Attachment B-9

ENDANGERED SPECIES ACT COMPLIANCE DETERMINATION

1. To: Well file, MI-075-2D-0009

Fr: Anna Miller

Re: Endangered Species Determination

December 8, 2011

2. The endangered, threatened, and candidate species present in (County) County as of December 8, 2011 are:

Species	**Status**	**Habitat**
Indiana bat (*Myotis sodalis*)	Endangered	Summer habitat includes small to medium river and stream corridors with well developed riparian woods; woodlots within 1 to 3 miles of small to medium rivers and streams; and upland forests. Caves and mines as hibernacula.
Eastern massasauga (*Sistrurus catenatus*)	Candidate	
Mitchell's satyr butterfly (*Neonympha mitchellii mitchellii*)	Endangered	Fens; wetlands characterized by calcareous soils which are fed by carbonate-rich water from seeps and springs
*Poweshiek skipperling (*Oarisma poweshiek*)	Candidate	Wet prairie and fens

3. The action area is a well pad about 200 feet by 200 feet, creation of an access road. Land disturbance includes removing top Heavy trucks will deliver rig components and a large rotary drill rig with support facilities will be utilized during drilling.

4. The previous and current land use is agricultural, with some residential at ¼ mile boundary.

5. Due to 1) there being no critical habitat in the action area, 2) there being no endangered species in immediate proximity to the action area, or 3) the non-disruptive and limited nature of the activities in the action area), I have determined that this well will have NO ADVERSE EFFECT on endangered species.

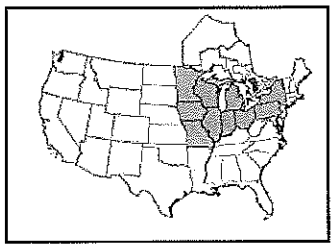

The eastern massasauga is generally found in small, isolated populations throughout its range.

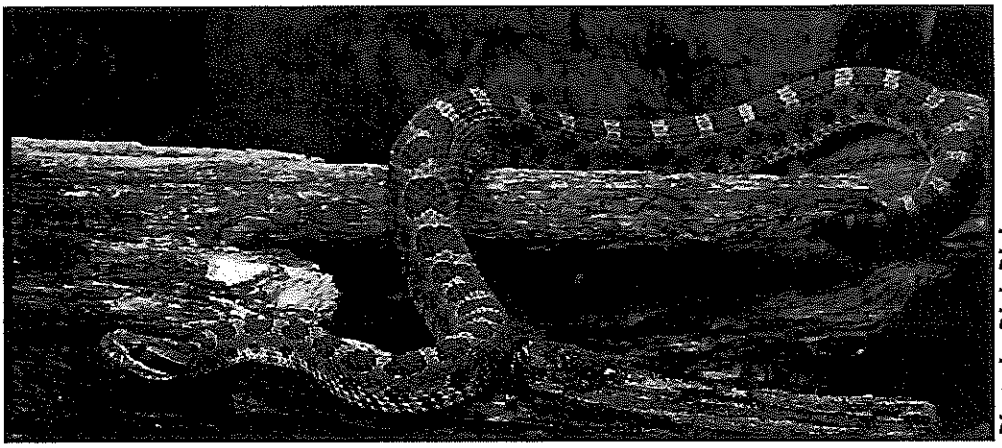

Photo by Dick Dickensen

Eastern Massasauga Rattlesnake

The eastern massasauga rattlesnake (*Sistrurus catenatus catenatus)* is a Federal candidate species. Candidate species are those species for which the Service has sufficient information on their biological status and threats to propose them as endangered or threatnened. Candidate species receive no legal protection, however, conservation is encouraged since they may warrant future protection under the Endangered Species Act.

What is an eastern massasauga rattlesnake?

Appearance - Massasaugas are small snakes with thick bodies, heart-shaped heads and vertical pupils. The average length of an adult is about 2 feet. Adult massasaugas are gray or light brown with large, light-edged chocolate brown blotches on the back and smaller blotches on the sides. The snake's belly is marbled dark gray or black and there is a narrow, white stripe on its head. Its tail has several dark brown rings and is tipped by gray-yellow horny rattles. Young snakes have the same markings, but are more vividly colored. The head is a triangular shape and the pupils are vertical.

Habitat - Massasaugas live in wet areas including wet prairies, marshes and low areas along rivers and lakes. In many areas massasaugas also use adjacent uplands during part of the year. They often hibernate in crayfish burrows but they may also be found under logs and tree roots or in small mammal burrows. Unlike other rattlesnakes, massasaugas hibernate alone.

Reproduction - Like all rattlesnakes, massasaugas bear live young. The young actually hatch from eggs while still in the female's body. Depending on the health of the individual, adult females may bear young every year or every other year. When food is especially scarce they may only have young every three years. Massasaugas that have young every year, mate in the spring and bear their young in late summer or early fall. In contrast, snakes that have young every other year, mate in autumn and bear young the next summer. Litter size varies from 5 to 19 young.

Feeding Habits - Massasaugas eat small rodents like mice and voles but they will sometimes eat frogs and other snakes. They hunt by sitting and waiting. Heat sensitive pits near the snakes' eyes alert the snake to the presence of prey. They can find their prey by sight, by feeling vibrations, by sensing heat given off by their prey, and/or by detecting chemicals given off by the animal (like odors).

Massasaugas are docile, secretive snakes that will try to escape rather than fight. But they will protect themselves and may bite if cornered. Be cautious in massasauga areas by wearing leather boots or shoes, watching where you place your hands and feet and walking around, rather than over, fallen logs. Treat massasaugas with respect, like any wild animal. If you are bitten by a massasauga, seek medical help immediately.

What is an eastern massasauga rattlesnake? (cont'd.)

Range - Eastern massasaugas live in an area that extends from western New York and southern Ontario to southern Iowa and a narrow band in northeastern Missouri. Historically, the snake's range covered this same area, but within this large area the number of populations and the number of snakes within populations have steadily shrunk. Today, the massasauga is listed as endangered, threatened, or a species of concern in every state and province in which it lives.

Why is the eastern massasauga a candidate species?

Eradication - People seem to have an innate fear of snakes and fear of poisonous snakes is particularly strong. Therefore, not only are massasaugas killed when they show up near homes or businesses, but people may go out of their way to kill or even eliminate them. Indeed, many states had bounties on all rattlesnakes, including massasaugas.

Habitat loss - Massasaugas depend on wetlands for food and shelter but often use nearby upland areas during part of the year. Draining wetlands for farms, roads, homes, and urban development has eliminated much of the massasauga habitat in many states. Also, massasaugas are not long distance travelers, so roads, towns, and farm fields prevent them from moving between the wetland and upland habitats they need. These same barriers also separate and isolate remaining populations from each other. Small, isolated populations often continue on a downward spiral until the massasauga is lost from those areas.

What is being done to conserve the eastern massasauga?

Research - Researchers are studying the eastern massasauga to learn about its life history, about how it uses its habitat, and how we can manage for it and its habitat.

Habitat Management - Many of the remaining populations of massasaugas are on public land and privately owned natural areas. Some land management practices on those properties harm massasaugas. The Service is working with willing land managers to practice techniques that allow traditional management goals to continue but avoid harming the massasauga and its habitat.

Education - Although many people have an innate fear of massasaugas, it is actually a secretive, docile snake that strikes humans only when it feels threatened and cornered. Living, working, or recreating in massasauga areas does require caution, but the massasauga is also an important and beautiful part of the natural heritage of those areas. We hope that education about the docile nature of the snake, its habits, and its role in the ecosystem will help people feel more comfortable living with this rare creature.

Why do we want to conserve the eastern massasauga?

Ecosystem Role - The massasauga plays an important role in its ecosystems, both as a predator on small mammals, other snakes, and amphibians and as prey for hawks, owls, cranes, and some mammals.

Indicator Species - The fact that massasaugas are in serious decline is a warning bell telling us that something is wrong. The story of the massasauga is similar to the story of many species of plants and animals that need wetlands and/or a combination of wetlands and uplands to survive. When we drain wetlands and develop in natural areas, we push our wild plants and animals onto ever smaller isolated islands of habitat where it is difficult for them to survive. By conserving massasaugas, we conserve natural systems that support many species of plants and animals.

S. Fish & Wildlife Service
Federal Drive
rt Snelling, Minnesota 55111-4056
2/713-5350
tp://midwest.fws.gov/endangered

October 1999

Attachment B-10

Geochimica et Cosmochimica Acta, 1958, Vol. 15, pp. 57 to 72. Pergamon Press Ltd., London

Mechanism of gypsification*

R. F. CONLEY† and W. M. BUNDY†

(*Received* 1 *April* 1957; *in revised form* 24 *February* 1958)

Abstract—Petrographic studies have shown that many gypsum deposits have been formed by the hydration of anhydrite, but the mechanism for hydration has not been fully explained. Gypsum has been produced experimentally by the agitation of anhydrite in pure water, a reaction that is accelerated by certain acids, bases, and salts, particularly alkali sulphates.

Phase investigations and reaction velocity studies indicate that accelerated hydration of anhydrite takes place through the medium of transient surface complexes in dilute solution. Concentrated solutions may precipitate double salts.

Contrary to recent hypotheses of gypsum dehydration by concentrated salt solutions, double salts and/or gypsum are stable phases below a temperature of 42°C. Above 42°C double salts may replace anhydrite as the stable phase. Gypsum, however, may remain a metastable phase indefinitely in its saturated solution below the hemihydrate transition temperature (98°C).

Experimental data indicate that precipitation of anhydrite from sea water is unlikely.

INTRODUCTION

HYDRATION of the mineral anhydrite ($CaSO_4$) to gypsum ($CaSO_4 \cdot 2H_2O$) has been a well-known phenomenon for many years. Although the hydration of anhydrite by pure water is extremely slow, it is accelerated in the presence of certain salts, alkalis and acids. The mechanism whereby this acceleration takes place has never been fully understood. This paper attempts to shed new light on the mechanism by which activation of anhydrite takes place.

PREVIOUS WORK

FARNSWORTH (1925) carried out hydration experiments using very finely ground anhydrite agitated in pure water. Several weeks were required for complete conversion. This reaction has been demonstrated by POSNJAK (1940) to take place via solution phase. His results are based on solubility data for calcium sulphate phases in water which show gypsum to be the least soluble phase below 42°C.

Thermodynamic studies by MACDONALD (1953) show that hydrostatic pressure assists hydration by driving the components of the following reaction to a state of lesser volume.

(A) $$CaSO_4 \text{ (anhydrite)} + 2H_2O \longrightarrow CaSO_4 \cdot 2H_2O \text{ (gypsum)}$$

However, when the lithostatic pressure exceeds the hydrostatic pressure, and confined water is allowed to escape, the equilibrium temperature for the above reaction is lowered. MACDONALD theorized that when pressure differential exists, gypsum in pure water could exist only at depths less than about 2500 ft.

Several investigators have also postulated that certain salt solutions decrease the solubility of anhydrite relative to gypsum to the point that anhydrite is the stable phase at temperatures well below 42°C. This change in solubility is based

* Published with the permission of the State Geologist, Indiana Department of Conservation, Geological Survey, Bloomington, Indiana.

† Present address; Georgia Kaolin Company, 433 North Broad, Elizabeth, New Jersey, U.S.A.

on the thermodynamic considerations of vapour pressure relationships by MacDonald and Posnjak and also Kelley, Southard and Anderson (1941). MacDonald proposed that concentrated saline solutions, as evaporating bodies of sea water, precipitate anhydrite at temperatures as low as 7°C.

Posnjak (1940) demonstrated the persistence of gypsum as a metastable phase up to 98°C (hemihydrate transition temperature) and this has been substantiated in the present investigation. Finely ground gypsum in contact with saturated NaCl solution remained unchanged at room temperature over a period of 6 months. Anhydrite nuclei added to this mixture were subsequently transformed to gypsum. Upon elevation of the solution temperature to 60°C, no alteration to anhydrite took place after 3 weeks. Other similar experiments with saturated solutions of sea water, $MgCl_2$, $CaCl_2$ and Na_2SO_4 over more extended periods of time gave the same results. Precipitated calcium sulphate formed by the following reaction occurs as gypsum up to about 70°C:

$$\text{(B)} \qquad CaCO_3 + 2H^+ + SO_4^{=} \xrightarrow{H_2O} CO_2\uparrow + Ca^{++}\,SO_4^{=} \longrightarrow \text{ppt.}$$

At higher temperatures hemihydrate precipitates and readily reverts to gypsum in water below 70°C. Hence, it may be concluded that the following reaction under standard conditions of temperature and pressure proceeds with extreme slowness, if at all:

$$\text{(C)} \qquad CaSO_4{\cdot}2H_2O(G) \xrightarrow[\text{soln.}]{\text{satd. salt}} CaSO_4(A) + 2H_2O$$

In contrast to the work of Posnjak and MacDonald showing that in certain salt solutions the gypsum–anhydrite transition temperature is lowered, several workers have demonstrated that these salts activate rather than inhibit hydration. This activation occurs even under conditions theoretically favouring anhydrite.

Hennicke (1923) introduced in Germany a mortar-forming process which utilized solutions of "alkali salts, acids and bases" with ground anhydrite. These solutions accelerated the hydration process. Further investigations of acceleration processes have been carried out by Randel (1933), Otteman (1950), and Gelmroth (1953).

Recent experiments (Leininger, Conley and Bundy, 1957) conducted to determine the relative effectiveness of activators yielded the following qualitative series:

$$K^+ \geqslant Na^+ \geqslant NH_4^+ > Mg^{++} > Fe^{++} > H^+ > Al^{+++} > Ca^{++}$$

$$\text{and } SO_4^{=} \geqslant Cl^- > OH^-$$

Although other ions may promote conversion, only these were studied because of their industrial and geochemical application. Potassium and sodium sulphate were investigated in detail because of their efficiency in activation and presence in natural waters.

Double Salt Formation

The reaction for the conversion of anhydrite to gypsum with activator solutions:

$$\text{(D)} \qquad CaSO_4\,(A) \xrightarrow[H_2O]{\text{act.}} Ca^{++} + SO_4^{=} \xrightarrow{H_2O} CaSO_4{\cdot}2H_2O\ (G)$$

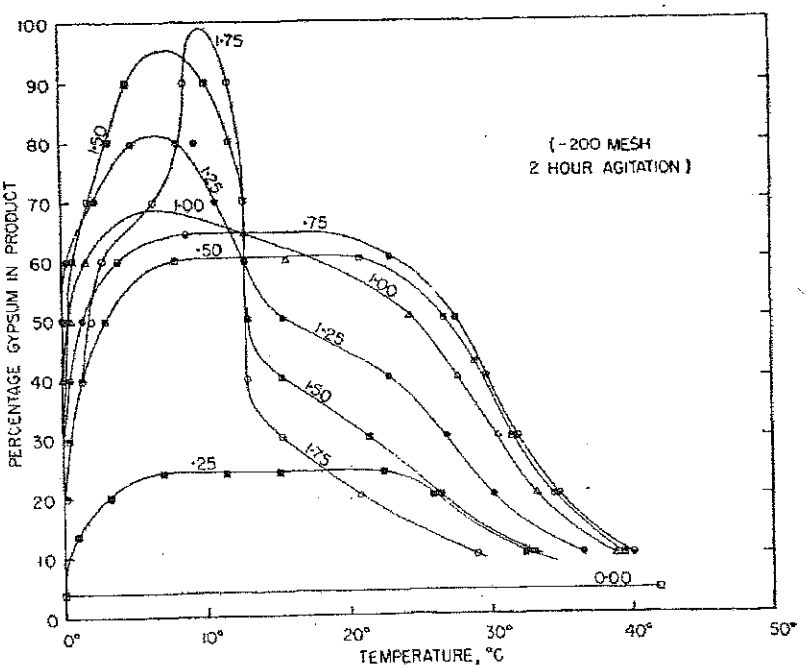

Fig. 1. Sodium sulphate isomolarity curves.

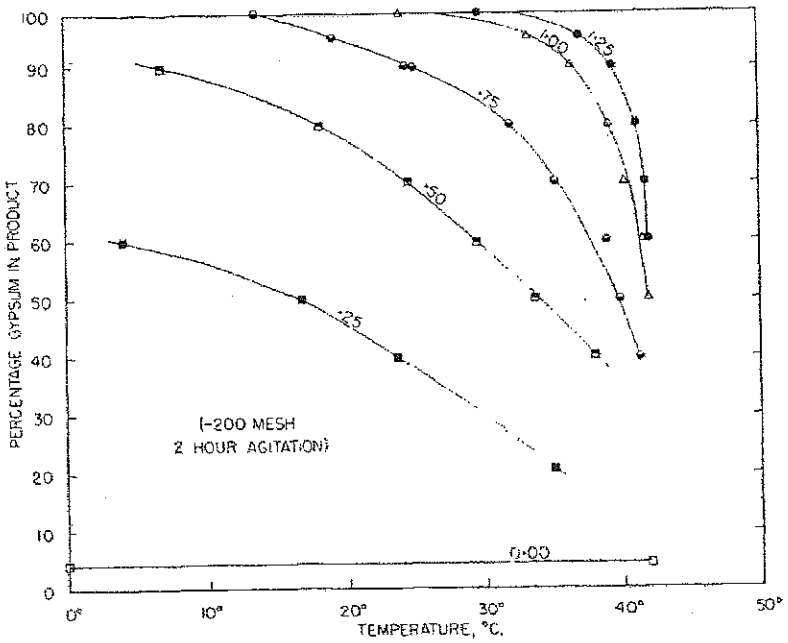

Fig. 2. Potassium sulphate isomolarity curves.

is primarily dependent upon solution temperature and concentration. Figs. 1 and 2 illustrate the effects of these parameters when sodium sulphate and potassium sulphate are used as activators and the product is removed and washed free of activator.* In this process gypsum results from decomposition of any double salt that has been formed. In Fig. 1 it is apparent that anomalous conversion to gypsum occurs at temperatures below 13°C and concentrations above 0·75M

* Gypsum content determined by standard A.S.T.M. gravimetric method.

Na_2SO_4. Experiments conducted within this field give rise to the formation of a stable double salt which subsequently decomposes upon washing. This double salt appears identical in composition with the sodium hemicalcium sulphate salt, $2Na_2SO_4 \cdot CaSO_4 \cdot 2H_2O$, designated as labile salt, and synthesized by Hill and Wills (1938) by the following method:

> A slight excess of gypsum is placed in a solution of sodium sulphate, 24·2 to 29·0 per cent by weight. The mixture is maintained in a sealed container at 75°C for 72 hr.

Table 1. Chemical analyses of labile salt

Component	Labile salt (theory)	Synthetic (Hill and Wills)	Synthetic (Conley and Bundy)
Na_2SO_4	62·27	61·6	69·4*
$CaSO_4$	29·83	29·7	23·8
H_2O	7·90	8·7	7·7
	100·00	100·0	100·9

* High sodium content due to activator contamination.

Table 1 includes chemical analyses of the double salt obtained from a solution at 6·5°C, the salt synthesized by Hill and Wills, and the stoichiometric composition of labile salt. X-ray spectrometer data of the synthesized salts are shown in Fig. 3.

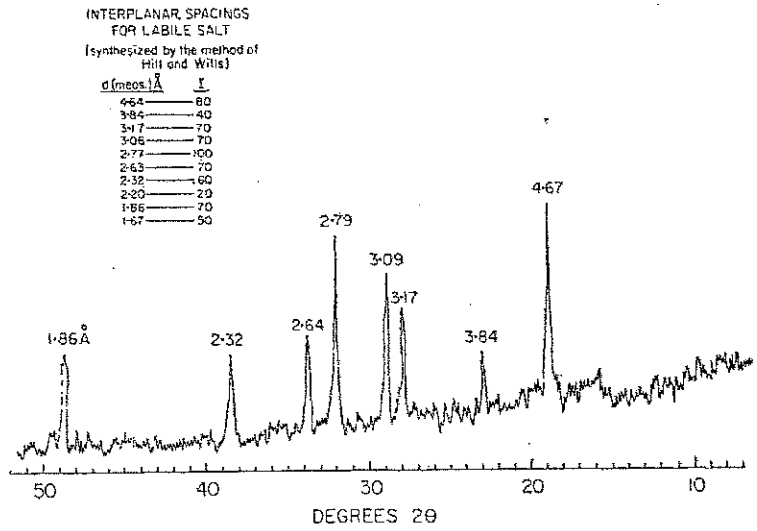

Fig. 3. X-ray spectrometer trace and interplane spacings for labile salt.

Fig. 2 shows that conversion is largely dependent upon K_2SO_4 concentration, and no critical temperature is observed below 42°C. Throughout the operating range 0–42°C and 0·25–1·25 M K_2SO_4 a double salt which corresponds to the mineral syngenite, $K_2SO_4 \cdot CaSO_4 \cdot H_2O$, is obtained. Chemical analyses for the double salt obtained in these experiments and the stoichiometric composition of

syngenite are given in Table 2. An X-ray spectrometric trace of the double salt is shown in Fig. 4. Although this pattern is not in complete accord with the A.S.T.M. data listed for syngenite,† it is believed that chemical and X-ray data are adequate to conclude that syngenite is present.

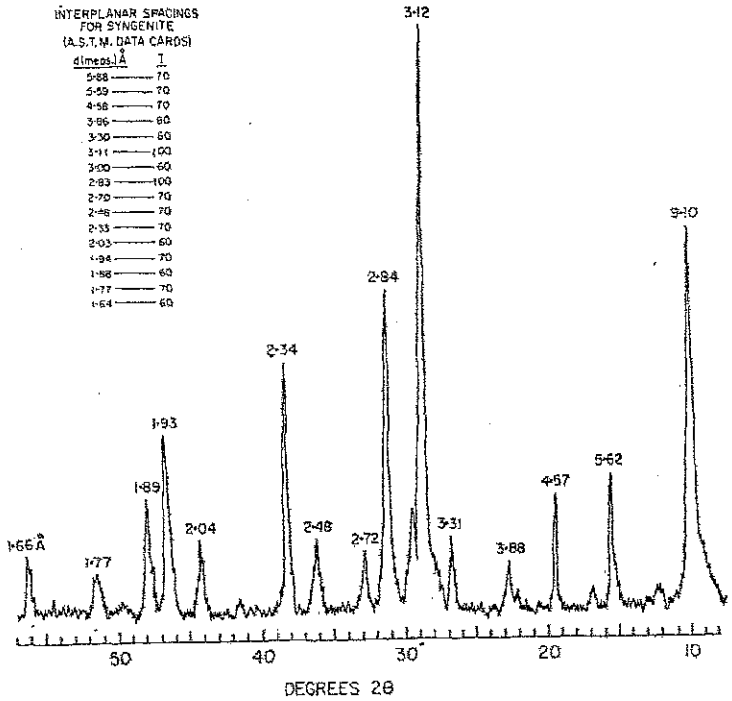

Fig. 4. X-ray spectrometer trace and interplane spacings for syngenite.

Phase Studies

Ternary phase diagrams for the systems $CaSO_4$–Na_2SO_4–H_2O and $CaSO_4$–K_2SO_4–H_2O have been constructed in order to obtain a better understanding of phase equilibria. Hill and Wills (1938) collected data for the former in the range 25°–100°C and Hill (1934) for the latter from 40°–100°C. These workers

Table 2. Chemical analyses of syngenite

Component	Syngenite (theory)	Synthetic (Conley and Bundy)
$CaSO_4$	41·46	41·0
K_2SO_4	53·06	53·5
H_2O	5·48	5·5
	100·00	100·0

† All the lines on the diagram that are within the range of those recorded on the A.S.T.M. card check to within 0·02 Å. The one line on the card that does not show up on the diagram (5·88 Å) is also missing from the syngenite pattern on file at the U.S. Geological Survey, so it is possible that it was due to an impurity in the material from which the pattern summarized on the A.S.T.M. card was made. Ed.

have demonstrated the stability of various double salts above 42°C. It was necessary to supplement these data with information obtained in the range 0–25°C.

For this purpose a warming-curve method modified after Tammann cooling-curves (1903) was employed. Fig. 5(a) shows the temperature change with time

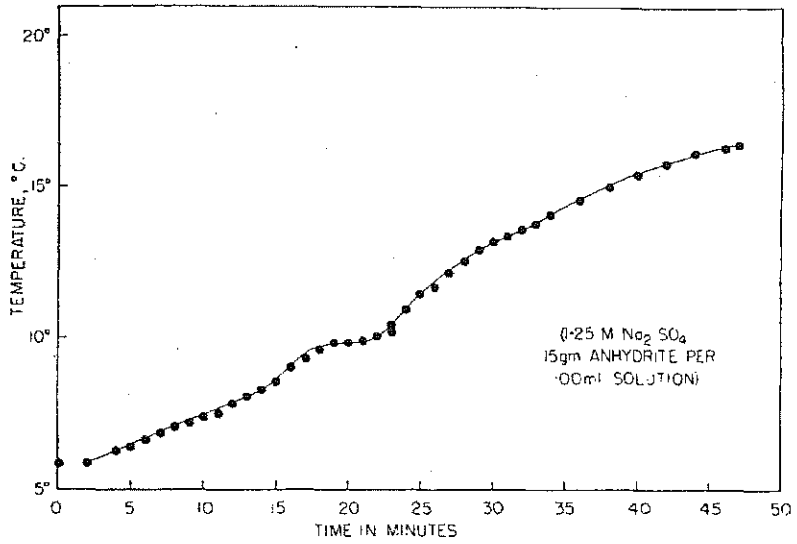

Fig. 5(a) Warming curve for the system Na_2SO_4–$CaSO_4$–H_2O.

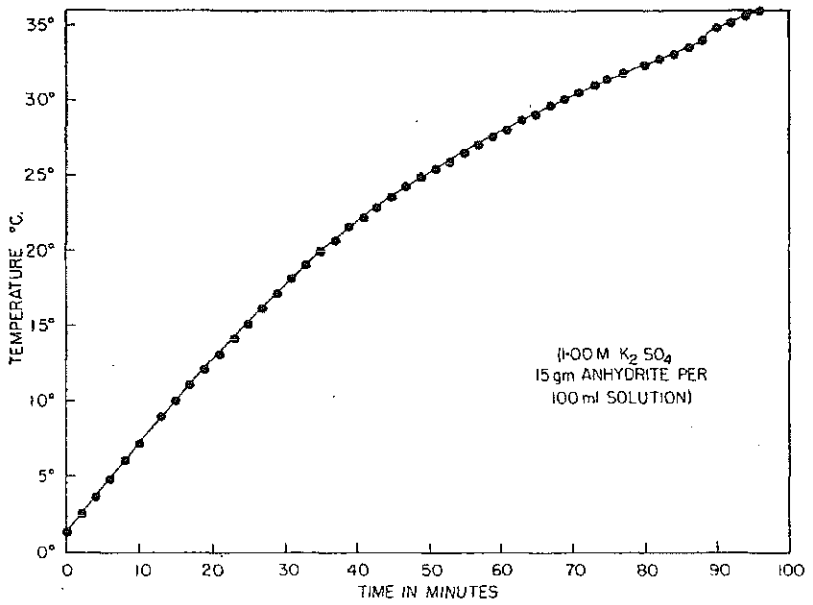

Fig. 5(b). Warming curve for the system K_2SO_4–$CaSO_4$–H_2O.

of a Na_2SO_4 activated suspension of anhydrite. The composition of this mixture was selected from the field of complex salt stability in Fig. 1. The mixture was agitated for 6 hr in a 2°C bath to obtain maximum double salt formation. The resulting mixture was removed from the bath and allowed to warm in air at room temperature. Temperature measurements of the warming solution were determined periodically with an N.B.S. calibrated thermometer graduated in 0·1°C.

A well-defined plateau in Fig. 5(a), originating from an endothermic reaction, is observed at 9·8°C. The change of slope above this temperature indicates the formation of a new phase. Results of X-ray analysis show that below 9·8°C labile

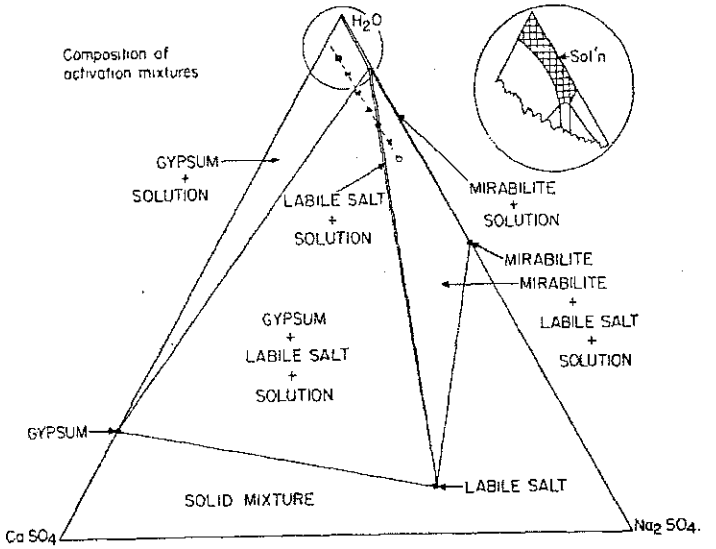

Fig. 6(a). Weight (%) ternary diagram of Na_2SO_4–$CaSO_4$–H_2O at 9°C.

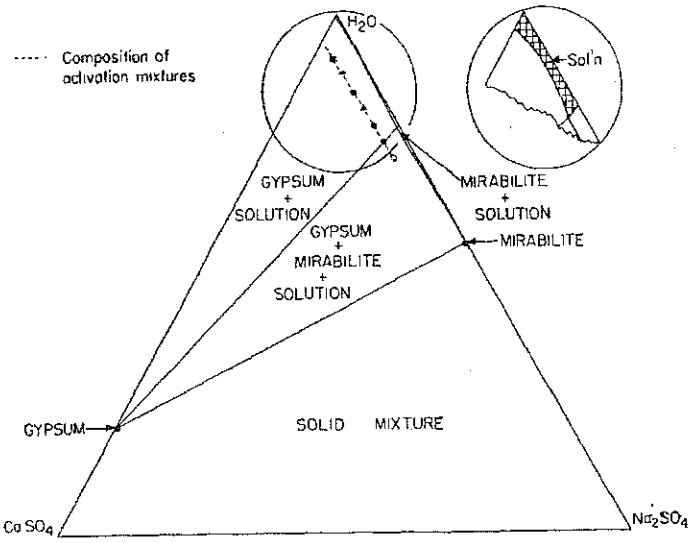

Fig. 6(b). Weight (%) ternary diagram of Na_2SO_4–$CaSO_4$–H_2O at 25°C.

salt and small quantities of gypsum exist as stable phases but above this temperature gypsum and mirabilite, $Na_2SO_4 \cdot 10H_2O$, are stable. Therefore, 9·8°C is the temperature at which labile salt begins to dissociate into gypsum and mirabilite (the solubility of labile salt equals the solubility of gypsum). It should be noted that the transition temperature 13°C apparent in Fig. 1, probably represents

equilibrium between the solubilities of the two metastable phases, labile salt and anhydrite. In Fig. 5(a) a very small break occurs at about 13°C. At this point equilibrium is believed to exist between metastable labile salt and the very small

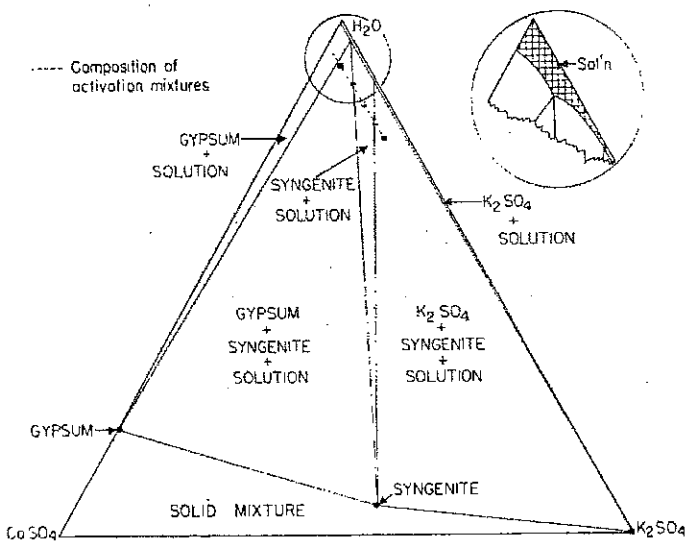

Fig. 6(c). Weight (%) ternary diagram of K_2SO_4–$CaSO_4$–H_2O at 25°C.

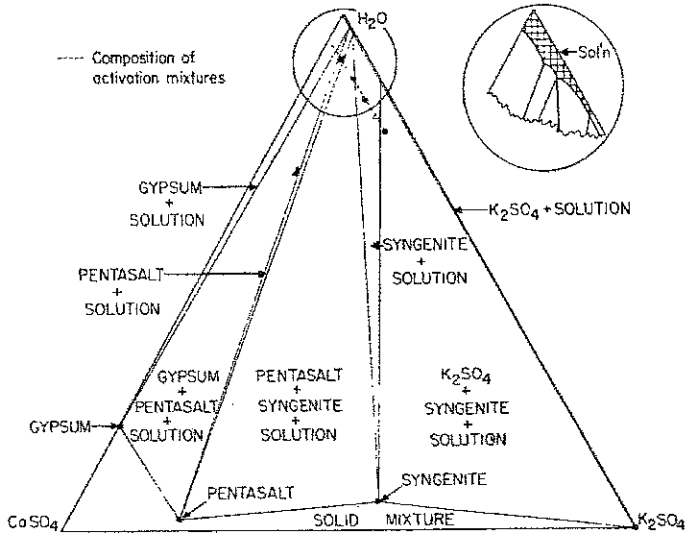

Fig. 6(d). Weight (%) ternary diagram of K_2SO_4–$CaSO_4$–H_2O at 40°C.

quantity of anhydrite remaining in the mixture. Other warming-curve data taken from an automatic recorder and plotted as the second derivative, d^2T/dt^2, support this interpretation.

The discontinuity occurring at a temperature lower than 9°C could not be interpreted with present phase information. A new phase region may be indicated by this break.

From the above determinations, along with $CaSO_4 \cdot 2H_2O$ and $Na_2SO_4 \cdot 10H_2O$ solubility data, the ternary diagram [Fig. 6(a)] was constructed. The extreme narrowness of the field, labile salt + solution, inhibits precise determination of the phase boundary, labile salt + solution/solution. The diagram was drawn in accordance with the general principles reviewed by MARSH (1935) and RIVETT (1923). A similar ternary phase diagram [Fig. 6(b)] was constructed from 25°C data to show the shift of the various stability fields.

A second warming curve [Fig. 5(b)] was obtained by using a K_2SO_4 activated suspension of anhydrite. The methods employed were similar to those used in obtaining the Na_2SO_4 warming curve. An exothermic reaction was obtained at about 34·5°C. This represents the equilibrium temperature between the fields of syngenite + gypsum and syngenite + pentasalt [$(CaSO_4)_5K_2SO_4 \cdot H_2O$]. No other phase changes were observed up to the terminal temperature, 60°C. These phases are substantiated by X-ray analysis, and the results are in agreement with conclusions of HILL (1934). Figs. 6(c) and 6(d) are two ternary phase diagrams constructed from 25°C and 40°C data. The greater efficiency of K_2SO_4 over Na_2SO_4 activation may be expected to result from the greater stability range of the K–Ca double salts. X-ray determinations and warming-curve data show syngenite to be stable throughout the temperature range in Fig. 5(b).

MECHANISM OF DOUBLE SALT FORMATION

The transition from anhydrite to a double salt and the decomposition of the double salt to gypsum by washing were observed to be relatively rapid processes. Transformation of anhydrite to gypsum by means of stable double salt formation and decomposition can therefore be readily understood. Comparison of Fig. 1 with Figs. 6(a) and (b) and Fig. 2 with Figs. 6(c) and (d) indicates that relatively rapid conversion also occurs outside the double salt stability fields. The reactions within these areas of complex salt instability require a more thorough explanation.

OTTEMAN suggested the formation of transient double salts as a possible mechanism of transformation. He further postulated that the increased solubility of anhydrite in concentrated Na_2SO_4 solution is a primary factor in this transformation process. Results of the present investigation are in agreement with OTTEMAN's "transient double salt" postulation; however, the writers do not believe that the slight increase in anhydrite solubility contributes significantly to the conversion process. The negligible effect of this solubility increase is shown in Fig. 7. Fig. 8 shows that after 2 hr of agitation in pure water 0·2 per cent of anhydrite is converted to gypsum, whereas under the same conditions with 0·75 M Na_2SO_4 in saturated $CaSO_4$ solution about 60 per cent of anhydrite is converted. The reaction rate is increased 300-fold, but the solubility-differential between anhydrite and gypsum for these two solutions shows only a slight increase.

This relation is further demonstrated by an analysis of the effects produced by NaCl activation. The solubility of calcium sulphate in 0·5 M sodium chloride solution is approximately three times greater than in an equivalent sodium sulphate solution (COMEY and HAHN, 1921). Conversely, the activating efficiency of the Na_2SO_4 is about fifty times greater than that of NaCl. It is concluded that both the cation and anion enter into an activation complex.

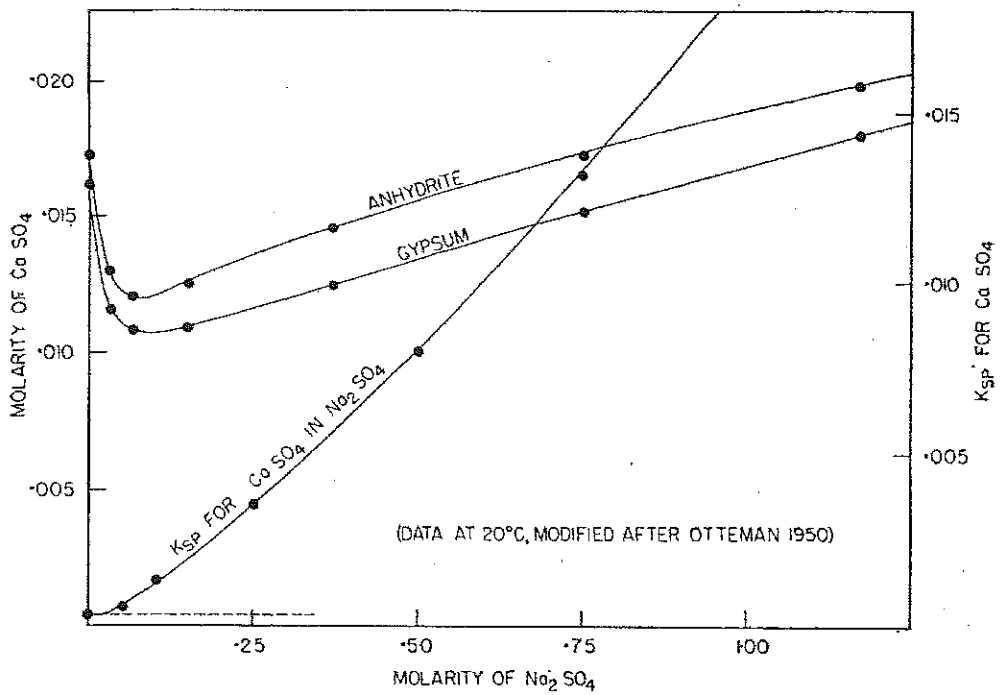

Fig. 7. Solubility and solubility product relationship of $CaSO_4$ in Na_2SO_4 solutions.

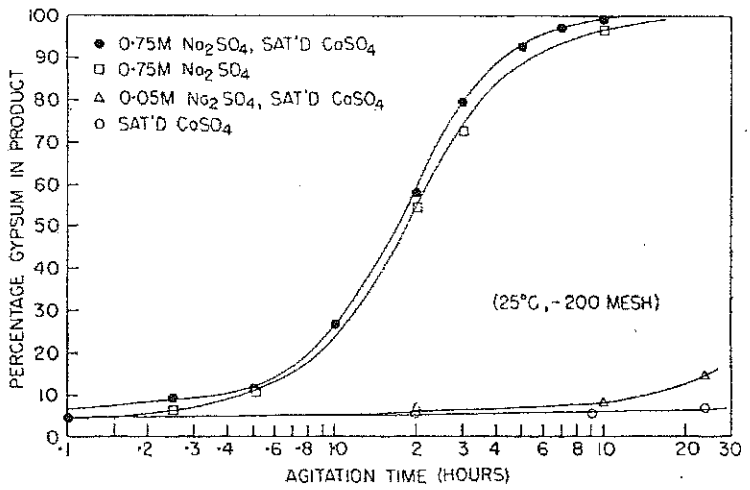

Fig. 8. Rate of gypsum formation in activating solutions.

Experimental work (LEININGER, CONLEY and BUNDY, 1957) indicates that sulphate salts are more effective activators than foreign anion salts. To comprehend better the effect of the anion upon activation, the following theoretical treatment is given. The surface of anhydrite* is considered as a network of alternating Ca^{++} and $SO_4^{=}$ ions. When this surface is in contact with a saturated

* Microscopic observations of anhydrite undergoing hydration by an activating solution show that the 100 plane is most susceptible to this attack (OTTEMAN, 1950).

calcium sulphate solution, the following transitions take place and approach equilibrium:

	Interfacial ion		Solvated ion
(E)	(Ca^{++})	$\rightleftharpoons$	Ca^{++}
(F)	$(SO_4^{=})$	$\rightleftharpoons$	$SO_4^{=}$

This exchange process is shifted slightly to the solution phase below 42°C and results in very slow rate of gypsum precipitation.

If the anhydrite surface is in contact with a calcium sulphate solution which contains a dissolved salt $M^{+a}X^{-b}$ of a given concentration, the following transitions can occur:

	Interfacial ion		Solvated ion
(E)	$1(Ca^{++})$	$\rightleftharpoons$	$1Ca^{++}$
(F)	$1(SO_4^{=})$	$\rightleftharpoons$	$1SO_4^{=}$
(G)	$1(Ca^{++})$	$\rightleftharpoons$	$2/aM^{+a}$
(H)	$1(SO_4^{=})$	$\rightleftharpoons$	$2/bX^{-b}$
(I)	$1(Ca^{++}SO_4^{=})$	$\rightleftharpoons$	$1M^{+a} + X^{-b}$

Only these ionic transitions permit the net surface charge to remain electrostatically unaltered. If the molar concentration of the salt $M^{+a}X^{-b}$ is large with respect to the concentration of calcium sulphate, transitions (G), (H) and I predominate.

It is apparent that when X^{-b} is the sulphate ion, the statistical probability of a surface transient complex formation is considerably higher than when X^{-b} is Cl^{-}, etc. Many investigators have reported double sulphate salts of Ca^{++} and cation M^{+a}, but relatively few complex salts which have a composition of the general type MX·NY (different cations and different anions) are known. The increased quantity of $SO_4^{=}$ ions in solution also increases the precipitation rate of gypsum by virtue of a greater number of Ca^{++}–$SO_4^{=}$ collisions in the solution phase.

The formation of surface transient complexes may then be considered as a statistical replacement process whereby M^{+a} ions are substituted randomly for Ca^{++} ions or adsorbed on the calcium sulphate surface. The adsorption of these foreign ions in localized areas produces surface deformities and reduces the surface energy. Because of surface energy reduction, more Ca^{++} and $SO_4^{=}$ ions are released per unit time. These, in turn, precipitate as gypsum from the already saturated calcium sulphate solution. The increased rate of gypsum formation is produced, therefore, by making the anhydrite more readily soluble.

If a double salt is the least soluble species under the conditions of the system, a double salt crystallite will be formed. Growth will occur upon the crystallite surface by depletion of Ca^{++}, M^{+a} and $SO_4^{=}$ ions from the surrounding solution. The solution is replenished by dissolution of the more soluble anhydrite and, if present, solid phase $M_{2/a}SO_4$. This process of precipitation may result in the inclusion of the anhydrite grain by peripheral double salt growth. Microscopic observations show this type of inclusion to occur.

Nuclei for double salt formation also may be provided by direct precipitation from solution. This type of nuclei formation can be observed during the interaction of saturated calcium sulphate solution with potassium sulphate solutions above approximately 0·2 M and concentrated $NaSO_4$ solutions below 9·8°C.

If the solubility of the double salt is greater than that of gypsum (the double salt is unstable under the conditions of the system), dissolution of the crystallite surface will occur and supersaturate the solution with resepct to $CaSO_4 \cdot 2H_2O$. Precipitation of $CaSO_4 \cdot 2H_2O$ then will occur either on the surface of existing nuclei or by spontaneous nucleation. Depletion of the solid phase anhydrite will be most rapid when the ratio of anhydrite to gypsum is large. As greater quantities of gypsum form, a competing reaction due to foreign cation adsorption on the gypsum surface will then decrease the anhydrite dissolution rate and, consequently, the gypsum formation rate. Therefore, an inflexion in the hydration rate curve would theoretically be obtained when the surface area (or surface activity) of calcium sulphate in the anhydrite phase is equal to that of the calcium sulphate in the gypsum phase. It is apparent from Fig. 8 that the data show a maximum for the rate change at about 50 per cent yield.

The precipitation of gypsum from a saturated calcium sulphate solution may then be considered as a two-stage process: (1) formation of incipient nuclei, and (2) crystal growth of these nuclei. The overall reaction may be represented by the following equation:

(J) $$n\mathrm{Ca}^{++} + n\mathrm{SO}_4^{=} + 2n\mathrm{H}_2\mathrm{O} \longrightarrow n\mathrm{CaSO}_4 \cdot 2\mathrm{H}_2\mathrm{O}.$$

If the mole fraction of water is large relative to the concentration of calcium and sulphate ions, the precipitation of gypsum will be limited primarily by the Ca^{++} and $SO_4^{=}$ ion concentrations. Crystallite formation is dependent upon the total number of anion–cation collisions which in turn are a function of the anion and cation concentrations. The rate of formation of nuclei is proportional to $[(Ca^{++})(SO_4^{=})]^{p/2}$ where p is the number of monomers, or ion members of a nucleus, required to sustain the crystalloid (O'Rourke and Johnson, 1955). With regard to nucleation, it must be pointed out that natural anhydrite may contain intrinsic gypsum and also may provide simultaneous growth planes (Spangenberg and Neuhaus, 1930; Turnbull and Vonnegut, 1952) for gypsum. Both of these processes would circumvent the necessity of incipient nuclei formation.

The precipitation rate of gypsum by crystal growth of nuclei is represented by the following solution equation:

(K) $$-\frac{dC}{dt} = k(C - C_s)^q$$

where C = concentration of monomers

C_s = concentration at saturation

q = number of monomers in the growth nucleus

Simply stated, the driving force for precipitation is a function of the concentration

of calcium and sulphate ions above the saturation concentration. The equation can be transformed to:

$$(L) \qquad -\frac{dC}{dt} = k\{\sqrt{([Ca^{++}]\,[SO_4^{=}])} - \sqrt{([Ca^{++}]_s[SO_4^{=}]_s)}\}^q.$$

The value $\sqrt{([Ca^{++}]_s[SO_4^{=}]_s)}$ can be equilibrated with the $(K_{sp})^{1/2}$ for calcium sulphate. As Fig. 7 shows, the K_{sp} varies strongly with $SO_4^{=}$ concentration. The growth order, q, and nucleation order, p, for the reactions are assigned the value of 4 based on the similar barium sulphate kinetic study by JOHNSON and O'ROURKE (1954). Hence, it is concluded that the rate of precipitation is $\alpha([Ca^{++}][SO_4^{=}])^2$ for nucleation and $\alpha\{\sqrt{([Ca^{++}][SO_4^{=}])} - \sqrt{K_{sp}}\}^4$ for growth.

The above treatment of solution kinetics has been incorporated to show that a sulphate activator provides greater precipitation rate for gypsum than other anion activators do. These kinetics also indicate that very dilute activator solutions, even in the range where calcium sulphate solubility is sharply depressed, are more efficient in producing hydration (as $[M_{2/a}SO_4] \rightarrow 0$) than water alone. This is substantiated by the 0·05M Na_2SO_4 data appearing in Fig. 8.

GEOLOGICAL APPLICATION

Gypsification of secondary anhydrite is believed to take place primarily by the action of activating cations. This concept of natural activation is supported both by the prevalence of saline solutions associated with gypsum–anhydrite deposits and by laboratory evidence.

The salinity of ground water associated with evaporite deposits is largely dependent upon beds of the more soluble K, Mg and Na salts. The prevalence of these salts in the Stassfurt evaporite deposits of Germany should result in the formation of concentrated salt solutions. It can be assumed, therefore, that activation of anhydrite through the formation of both stable and unstable double salts is a significant process in these deposits. Some of the complex salts which occur in the Stassfurt deposits and which may be related to activation processes (CLARKE, 1924) are:

Glauberite	$CaSO_4 \cdot Na_2SO_4$
Polyhalite	$2CaSO_4 \cdot MgSO_4 \cdot K_2SO_4 \cdot 2H_2O$
Krugite	$4CaSO_4 \cdot MgSO_4 \cdot K_2SO_4 \cdot 2H_2O$ (polyhalite admixed with anhydrite (FORD, 1947))
Syngenite	$CaSO_4 \cdot K_2SO_4 \cdot H_2O$

Obviously, the stable double salts persist only as long as their environments lie within their fields of stability. Dilution of the salt solutions and, with some salts, change of temperature result in their decomposition and subsequent precipitation of calcium sulphate as gypsum.

In contrast to the Stassfurt deposits the evaporites occurring in south-western Indiana (MCGREGOR, 1954) are limited to anhydrite and gypsum. The ground water associated with these deposits contains relatively little solute. Chemical

analyses of water samples from the National Gypsum Co. and United States Gypsum Co. mines near Shoals, Ind., show a salinity of less than 20 parts per thousand. The following analysis (Table 3) of a sample taken from the National Gypsum Co. mine indicates the dilute character of the subsurface water:

Table 3. Analysis of mine water (National Gypsum Co., Shoals, Ind.)

Constituent	Concentration (%)
Na	0·56
Ca+Mg	<0·1
Cl	0·59
SO_4	0·43
B	trace
Fe	trace
K	trace
Li	trace
Sr	trace
S (as sulphide)	trace
Total dissolved solids	1·78
pH	8·0

The constituents of these subsurface waters may have been derived from any of the following sources:

(1) Connate water. Occurs as liquid inclusions in mineral grains and pore fluids within rock strata.

(2) Disseminated salts. Minute crystals included in the anhydrite–gypsum beds.

(3) Adsorbed ions. On clay structures by ion exchange.

(4) Previous salt deposits. Although petrographic evidence does not indicate the presence of soluble K, Na and Mg salts, these may have been removed by the action of ground water.

The relative rate of hydration produced by dilute solutions is illustrated in Fig. 8. The amount of conversion obtained by using a 0·75M Na_2SO_4 activator solution is shown by the upper two curves. The time lag between these two curves indicates the necessity of calcium sulphate saturation before gypsum precipitation can occur. At 0·75M sodium sulphate concentration the anhydrite solubility is noticeably increased with respect to dilute Na_2SO_4 solutions (see Fig. 7). The curve obtained with 0·05M Na_2SO_4, where anhydrite solubility is depressed, shows that activation occurs even in very dilute solutions. Although dilute solutions do not greatly accelerate hydration, the slight rate increase over pure water is significant when geologic time is considered. This observation becomes important when applied to geologic conditions in which the number of nuclei and amount of reaction surface are comparatively small.

On the assumption that crystallites of anhydrite form in sea water, as postulated by earlier workers, the present investigation indicates that activating constituents

contained therein would bring about almost immediate conversion to gypsum and/or double salts. Gypsum formation requires that temperatures during precipitation do not greatly exceed 42°C. The activating effect of sea water is shown in Fig. 9.* A second curve of activation by NaCl is included for comparison. The greater efficiency of sea water activation can be accounted for by the presence of small quantities of sulphate ion in sea water. It can be seen that above 214 parts per thousand salinity for sea water and 196 parts per thousand for NaCl, anhydrite is still converted to gypsum. Above these concentrations, theoretical vapour

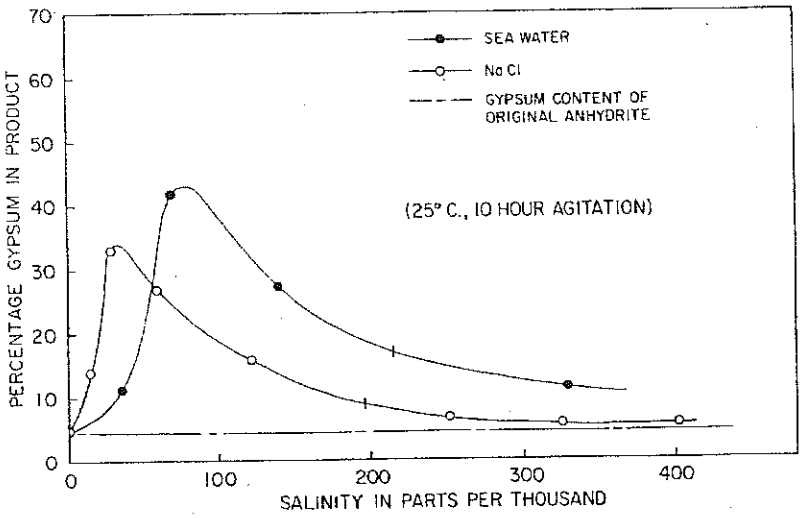

Fig. 9. Activation effect of sea water and NaCl.

pressure calculations indicate that at 25°C only anhydrite can be precipitated from solution. It must be concluded, therefore, that former thermodynamic applications based on vapour pressure relationships, which predict the formation of anhydrite from gypsum in concentrated salt solutions are incomplete. These applications do not incorporate the lattice alterations and intermediate calcium sulphate–activator complexes which influence the reaction kinetics.

It appears more reasonable to assume that anhydrite is formed, given sufficient time, only after burial when gypsum is subjected to directed stresses and increased temperatures.

Summary

(1) The hydration of anhydrite is accelerated by certain acids, bases, and salts. Alkali sulphates are the most effective of these activators.

(2) In dilute activating solutions hydration proceeds via transient complexes. Depending upon temperature, double salts can be stable in concentrated activator media. The formation of complexes is believed to be a surface ionic transfer process and is a function of probability.

(3) Hydration of anhydrite in nature is believed to take place primarily by action of the activating cations occurring in ground water.

(4) Primary precipitation of anhydrite from sea water is improbable. The

* Robert F. Conley (1957) Unpublished manuscript.

relative ease of crystallization of metastable gypsum within the anhydrite stability field prevents sufficient supersaturation for nucleation of anhydrite. Abundant activating cations present in sea water further inhibit the formation of anhydrite.

Acknowledgement—The authors are indebted to Dr. RALPH L. SEIFERT, Indiana University, for his assistance and suggestions in the construction of the phase diagrams.

REFERENCES

CLARKE F. W. (1924) *U.S. Geol. Surv. Bull.* 770.
COMEY A. M. and HAHN D. A. (1921) *A Dictionary of Chemical Solubilities, Inorganic* (2nd Ed.). Macmillan, New York.
FARNSWORTH M. (1925) *Amer. Pat.* 1566186.
FORD W. E. (1947) *A Textbook of Mineralogy.* John Wiley, New York.
GELMROTH W. *Silikattechnik* **4,** 21–24.
HENNICKE R. (1923) *Amer. Pat.* 1442406.
HILL A. E. (1934) *J. Amer. Chem. Soc.* **56,** 1071–1078.
HILL A. E. and WILLS J. H. (1938) *J. Amer. Chem. Soc.* **60,** 1647–1655.
JOHNSON R. A. and O'ROURKE J. D. (1954) *J. Amer. Chem. Soc.* **76,** 2124–2126.
KELLEY K. K., SOUTHARD J. C. and ANDERSON C. F. (1941) *U.S. Bur. Mines Tech. Paper* 625.
LEININGER R. K., CONLEY R. F. and BUNDY W. M. (1957) *Indust. Engng. Chem.* **49,** 818–821.
MACDONALD G. J. (1953) *Amer. J. Sci.* **251,** 883–898.
MCGREGOR D. J. (1954) *Indiana Geol. Survey, Rept. Progress* 8.
MARSH J. S. (1935) *Principles of Phase Diagrams* pp. 99–170. McGraw-Hill, New York.
O'ROURKE J. D. and JOHNSON R. A. (1955) *Analyt. Chem.* **26,** 1699–1704.
OTTEMAN J. (1950) *der Geol. Landesanstalt,* No. 219.
POSNJAK E. (1940) *Amer. J. Sci.* **238,** 559–568.
RANDEL W. S. (1933) *Amer. Pat.* 1941188 (to U.S. Gypsum Co.).
RIVETT A. C. (1923) *The Phase Rule* pp. 93–125. Oxford University Press, London.
SPANGENBERG K. and NEUHAUS A. (1930) *Chemie Der Erde* **5,** 437–529.
TAMMANN G. (1903) *Z. anorg. Chem.* **37,** 303–313.
TURNBULL D. and VONNEGUT B. (1952) *Industr. Engng. Chem.* **44,** 1292–1297.

Attachment B-11

THE AMERICAN MINERALOGIST, VOL. 52, JANUARY-FEBRUARY, 1967

THE GYPSUM—ANHYDRITE EQUILIBRIUM AT ONE ATMOSPHERE PRESSURE[1]

LAWRENCE A. HARDIE, *Department of Geology, The Johns Hopkins University, Baltimore, Maryland*

ABSTRACT

The equilibrium temperature for the reaction $CaSO_4 \cdot 2H_2O = CaSO_4 + 2H_2O_{(liq.\ soln)}$ has been determined as a function of activity of H_2O (a_{H_2O}) of the solution. Synthetic gypsum and anhydrite or 1:1 mixtures were stirred in solutions of known a_{H_2O} (calculated from vapor pressure data for the Na_2SO_4 and H_2SO_4 solutions), at constant temperature for as much as 12 months. The reversible equilibrium was approached from both sides and is defined by: $a_{H_2O} = 0.960$ at 55°, 0.845 at 39°, 0.770 at 23°C. Provided the solids do not change in composition, the equilibrium at constant P and T is a function of a_{H_2O} only and is independent of the constituents in solution. Extrapolation to the bounding system $CaSO_4$-H_2O ($a_{H_2O} = 1.000$) yields 58° ± 2°C. This is within thermodynamic calculations (46° ± 22°C) but higher than solubility measurements (38° to 42°C). The new data indicate that in seawater saturated with halite and gypsum should dehydrate above 18°C. The scarcity of anhydrite in modern evaporite deposits is predicted by the present results. The available data on the temperature-salinity conditions under which anhydrite and gypsum exist in the Recent supratidal flat sediments of the Trucial Coast, Persian Gulf, are compatible with the present experimental data.

INTRODUCTION

The stability relations of gypsum ($CaSO_4 \cdot 2H_2O$) and anhydrite ($CaSO_4$) are of considerable interest because most natural marine evaporite deposits consist essentially of gypsum and/or anhydrite interbedded with dolomite, limestone and clastic sediments (*e.g.*, Stewart 1963, Table 18). In the binary system $CaSO_4$-H_2O, the reaction $CaSO_4 \cdot 2H_2O \rightleftharpoons CaSO_4 + 2\ H_2O_{(liq.)}$ has been studied experimentally at one atmosphere pressure by van't Hoff *et al* (1903), Partridge and White (1929), Toriumi and Hara (1934), Hill (1934), Posnjak (1938) and D'Ans *et al* (1955). Kelley, Southard and Anderson (1941) measured the thermochemical properties of the solid phases of the system at atmospheric pressure, and from these data calculated an equilibrium temperature for the gypsum-anhydrite transition. Marsal (1952), MacDonald (1953), Zen (1965) and Hardie (1965, pp. 25–30) calculated the effect of pressure on the reaction.

The effect of salt solutions on the gypsum-anhydrite equilibrium at atmospheric pressure has been considered in some detail by several workers, all of whom have verified that the transition temperature is lowered with increasing salinity. The system $CaSO_4$-NaCl-H_2O has been investigated experimentally by van't Hoff *et al* (1903), D'Ans *et al* (1955), Madgin and Swales (1956), Bock (1961) and Zen (1965). MacDonald

[1] This paper is taken from a Ph.D. dissertation submitted by L. A. Hardie to the Department of Geology, The Johns Hopkins University, Baltimore, Maryland.

(1953) calculated the effect of NaCl solutions on the equilibrium temperature. The transition in sea water has been studied by Toriumi *et al* (1938) and Posnjak (1940). Other pertinent laboratory studies are those of Hill and Wills (1938) and Conley and Bundy (1958) in the system $CaSO_4$-Na_2SO_4-H_2O, D'Ans and Hofer (1937) in the system $CaSO_4$-H_3PO_4-H_2O, and Ostroff (1964), who converted gypsum to anhydrite in NaCl-$MgCl_2$ solutions.

For the most part the results of the different workers are in poor agreement. For this reason, and because the methods used were largely indirect (*e.g.* solubility and dilatometer measurements, thermodynamic calculation), a re-examination of the problem, using a different laboratory approach, seemed desirable.

The conversion of gypsum to anhydrite, and anhydrite to gypsum, was studied at atmospheric pressure as a function of temperature and activity of H_2O (a_{H_2O}). For the reaction

$$CaSO_4 \cdot 2H_2O_{(s)} \rightleftharpoons CaSO_{4(s)} + 2H_2O_{(\text{liquid, in solution})}$$

the equilibrium constant may be defined in terms of activities, as follows:

$$(K_a)_{p,T} = \frac{a_{CaSO_4} \cdot a^2_{H_2O}}{a_{CaSO_4 \cdot 2H_2O}}$$

If the standard states of the components of the reaction are considered to be pure H_2O liquid water, pure crystalline $CaSO_4$ and pure crystalline $CaSO_4 \cdot 2H_2O$ at one atmosphere total pressure and at the temperature of reaction, the equilibrium constant simplifies to

$$(K_a)_{T,p=1} = a^2_{H_2O}$$

It follows that the dehydration of gypsum to anhydrite, at atmospheric pressure, is a function of temperature and activity of H_2O only. Therefore, provided the solids do not change in composition, the equilibrium is independent of the components in the co-existing solution.

The activity of H_2O of the solutions co-existing with gypsum or anhydrite was varied by adding Na_2SO_4 or H_2SO_4: these were chosen because the gypsum$\rightleftharpoons$anhydrite conversion rates were found to be relatively rapid in sodium sulfate or sulfuric acid solutions. In the system $CaSO_4$-Na_2SO_4-H_2O neither gypsum nor anhydrite can co-exist with a solution of Na_2SO_4 concentration greater than that fixed by the one atmosphere isothermally invariant assemblage gypsum (or anhydrite)+glauberite ($CaSO_4 \cdot Na_2SO_4$)+solution+vapor. The a_{H_2O} of the invariant solutions varies from about 0.90 at 25°C to about 0.96 at 70°C. This limits the

study to very dilute solutions only, a considerable disadvantage because many natural calcium sulfate deposits must have formed in brines with activities of H_2O at least as low as 0.75, as defined by the assemblage gypsum (or anhydrite)+halite+solution+vapor in the "haplo-evaporite" (Zen, 1965, p. 125) system $CaSO_4$-NaCl-H_2O. In the system $CaSO_4$-H_2SO_4-H_2O, however, the stability fields of gypsum and anhydrite are not limited by double-salt formation. Thus, the reaction may be studied in H_2SO_4 solutions which have a range of activity of H_2O comparable to that found in natural waters, that is, from near 1.00 to about 0.70.

Experimental Methods

Starting Materials. The solid starting materials were artificial $CaSO_4 \cdot 2H_2O$, $CaSO_4$ (anhydrous) and Na_2SO_4 (anhydrous) of reagent grade.

The $CaSO_4 \cdot 2H_2O$ (Baker Analyzed, Lots No. 25692 and 25286) was fine-grained but variable-sized material (0.1 mm to less than 0.01 mm), which showed the characteristic morphology of gypsum euhedra. The X-ray diffraction pattern was indistinguishable from that of natural gypsum, and the material was used as such with no further treatment. The $CaSO_4$ (Baker Analyzed anhydrous [*sic*] Lot No. 90128) yielded an X-ray pattern consistent with bassanite $CaSO_4 \cdot nH_2O$ ($n \leq 0.5$). When this material was heated at 450°C to 550°C for 2 to 5 days, a very fine-grained powder was produced which gave an excellent anhydrite X-ray pattern. In the experimental runs with anhydrite as a starting material, the heat-treated $CaSO_4$ was used. Zen (1965, p. 151) found that artificial anhydrite, prepared by dehydrating gypsum overnight at 300°C, readily reverted to gypsum when brought into contact with water; he therefore considered such anhydrite unsuitable as a starting material. In the present investigation no such rehydration of artificial anhydrite occurred—even in stirred runs of 6 months duration—under conditions where anhydrite was considered to be stable. Critical experiments however, were repeated using natural gypsum and/or anhydrite. The gypsum was large clear selenite plates from Montmartre, Paris, and the anhydrite was massive fine-grained material from Richmond Co., Nova Scotia (Williams Collection, The Johns Hopkins University).

The Na_2SO_4 (Baker Analyzed, anhydrous, Lots No. 25581 and 22088) gave a sharp thenardite X-ray pattern and was used without further refinement.

The sulfuric acid solutions were prepared by diluting Baker Analyzed 95 percent H_2SO_4 with double-distilled water to the required concentrations. The exact concentration in weight percent H_2SO_4 was then deter-

mined by titration of carefully weighed aliquots of each solution against 1N NaOH solution (CO_2 free) using methyl orange as an indicator (Welcher, 1962, p. 540). The results were checked against the H_2SO_4 concentration determined by specific gravity measurements, using the calibration curve of Hodgman (1953, p. 1894).

Experimental procedure

(a) Static Method. At the start of the study a technique similar to that used in hydrothermal work was employed. Finely ground mixtures of anhydrite, or gypsum, and thenardite were accurately weighed, with the required amount of distilled water, into pyrex glass tubes (7×60 mm) which were then sealed using an oxy-acetylene torch. Loss of distilled water was successfully avoided during the sealing process by wrapping the tubes in wet filter paper. The sealed tubes were then totally immersed in thermostatically controlled water-baths. At the end of the run periods, which varied from several days to many months, the tubes were broken open and the solid products separated from the solution on absorbent paper. Samples were immediately examined, both under the microscope and by X-ray diffraction. Although by this technique many runs can be carried out simultaneously, it has the obvious disadvantage that the solution volumes are too small for analysis. Unfortunately, the method proved to have an even greater disadvantage; in many runs equilibrium was not attained even after periods of many months. When it was apparent that some form of agitation was required to promote the reactions, the static method was abandoned. However, it was possible to salvage enough significant information to warrant discussion and comparison with the results of runs carried out with the dynamic method (continuous stirring of the charge), which was used through the rest of the study.

(b) Dynamic Method. Approximately 200g of starting materials were weighed (±0.1%) into a 250-ml Erlenmeyer flask, fitted with a mercury-in-glass air-tight seal through which the solution was stirred sufficiently to keep all the solid material in constant agitation. The charged reaction vessels were immersed in water baths of capacity 30 liters, thermostatically controlled to ±0.1°C.

A maximum variation of ±0.5°C was observed over a period of six months.

At intervals, one milliliter of the suspension-charged solution was withdrawn with a pipette and rapidly pressure-filtered through a Buchner funnel: this removed almost all the solution. The solid material was immediately washed several times with acetone and air-dried. A portion of the sample was examined under the petrographic microscope; the re-

mainder was hand-ground under acetone and a smear mount prepared for x-ray diffraction.

Determinations of activity of H_2O in solutions. The activity of any constituent of a solution is given by the ratio of the fugacities:

$$a_i = f_i/f_i^0$$

At one atmosphere total pressure, water vapor may be regarded as an ideal gas so that the fugacities may be safely replaced by the partial pressures of H_2O:

$$a_{H_2O} = p_{H_2O}/p^0_{H_2O}$$

The standard state is taken as pure liquid water, at one atmosphere pressure and at the temperature of reaction, for which the activity is unity.

The solubilities of gypsum and anhydrite in sodium sulfate and sulfuric acid solutions are very low (less than 0.25 percent by weight). Therefore, the vapor pressures of these solutions saturated with $CaSO_4$ are given, within experimental measurement, by the vapor pressures of the *$CaSO_4$-free* solutions.

For the sodium sulfate solutions the vapor pressure data given in International Critical Tables (III, p. 371) were used to calculate a_{H_2O}. The a_{H_2O} of each solution was computed at the temperature of each experiment. At the end of a run the total dissolved solids content of the equilibrium solution was determined. This value was compared with the starting Na_2SO_4 content to provide a check on the assigned a_{H_2O} value. The activities of H_2O of the sulfuric acid solutions were taken from Harned and Owen (1958, p. 574). These data, reproduced in Table 1, show that within the range of H_2SO_4 concentration used in the study, a_{H_2O} values determined by EMF measurements are in excellent agreement with those calculated from vapor pressure measurements. The initial gypsum and (or) anhydrite constituted only about 3 percent of the total charge. Consequently the H_2SO_4 concentration of the solution, and hence the activity of H_2O, was not significantly changed by the H_2O released or absorbed by the gypsum-anhydrite conversion. The H_2SO_4 content of the solution was checked by titration at the completion of each run.

The a_{H_2O} of the final solution in each of two runs (one in H_2SO_4 and one in Na_2SO_4) was measured directly using an H_2O-sensing apparatus (Hardie, 1965a, p. 252); the values did not differ measurably from the activities of H_2O determined in the $CaSO_4$-free solutions.

TABLE 1. ACTIVITY OF H_2O IN AQUEOUS SULFURIC ACID SOLUTIONS
(After Harned and Owen, 1958, p. 574)

Moles H_2SO_4/1000 moles H_2O	Wt. % H_2SO_4	25°C		40°C	60°C
		emf	v.p.	emf	emf
1	8.93	0.9620	0.9620	0.9624	0.9630
1.5	12.82	0.9391	0.9389	0.9402	0.9415
2	16.40	0.9136	0.9129	0.9155	0.9180
3	22.73	0.8506	0.8514	0.8548	0.8602
4	28.18	0.7775	0.7795	0.7850	0.7950
5	32.90	0.6980	0.7030	0.7086	0.7229
6	37.05	0.6200	0.6252	0.6288	0.6505
7	40.71	0.5453	0.5497	0.5608	0.5815

DESCRIPTION AND PROPERTIES OF THE SOLID PHASES

The gypsum synthesized by hydration of anhydrite (hereinafter referred to as "synthetic gypsum") commonly consists of thin plates flattened parallel to (010), with the characteristic monoclinic outline (Fig. 1). Between crossed nicols the thin plates show first-order white or grey interference colors and oblique extinction. In runs where gypsum was converted to anhydrite, the first stage of the process was recrystallization of the fine-grained artificial gypsum used as a starting material to coarser bladed crystals. This recrystallized gypsum, seemingly of a more

FIG. 1. Photomicrograph of synthetic gypsum, prepared from anhydrite at 40°C and 1 atmosphere in 22% H_2SO_4 solution, with seeding, in 50 days (Run LS 23). Average length of crystals 0.2 to 0.3 mm.

stable habit than the original smaller crystals, was morphologically and optically indistinguishable from the synthetic gypsum.

The optical properties of the synthetic gypsum were not significantly different from those of the natural material.

Wooster (1936) has determined the crystal structure of gypsum. In the *ac* plane two sheets of SO_4 tetrahedra are bound by Ca atoms within them. Between these sheets lie layers of water molecules. The Ca atoms are linked to 6 oxygens of SO_4 tetrahedra and to 2 water molecules. Water molecules thus occupy important structural positions and even partial dehydration must result in the destruction of the gypsum structure.

Unit cell parameters of the synthetic gypsum were determined by X-ray powder diffraction methods with either silicon or quartz as internal standard, and found to be in excellent agreement with those given by Deer *et al.* (1962) for natural gypsum.

Anhydrite synthesized from gypsum appeared under the microscope as a mass of minute birefringent grains; individual crystal outlines were barely distinguishable under high power, and refractive index measurements were unreliable.

The presence of synthetic anhydrite could be readily detected in the reaction flask by inspection: a fine white mass stayed in suspension long after the stirrer was stopped. In contrast, the well-crystallized synthetic and seed gypsum settled very rapidly, leaving, in the absence of anhydrite, a remarkably clear solution.

In one run (LS 51, Table 2), anhydrite grains as large as 0.3 mm across were synthesized from gypsum in 22 percent sulfuric acid solution at 50°C. They showed a stubby prismatic to equant shape with very high interference colors and parallel extinction.

The cell parameters of synthetic anhydrite were in excellent agreement with those given by Swanson *et al.* (1955).

Bassanite ($CaSO_4 \cdot nH_2O$, $n \leq 0.5$) was encountered only in static runs in which NaCl had been added to the charges. It was identified by X-ray diffraction techniques only, using the data of Posnjak (1938, p. 253). No distinction was made between calcium sulfate hemidydrate ($CaSO_4 \cdot 1/2H_2O$) and soluble anhydrite ($CaSO_4$) because there is considerable uncertainty as to the relationship between these two phases (Deer, Howie and Zussman, 1962, v. 5, pp. 207–208).

Experimental Results

Results of dynamic runs. The data used to define the position of the a_{H_2O}-temperature equilibrium curve for the reaction

$$\text{gypsum} = \text{anhydrite} + 2H_2O_{(\text{liquid, in solution})}$$

are given in Table 2 and plotted in Figure 2.

Determination of the curve rested on the ability to convert gypsum to anhydrite, and *vice versa*, and on the ability to reverse the conversion when either one of the parameters was varied.

A run in which no change occurred in the starting phase, even after a reaction time of many months, was not considered evidence of stability of that phase, although in many cases such data provided confirmation of reversed runs. Taken by itself, a run in which no reaction occurs is at best inconclusive since metastable persistence of starting phases is commonly encountered in experimental studies of mineral equilibria. In the present study this was particularly true of the rehydration of anhydrite in sulfuric acid solutions, and induced nucleation by seeding proved necessary. Anhydrite remained unchanged in most unseeded runs for up to eight months; the addition of seeds of gypsum promoted relatively rapid conversion of the anhydrite (compare runs LS 5 and LS 14 at 35°C, Table 2). In the system $CaSO_4$-H_2O, the dehydration of gypsum to anhydrite has been shown to be incredibly slow (*e.g.* run AG 1, 70°C, Table 2) but, according to Posnjak (1938, p. 262) seeds of anhydrite do initiate the reaction.[1] Considerable doubt has been thrown on the determination of stability by experiments in which seeds have been added to the charge because metastable growth of a phase from solution on seeds of its own kind is known to occur (Fyfe *et al.*, 1958, p. 83). However, it has never been demonstrated that seeding would promote the disappearance of a stable phase and growth of a less stable one. In the present study, charges containing equal parts by weight of gypsum and anhydrite were used. The proof of stability in these seeded runs was growth of one phase and disappearance of the other. When the extent of reaction exceeded about 7 to 10 percent, metastable precipitation of either phase on seeds could be ruled out. This follows from a consideration of the solubilities of gypsum and anhydrite in Na_2SO_4 and H_2SO_4 solutions (maximum about 0.3 percent $CaSO_4$ by weight), the mass of solution in the reaction vessel (about 200–250 g) and the mass of excess starting solids (about 10 g). The extent of reaction was gauged by microscope and X-ray examination of a series of samples taken from the reaction vessel at intervals. From the X-ray diffraction patterns, the relative intensities of the 020 peak of anhydrite (3.499 Å) and the 140 peak of gypsum (3.065 Å) were measured. The amount of gypsum in each sample was read from a calibration

[1] This was not substantiated in the present work, perhaps because the runs were not of sufficient duration. However, it was found that the presence of lime-water ($a_{H_2O}=1.00$, pH=12.4), with no seeding, markedly increased the dehydration rate where a seeded run in distilled H_2O showed no reaction (compare AG 1 and AG 5, 70°C, Table 2).

TABLE 2. EXPERIMENTAL DATA FOR GYPSUM AND ANHYDRITE STABILITY AS A FUNCTION OF ACTIVITY OF H_2O AND TEMPERATURE AT ATMOSPHERIC PRESSURE. RESULTS OF DYNAMIC RUNS ONLY

Run no.	Starting materials: Solid phases	Starting materials: Solution (wt. %) Na_2SO_4	Starting materials: Solution (wt. %) H_2SO_4	a_{H_2O} sol'n	Temp. °C	Time days	Solid products	Result
AG1	95g, 5a	100% H_2O		1.000	70°	359	95g, 5a	n.c.
AG5	100g	limewater		1.000	70°	193	93g, 7a	g→a
LX9	100g	12.3		0.965	70°	6	100g	
						19	42g, 58a	
						46	5g, 95a	
						147	100a	g→a
LX22	g, gl	12.3		0.965	70°	26	100a	g→a
LX25	100g	18.9		0.942	70°	9	gl, a	g→a
LS30-2	90g, 10a*		9.43	0.961	60°	43	45g, 55a	g→a
LX49-2	100g	15.0		0.955	60°	46	94g, 6a	g→a
LS20	50g, 50a		4.03	0.985	55°	42	94g, 6a	a→g
LS22	50g, 50a		9.43	0.961	55°	51	100g	a→g
LS30-1	50g, 50a*		9.43	0.961	55°	51	90g, 10a	a→g
LS8	100g		9.56	0.960	55°	35	55g, 45a	g→a
LX49-1	100g	15.0		0.954	55°	50	100g	n.c.
LX46-1	a, gl	19.3		0.941	55°	99	a, gl	n.c.
LS52	100g		22.24	0.866	55°	99	100a	g→a
LS21	50g, 50a		4.03	0.985	52.5°	42	95g, 5a	a→g
LS18	50g, 50a		9.56	0.960	52.5°	35	95g, 5a	a→g
AG3	95g, 5a	100% H_2O		1.000	50°	278	95g, 5a	n.c.
LS1	100g		9.56	0.960	50°	262	100g	n.c.
LS16	50g, 50a		9.56	0.960	50°	25	95g, 5a	a→g
LX17	100g	15.0		0.953	50°	155	100a	n.c.
LX11	100g	15.0		0.953	50°	47	100g	
						94	95g, 5a	
						319	95g, 5a	g→a(?)
LX48	a, gl	20.6		0.930	50°	23	a, gl, (g)	a→g(?)
LS51	100g		22.24	0.863	50°	211	50g, 50a	g→a
LS32-2	80g, 20a*		22.24	0.863	50°	111	60g, 40a	g→a
LS2	100g		9.56	0.959	45°	148	100g	n.c.
LS7	100a		9.56	0.959	45°	127	100a	n.c.
LS15	50g, 50a		9.56	0.959	45°	138	100g	a→g
LX15	100g	15.0		0.952	45°	156	100g	n.c.
LX16	100a	15.0		0.952	45°	156	70g, 30a	a→g
LS50	100g		22.24	0.862	45°	211	93g, 7a	g→a
LS4-2	100g		23.60	0.846	45°	62	65g, 35a	g→a
AG4	95g, 5a	100% H_2O		1.000	40°	277	100g	a→g
LS9	50g, 50a		9.56	0.959	40°	55	100g	a→g
LX12	100a	15.0		0.951	40°	255	93g, 7a	a→g
LX18	100g	21.0		0.926	40°	88	100g	n.c.
LX19	100g	22.2		0.922	40°	88	100g	n.c.
LS23	50g, 50a		22.24	0.860	40°	50	95g, 5a	a→g
LS33-1	50g, 50a*		22.24	0.860	40°	49	75g, 25a	a→g

g—gypsum
a—anhydrite
gl—glauberite
th—thenardite
mr—mirabilite
n.c.—no detectable change
*—natural gypsum and anhydrite
( )—trace

TABLE 2—(*Continued*)

Run no.	Starting materials: Solid phases	Solution (wt.%): Na_2SO_4	Solution (wt.%): H_2SO_4	a_{H_2O} sol'n	Temp. °C	Time days	Solid products	Result
LS3-1	100g		23.60	0.845	40°	23	100g	n.c.
LS3-2	100g		23.60	0.845	40°	40	20g, 80a	g→a
LS19	50g, 50a		23.60	0.844	37.5°	35	95g, 5a	a→g
LS32-1	50g, 50a*		22.24	0.859	35°	51	80g, 20a	a→g
LS4-1	100g		23.60	0.843	35°	21	100g	n.c.
LS5	100a		23.60	0.843	35°	232	100a	n.c.
LS14	50g, 50a		23.60	0.843	35°	83	94g, 6a	a→g
LX40	g, th	24.5		0.907	30°	195	g, gl	n.c.
LS4-3	50g, 50a		23.60	0.842	30°	56	100g	a→g
LS6	100a		23.60	0.842	30°	197	100a	n.c.
LS11	100g		28.61	0.773	30°	67	90g, 10a	g→a
LY5	100a	14.3		0.952	25°	189	80g, 20a	a→g
LY6	100a	15.8		0.948	25°	189	80g, 20a	a→g
LS10	50g, 50a		23.60	0.840	25°	55	100g	a→g
LS12	100g		28.61	0.771	25°	67	40g, 60a	g→a
LS17	50g, 50a		28.61	0.771	25°	69	20g, 80a	g→a
LY1	100a	16.1		0.943	20°	28	g, mr	a→g
LG2-1	100a	16.1		0.943	20°	1	a, g, mr	a→g
LS13	100a		28.61	0.768	20°	67	45g, 55a	a→g

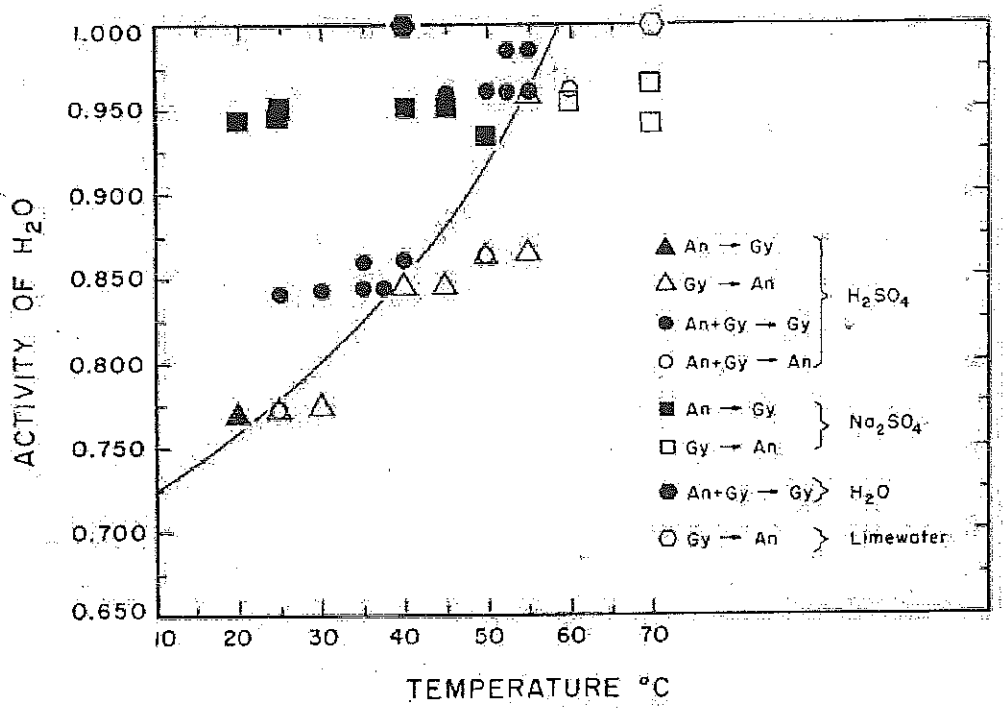

FIG. 2. The stability of gypsum and anhydrite determined experimentally as a function of temperature and activity of H_2O at atmospheric pressure. Only runs in which a conversion was achieved are plotted.

curve of I(anhydrite)/I(gypsum) against weight percent gypsum with a reproducibility of better than 2 percent.

Because of the time limit, most of the runs were stopped before complete conversion of one phase to the other had occurred. Those runs which were allowed to react completely provided material for optical and X-ray studies.

Figure 2 shows that the experimental data, in general, are consistent. However, some exceptions must be noted. At 50°C, in 15 percent sodium sulfate solution ($a_{H_2O}=0.953$), anhydrite started growing at the expense of gypsum after about 90 days reaction time (run LX 11, Table 2).

TABLE 3. ACTIVITY OF H_2O AND TEMPERATURE THAT DEFINE THE EQUILIBRIUM GYPSUM = ANHYDRITE + 2 $H_2O_{liq.\ soln.}$ AT ATMOSPHERIC PRESSURE

Temperature °C(±2°)	a_{H_2O} (±0.005)	Remarks
58°	1.000	extrapolated
55°	0.960	measured
50°	0.915	interpolated
45°	0.880	interpolated
39°	0.845	measured
35°	0.825	interpolated
30°	0.800	interpolated
23°	0.770	measured
18°	0.750	extrapolated
12°	0.725	extrapolated

However, the reaction apparently stopped (!) as no further growth of anhydrite occurred in 10 months. Under the same conditions, anhydrite as a starting phase remained unaltered after 5 months (run LX 17). With sulfuric acid of about the same activity of H_2O, anhydrite was converted to gypsum at 50°C in a seeded run within a month (run LS 16), while gypsum was unchanged in an unseeded run of 9 months (run LS 1). The anomaly remains unexplained. An inconsistent result was also obtained at 55°C and $a_{H_2O}=0.96$. In an unseeded run, gypsum was converted to anhydrite in sulfuric acid solution (run LS 8, about 50 percent reaction); in seeded runs both synthetic and natural anhydrite were transformed into gypsum (runs LS 22 and LS 30-1). These results are taken to indicate that the runs are very close to the equilibrium curve.

With the exception of run LX 11, then, the results obtained using sulfuric acid solutions are perfectly consistent with those obtained using sodium sulfate solutions.

The a_{H_2O}-T values which define the equilibrium curve are given in Table 3.

Results of static runs. The results of experiments on the gypsum-anhydrite reaction carried out under static conditions are not included in Figure 2 or Table 2 because the method was soon abandoned in favor of agitated runs. A discussion of the data, however, is warranted. All the static runs were made with sufficient Na_2SO_4 to produce glauberite ($CaSO_4 \cdot Na_2SO_4$) as an additional phase. Synthetic anhydrite was the starting solid, although in a few runs natural anhydrite or synthetic gypsum were used instead. Seeds were not added to any of the charges. Reaction times varied from a few days to over 12 months. The results were most unexpected: anhydrite was found to rehydrate to gypsum at temperatures as high as 75°C. The reverse reaction, the dehydration of gypsum to anhydrite, was never achieved. Several possible explanations come to mind. First, the properties of the synthetic anhydrous $CaSO_4$ may be different from those of natural anhydrite. However, the results of the dynamic runs indicate that the differences, if any, are not significant. Another possibility is solid solution between gypsum and sodium sulfate. Unfortunately, this could not be checked by chemical analysis due to separation difficulties. However, no significant change in cell dimensions of the gypsum was observed, which suggests little or no substitution of Na^+ for Ca^{++} in the gypsum structure. Indeed, a direct substitution is impossible since it would create a charge imbalance. The substitution of Na^+ for Ca^{++} perhaps could be achieved if accompanied by an HSO_4^- for $SO_4^=$ substitution. Chemical analyses of natural gypsum and anhydrite (Stewart, 1963, p. 33; Deer, Howie and Zussman, 1962, p. 206 and p. 221) show no evidence of this: sodium only occurs in trace amounts, if at all.

A third possibility is related to the experimental method. In the preparation of the charges, water was added to a solid mix of anhydrite +thernardite. Local high concentrations of sodium sulfate solution certainly existed, and probably persisted, in the initial stages of the runs. Conley and Bundy (1958) and Hardie (1965, p. 126) have shown that anhydrite reacts very rapidly with concentrated Na_2SO_4 solutions to form Ca-Na double sulfates. These double-salts are unstable in dilute Na_2SO_4 solutions (Hardie, 1965, p. 136; Hill and Wills, 1938, p. 1652) and decompose to gypsum and/or glauberite. In distilled water they immediately decompose to gypsum+Na_2SO_4 solution at all temperatures up to 100°C. It is possible, therefore, that in the static runs early formation of double-salts occurred in the regions of local high Na_2SO_4 concentration. This reaction removed anhydrite from the system. With time, diffusion led to a uniformly concentrated solution too low in Na_2SO_4 content for double-salt stability. Decomposition followed, giving gypsum+glauberite as products. Then, with prolonged time the gypsum should convert

to anhydrite. This is a plausible explanation because in all runs (static or stirred) in which the starting anhydrite was added to pre-mixed, uniformly concentrated sodium sulfate solution, no anomalous formation of gypsum was observed.

The work of Conley and Bundy (1958) is pertinent here since they proposed essentially this mechanism for the conversion of anhydrite to gypsum in salt solutions. They suggested that the reaction for the conversion with activator solutions such as sodium or potassium sulfate is:

$$CaSO_4 \xrightarrow[H_2O]{act.} Ca^{++} + SO_4^{=} \xrightarrow{H_2O} CaSO_4 \cdot 2H_2O$$

and is primarily dependent upon temperature and concentration. However, they achieved the conversion only by washing the reaction products with water. This in fact really only demonstrates that anhydrite will react rapidly at low temperatures and high alkali sulfate concentrations (see Conley and Bundy, 1958, Figs. 1 and 2) to form double-salts which decompose in water to give gypsum and salt solution. It certainly does not prove, as they maintained in the abstract of their paper (p. 57), that "contrary to recent hypothesis of gypsum dehydration by concentrated salt solutions, double salts and/or gypsum are stable phases below a temperature of 42°C."

Comments on the mechanism of dehydration of gypsum to anhydrite. Three different mechanisms by which gypsum in contact with an aqueous medium could dehydrate to anhydrite appear possible:

(1) a solution-precipitation process.
(2) direct dehydration to anhydrite (loss of structural water).
(3) step-wise dehydration through the intermediate hydrate, bassanite.

The present experimental results throw some light, albeit very diffuse, on the problem.

In a few of the runs in which anhydrite was produced from gypsum, a rind, presumed from X rays to be anhydrite, was observed on the surface of, and along cleavage cracks in, gypsum crystals (Fig. 3). It is conceivable that the rind material is bassanite, formed as an intermediate dehydration product, but no trace of this phase was identified in the charges by X rays even though perhaps as many as 10 to 15 percent of the gypsum grains showed some alteration. If the rind is anhydrite, the process would appear one of direct dehydration to anhydrite beginning at the crystal surfaces where H_2O may be transferred to the solution phase. The effect of seeding on the dehydration rate could not be gauged with any certainty because too few duplicate runs were made. However, in

those runs which were strictly comparable (*e.g.* LS 17 and LS 12 at 25°C; LS 51 and LS 32-2 at 50°C, Table 2), no significant rate increase, which would have suggested a solution-precipitation mechanism, was observed. In this respect the results of Zen's (1965) precipitation experiments loom large: direct precipitation of anhydrite from super-saturated solutions could not be achieved at temperatures up to 70°C, even with seeding. Similar attempts by the present author also failed. Gypsum

FIG. 3. Photomicrograph of a dark rind of anhydrite (?) on a prismatic grain of gypsum (colorless). Note incipient development of rind material in cleavage crack of large, colorless (recrystallized) gypsum plate. Data: Run LS 51, gypsum stirred in 22% H_2SO_4 solution at 50°C and 1 atm for 211 days. About 50% conversion to anhydrite at end of run. No reaction was observed until 146 days. Magnification about 250×.

always precipitated under conditions where anhydrite was presumed stable. This inability to precipitate anhydrite must remain the most telling evidence against a solution-precipitation mechanism for the dehydration of gypsum to anhydrite in aqueous media. On the other hand, the reverse reaction, the hydration of anhydrite, may well be accomplished through a solution-precipitation process because the hydration rate is measurably increased (in sulfuric acid solutions, at least) by the addition of seeds (compare runs LS 7 and LS 15 at 45°C; LS 5 and LS 14 at 35°C; LS 6 and LS 4-3 at 30°C: Table 2).

Ostroff (1964) observed the formation of calcium sulfate hemihydrate as an intermediate step during the conversion of gypsum to anhydrite in sodium-magnesium chloride solutions at 90.5°C. That this is not the

invariable mechanism is proved by the present experiments: bassanite was not formed in any of the sodium sulfate or sulfuric acid runs. With NaCl solutions, however, bassanite rather than anhydrite was the dehydration product of gypsum (Hardie, 1965, Table 30, p. 185). Zen (1965) also found bassanite instead of anhydrite in concentrated NaCl solutions. Apparently sodium chloride solutions promote a step-wise dehydration process. The picture remains unclear and an exhaustive study of the kinetics of the reaction using more sensitive methods is obviously needed.

Comparison of the Results with Previous Work

Extrapolation of the measurements of the present study to solutions in the system $CaSO_4$-H_2O ($a_{H_2O}=1.00$) gives a transition temperature of $58°\pm2°C$, slightly lower than that of van't Hoff *et al.* (1903) but significantly higher than the oft-quoted temperature of $42°\pm2°C$ given by Posnjak (1938) from solubility measurements. This discrepancy was puzzling, at first, because the solubility data seemed well supported by the thermodynamic data of Kelley *et al.* (1941), who calculated an equilibrium temperature of 40°C. Zen (1962), however, pointed out that these calculations employed internally inconsistent data. Recalculation put the transition temperature at $46°\pm21°C$, and Zen considered the agreement with the solubility measurements as fortuitous, a conclusion supported by the present calculations (Appendix). Indeed, re-examination of the solubility data indicates that the value of 42°C is by no means securely established. In Figure 4 are compiled all the available solubility measurements on gypsum and anhydrite in the system $CaSO_4$-H_2O; in large part the older data were taken from the tables of D'Ans (1933, pp. 203–205). If curves are drawn to enclose the maximum density of each set of points, a transition temperature of anywhere between 38° and 50° is indicated (see shaded area in Fig. 4). An uncertainty may well be real, since, as Zen (1965, p. 126) pointed out, all the available measurements were made by approaching the equilibrium solubility curves from the side of undersaturation only. This is, of course, a serious drawback in any solubility study but is particularly crucial in the case of poorly soluble substances. For example, Backström (1921) measured the solubility of calcite and aragonite by approaching the equilibrium curves from both sides: he found that after a few days the rate of change of the solubility had reached zero but that the supersaturation and undersaturation values differed by as much as 5 percent. Alexander *et al.* (1954) and Krauskopf (1956) obtained similar results for amorphous silica: even greater deviations were the case here. There is no guarantee, then, that the equilibrium saturation value of either gypsum or anhydrite had been reached in any except Zen's (1965) gypsum determinations. The available

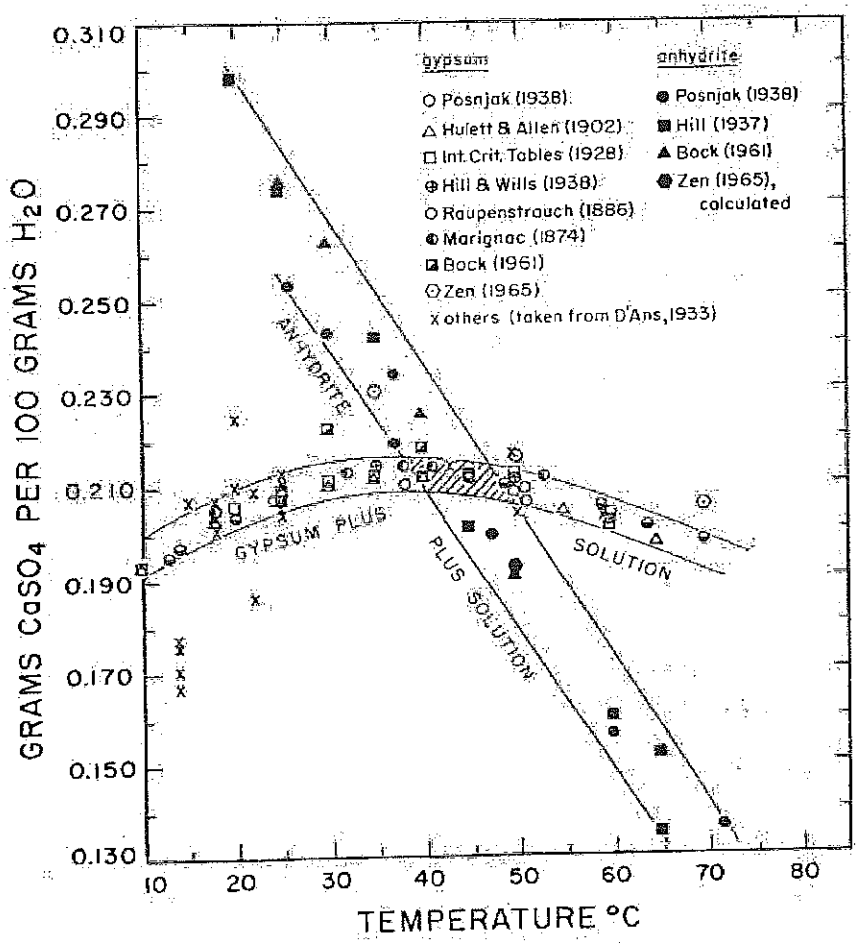

FIG. 4. The solubility relations of gypsum and anhydrite in the system $CaSO_4$-H_2O as a function of temperature at atmospheric pressure: a compilation of previous work.

solubility data therefore must be regarded as yielding minimum values only. The argument is crucial, for if the points plotted in Figure 4 for anhydrite are indeed minimum values then the transition point must lie at some temperature above at least 44°C, Zen's (1965) data being taken as the upper limit of gypsum solubility. Hill (1934, 1937) did recognize the necessity for approaching a solubility curve from both sides, and, indeed, reported his anhydrite values as obtained from both undersaturated and supersaturated solutions. The data, however, were extrapolated from solubilities measured in potassium sulfate solutions because he was unable to achieve supersaturation with respect to anhydrite using pure water at temperatures below 65°C. At this and higher temperatures he apparently was successful, but, unfortunately, he neither described the procedure nor reported direct precipitation of anhydrite from solution.

A similar criticism applies to the available gypsum and anhydrite solubility measurements made in salt or acid solutions, and probably explains why the results of different workers are in such poor agreement. Comparison of the results of these workers is most easily made by computing the activity of H_2O of the solutions reported to be in equilibrium with gypsum+anhydrite. Because the $CaSO_4$ content of these solutions

TABLE 4. THE EFFECT OF SALT SOLUTIONS ON THE GYPSUM—ANHYDRITE TRANSITION: A COMPARISON OF PREVIOUS WORK

Investigator	Trans. temp. °C	Co-existing solution	a_{H_2O}
van't Hoff *et al.* (1903)	50°	sat'd. $NaBrO_3$	0.900
Hill & Wills (1938)	45°[1]	20.0 % Na_2CO_4	.932
Bock (1961)	40°	5.88% NaCl	.965
Taperova & Shulgina (1945)	40°[1,2]	31.0 % H_3PO_4	.885
Bock (1961)	35°	11.85% NaCl	.920
Zen (1965)	35°	15.25% NaCl	.891
D'Ans *et al.* (1955)	34°	6.09% NaCl	.963
Bock (1961)	30°	16.09% NaCl	.883
Posnjak (1940)	30°	13.06% NaCl 1.82% $MgCl_2$ 0.82% $MgSO_4$ 0.43% K_2SO_4	.89
van't Hoff *et al.* (1903)	30°	sat'd. NaCl	.754
D'Ans *et al.* (1955)	28.5°	11.49% NaCl	.922
Bock (1961)	25°	20.08% NaCl	.840
Madgin & Swales (1956)	25°	18.02% NaCl	.864
D'Ans & Hofer (1937)	25°	45.36% H_3PO_4	.790
Taperova (1940)	25°[1,2]	40.0 % H_3PO_4	.845
D'Ans *et al.* (1955)	24°	16.33% NaCl	.881
D'Ans *et al.* (1955)	20.5°	20.6 % NaCl	.835
D'Ans *et al.* (1955)	18°	26.31% NaCl	.751

[1] Extrapolated by the present author.

[2] The results of these two studies were taken from Seidell (1958, pp. 665–667).

is very low, activity of H_2O may be obtained with considerable accuracy from the water vapor pressures of the $CaSO_4$-free salt or acid solutions. The vapor pressure data for the NaCl and Na_2SO_4 equilibrium solutions were taken from the International Critical Tables (1928, III, pp. 370–371) and those of sea water from Arons and Kientzler (1954). For the phosphoric acid solutions the vapor pressure values of Kablukov and Zagwosdkin (1935) were used. The results are summarized in Table 4 and shown graphically in Figure 5.

The values of van't Hoff *et al* (1903) alone are higher than those of the

present study. The approach of van't Hoff and his co-workers to the problem was brilliantly conceived. They first partially converted gypsum to anhydrite in saturated sodium chloride solution in a dilatometer at 70°C. The rate of conversion of gypsum to anhydrite and *vice versa* at different temperatures was then measured by the rate of change of volume of the contents of the dilatometer. At the equilibrium temperature there should be no volume change. They observed a volume decrease at 25°C and an increase at 35°C, so the transition temperature was taken as 30°C. The partial pressure of H_2O of the solution co-existing with

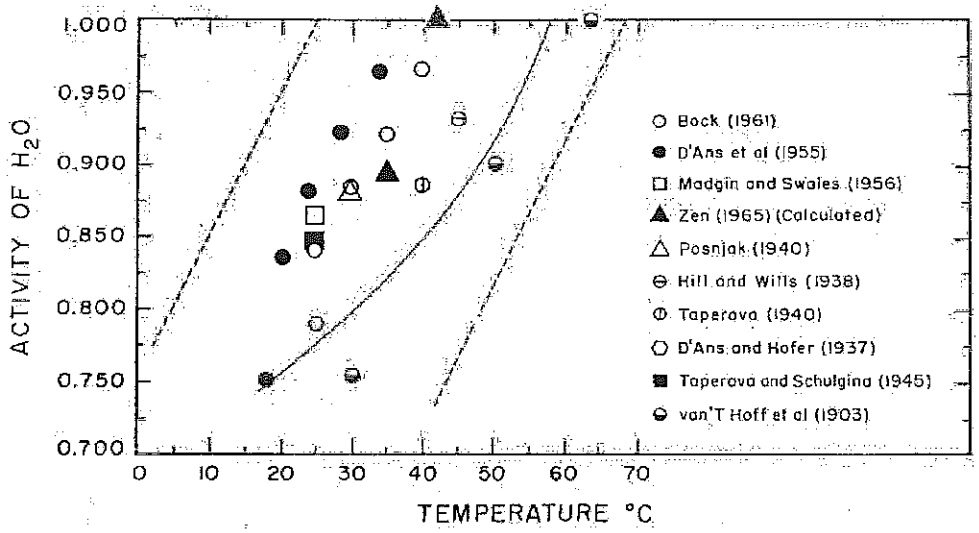

FIG. 5. Temperature-activity of H_2O relations of gypsum and anhydrite at atmospheric pressure; a comparison of previous work. Solid curve: this study; dashed curves: maximum and minimum limits predicted by thermodynamic calculations.

gypsum, anhydrite and halite at 30°C was then measured, giving a value of 24 mm. The method was repeated using saturated sodium bromate solution and a transition temperature of 50°C was obtained; the water vapor pressure of the equilibrium solution was measured as 83.3 mm. Using these two points in the relationship

$$\log p = \log p^\circ + A - B/T$$

they were able to extrapolate to solutions in the system $CaSO_4$-H_2O. Implicit in this approach is the principle that the gypsum-anhydrite transition is independent of the constituents in solution and that the equilibrium temperature is a function of the ratio p/p°. This is, of course, the principle on which the present study is based!

Figure 5 also shows that although the results of different workers are in very poor agreement, they all fall within the limits predicted by the thermodynamic calculations (Appendix)!

Geological Implications

It has been suggested by some workers that most, if not all, calcium sulfate of natural evaporites was originally deposited as gypsum (Posnjak, 1940; Bundy, 1956; Conley and Bundy, 1958; Murray, 1964; Zen, 1965). The agrument is based on (1) petrographic observations that much anhydrite is pseudomorphous after twinned gypsum, (2) the scarcity of anhydrite in modern evaporites deposits, and (3) experimental evidence that anhydrite cannot be synthesized under pressure-temperature conditions consistent with natural evaporite environments.

It is clear that the present relationship between gypsum and anhydrite in the pre-Recent marine evaporites of the world, to a great extent, is secondary, due to the effects of post-depositional burial. Gypsum at surface may be traced downward into anhydrite so that at depths below about 2000–3000 feet gypsum is practically absent (MacDonald, 1953; Stewart, 1963). Evidence of replacement is abundant. Anhydrite psuedomorphous after twinned gypsum has been reported by Schaller and Henderson (1932) in the Salado formation of Texas and New Mexico, by Stewart (1953) in the Permian evaporites of Yorkshire, England, and by Borchert and Baier (1953) in the German Zechstein. At shallower depths gypsum has been shown to have replaced anhydrite (Stewart, 1953; Goldman, 1952; Ogniben, 1955; Sund, 1959); such replacement has been recorded recently at a depth as great as 3500 feet (Murray, 1964). Therefore, both gypsum and anhydrite in sedimentary deposits may be metamorphic but this evidence does not prove that the replaced gypsum, or anhydrite, was primary in origin, a point emphasized by Zen (1965, p. 147).

More significant evidence is provided by the distribution of gypsum and anhydrite in Recent marine and nonmarine evaporites where effects due to burial are not involved. In these deposits gypsum is ubiquitous and, in all certainty, primary (Bramkamp and Powers, 1955; Morris and Dickey, 1957; Masson, 1955; Phleger and Ewing, 1962; Wells, 1962; and others) whereas anhydrite has been reported from only one locality, in supratidal flat sediments on the Trucial Coast, Persian Gulf (Curtis *et al*, 1963; Kinsman, 1964).[1] This single occurrence of Recent sedimentary

[1] Other occurrences of Recent anhydrite have been reported recently by Hunt *et al.* (1966, p. 59) as a surface layer in Death Valley, California, and by Moiola and Glover (1965) from a sediment dump on Clayton Playa, Nevada. In both cases the anhydrite has formed from gypsum, via bassanite, in the absence of a liquid phase. This dehydration process

$$CaSO_4 \cdot 2H_2O \rightleftharpoons CaSO_4 \cdot \tfrac{1}{2}H_2O + 1\tfrac{1}{2}H_2O\ (g)$$
$$CaSO_4 \cdot \tfrac{1}{2}H_2O \rightleftharpoons CaSO_4 + \tfrac{1}{2}H_2O\ (g)$$

involves a set of thermochemical conditions very different from those encountered in "wet" evaporite deposits.

anhydrite is of great import because, if not evidence of primary precipitation of anhydrite, it is, at least, proof that metamorphism of gypsum on burial is not *essential* to anhydrite formation. Even accepting that anhydrite can be primary, an inconsistency between the field evidence from modern evaporites and available experimental evidence exists. Temperature-salinity conditions necessary for anhydrite stability, as predicted from solubility experiments and thermodynamic calculations, are commonly found in modern evaporite environments, yet gypsum is the common phase of such deposits. This observation, coupled with the inability of experimenters to synthesize anhydrite at low temperatures, has led workers such as Murray (1964) to conclude that gypsum is always the primary precipitate. Further, under conditions theoretically favoring anhydrite, this gypsum will persist metastably (except where temperatures at surface are very high) until burial causes dehydration to anhydrite.

The present experimental results have a two-fold bearing on the problem. First, it is demonstrated that anhydrite can be synthesized at one atmosphere pressure under geologically reasonable conditions of temperature and activity of H_2O in a geologically reasonable time, reckoned in months. Primary precipitation of anhydrite, however, could not be achieved, indeed, has not been achieved by previous workers. This would suggest, but, of course, not prove, that gypsum is always the first formed $CaSO_4$ phase on evaporation of natural waters.[1] Be that as it may, the experiments do show that gypsum, maintained in the stability field of anhydrite, would be dehydrated to anhydrite soon after deposition. Second, it is demonstrated that higher temperatures than previously were entertained are required for anhydrite formation. This, qualitatively, is more in keeping with the observation that gypsum is the common phase in Recent evaporites.

Quantitative application of the experimental results to natural deposits is valid and possible but is hindered by the paucity of precise information on the temperature and a_{H_2O} of natural solutions co-existing with gypsum and anhydrite. Fortunately, the Persian Gulf deposit is an important exception. Quantitative data have been collected by D. J. J. Kinsman (personal communication, 1964). Brine temperatures range from 24° to 39°C and anhydrite is found in carbonate muds of the *sabkha*, or supratidal salt flat, where ground water chlorinities exceed about 130°/$_{oo}$ (about 24 percent salinity). Part of the anhydrite deposit

[1] It is possible, of course, that natural waters differ from experimentally tested solutions in that they contain additional components which would induce direct precipitation of anhydrite, as, for example, trace elements ("impurities") have been found to influence the nucleation of aragonite and calcite (Wray and Daniels, 1957).

TABLE 5. DATA ON SOLUTIONS CO-EXISTING WITH GYPSUM OR ANHYDRITE IN NATURAL EVAPORITE DEPOSITS

Locality	Mineral Assemblage	Solution			Investigator
		T°C	Chlorinity °/₀₀	a_{H_2O}	
	gypsum	27–34°	50–110	0.95–0.85	Bramkamp & Powers (1955)
Trucial Coast, Persian Gulf	gypsum, carbonate	24°	64 91 96	0.93 .88 .87	D. J. J. Kinsman (written communication, 1964)
	anhydrite, carbonate	to 39°	134[1] 152[1] 159 166	.80 .77 .75 .73	
Boccana de Virrila, Peru	gypsum	27°[2]	108[2]	.85	Morris & Dickey (1957)
Saline Valley, Calif.	gypsum	9–39°	16–30	0.99–0.95	Hardie (1965)
Salina fm., Mich. (Silurian)	anhydrite, halite[3]	32–48°	satd. NaCl	≤0.75	Dellwig (1955)

[1] Anhydrite in the zone of capillary draw. Chlorinities as given are for the underlying groundwaters. Actual solutions in which anhydrite formed presumably were more concentrated.

[2] Precise location in Boccana where gypsum is precipitating is difficult to read from Morris and Dickey's descriptions. Value given here is taken from their data for location C, which may be incorrectly interpreted by the present author as the gypsum site.

[3] Delicately preserved "hopper" crystals which have clearly not suffered alteration since their formation. The same argument must apply to the intimately associated anhydrite. Temperatures of formation of the hopper halite was determined by fluid inclusion studies.

occurs in the zone of capillary draw above the present water table but, more important, anhydrite is found in direct contact with brine (Table 5). Where ground waters are less concentrated (up to about 96°/₀₀ chlorinity) gypsum is precipitated within the carbonate muds. These data, together with the limited information from a few other deposits, are summarized in Table 5. To compare these data, chlorinity values

have been recalculated to activities of H_2O using the vapor pressure data for seawater of different chlorinities given by Arons and Kientzler (1954). The natural brine data and the equilibrium curve determined in the present study are plotted in Figure 6. Included in this figure is a gypsum-anhydrite transition curve computed from the solubility measurements of Bock (1961) in the haplo-evaporite system $CaSO_4$-NaCl-H_2O. His results are considered representative of the stability range for gypsum and anhydrite predicted by most existing solubility studies (see Fig. 5). If the natural deposits are to be interpreted in terms of this transition curve, then it is clear from Figure 6 that metastable persistence of gypsum in natural brines is the rule. On the other hand, the equilibrium curve of the present study is remarkably compatible quantatively with the data from the natural deposits, particularly that of the Persian Gulf (Fig. 6). This would strongly suggest that chemical equilibrium prevails in each of these deposits. Taken one step further, this could mean that the scarcity of anhydrite in modern evaporite deposits is simply a reflection that the conditions for its formation are seldom reached, or, at least, maintained for any length of time. Metastable persistence of gypsum would not be a necessity.

While this is most plausible it is surely an oversimplification because gypsum is found under nonequilibrium conditions in some modern evaporitic environments. For example, in Laguna Ojo de Liebre, Baja California, gypsum co-exists with halite at temperatures up to 27°C (Phleger and Ewing, 1962) whereas the present experimental data predict that in a seawater brine saturated with halite ($a_{H_2O} \leq 0.75$) gypsum should dehydrate to anhydrite at temperatures above about 18°C (see Fig. 2).

The questions this discussion raises are intriguing. Does the Persian Gulf, where anhydrite is forming, combine a freakish set of chemical and/or physical circumstances not found in other modern evaporite environments? Or, are the conditions under which gypsum is found in Baja California (and perhaps other areas) not maintained for long enough periods of time each year to produce anhydrite? It is clear that the problem is one of kinetics which must, therefore, become a most important consideration in interpreting gypsum-anhydrite deposits, modern or ancient.

Summary

1. The present results show that anhydrite can be synthesized experimentally from gypsum under p, t and a_{H_2O} conditions reasonable for natural evaporite environments.

2. The gypsum-anhydrite equilibrium temperatures determined in the

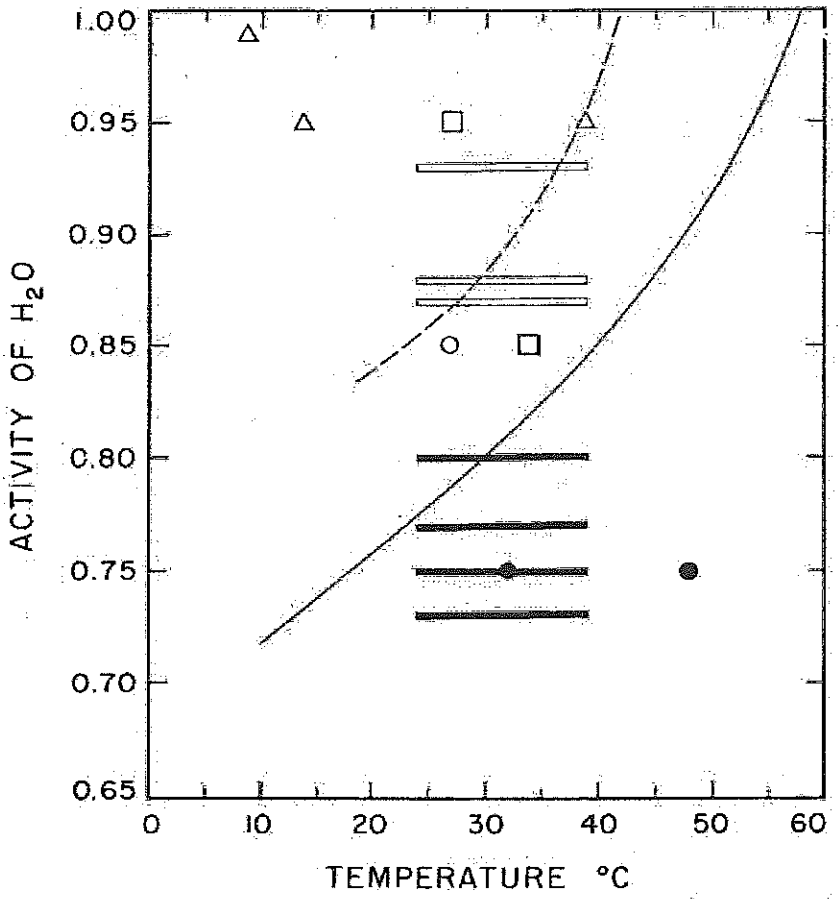

FIG. 6. Temperature-activity of H_2O relations of brines co-existing with gypsum and anhydrite in natural evaporite deposits. Experimentally determined equilibrium relations are shown as curves: *solid curve:* this study; *dashed curve:* solubility data of Bock (1961). The open symbols represent solutions in contact with gypsum and the solid symbols are those in contact with anhydrite.

Open circle:	Morris & Dickey (1957)
Squares:	Bramkamp & Powers (1955)
Triangles:	Hardie (1965)
Solid circles:	Dellwig (1955)
Bars:	Kinsman (pers. comm., 1964)

present study are considerably higher than those based on solubility measurements and on thermodynamic calculations. The new data are considered more reliable than the existing data because (a) the present results are based on reversible reactions whereas in available solubility studies the saturation curves for gypsum and anhydrite were approached only from the side of undersaturation and, therefore, do not necessarily represent equilibrium curves; (b) significant uncertainties exist in the available thermochemical values for gypsum and anhydrite.

3. The new equilibrium values of this study are more compatible with the field observations that gypsum is the common phase, and anhydrite rare, in unmetamorphosed evaporite deposits. Further, these values are quantitatively consistent with the a_{H_2O}-T conditions under which gypsum and anhydrite are found in the Recent evaporite deposit of the Trucial Coast, Persian Gulf.

Acknowledgments

Professor Hans P. Eugster suggested the project, guided the research and critically reviewed the manuscript. To him, I am deeply indebted. The manuscript was also reviewed by Owen P. Bricker, James L. Munoz and George B. Skippen and their comments led to a considerable improvement in the manuscript. Mr. Arthur Everhart designed and built the relays used to control the water-bath units. A special tribute must be paid to the late Thomas Banks (The Johns Hopkins University and Harvard University) for helpful discussions and stimulation during the latter part of the study.

The research was supported, in part, by Grant 680-A from the Petroleum Research Fund to The Johns Hopkins University.

Appendix. Thermodynamic Considerations

Calculation of the gypsum-anhydrite transition temperature in the system $CaSO_4$-H_2O at one atmosphere pressure. Kelley, Southard and Anderson (1941) measured the thermochemical properties of the solid phases of the system $CaSO_4$-H_2O (Table 6).

For the reaction

$$CaSO_4 \cdot 2H_2O = CaSO_4 + 2H_2O_{(l)}$$

Kelley *et al.* (1941, p. 44) obtained

$$\Delta G^\circ_T = -2495 - 65.17\,T \log T + 0.0215\,T^2 + 163.89\,T \qquad (1)$$

This equation gives 313°K (40°C) as the temperature at which gypsum, anhydrite and liquid water are in equilibrium at one atmosphere total pressure, in surprisingly good agreement with the value of 42°C derived from solubility data (Hill, 1937; Posnjak, 1938).

Zen (1962; 1965) has pointed out that equation (1) was obtained from inconsistent data. The present calculations confirm Zen's criticism. Differentiation of equation (1) with respect to temperature, $-d\Delta G^\circ/dT = \Delta S^\circ$, yields

$$\Delta S^\circ_T = -135.59 + 65.17 \log T - 0.043\,T \qquad (2)$$

and a value of 12.85 cal/deg for 298°K. This is inconsistent with the sum of the individual entropies at 298°K as given by Kelley *et al.* (see Table 6), that is,

$$\Delta S^\circ_{298} = 25.5 + (2 \times 16.8) - 46.4 = 12.7 \text{ cal/deg}$$

The discrepancy arises from the use of an integration constant of −33.18 which is the mean of their own consistent value of −33.03 and the value of −33.34 obtained from the indirect vapor pressures of Toriumi and Hara (1934). The resulting small error in entropy has a con-

TABLE 6. THERMOCHEMICAL PROPERTIES OF THE PHASES OF THE SYSTEM $CaSO_4$-H_2O

Phase	C_p, cal/deg mole (298°–450°K)	$S°$ (298°K) cal/deg mole	Reference[1]
$CaSO_4 \cdot 2H_2O$ gypsum	$21.84+0.076T$	46.4 ± 0.4	I (p. 36 & p. 19)
$CaSO_4$ anhydrite	$14.10+0.033T$ $16.78+0.0236T$	25.5 ± 0.4	I (p. 36 & p. 19) III (p. 46)
H_2O (liquid) water	18.02 18.04	16.8 16.75 ± 0.03	I (p. 36) II (p. 105) III (p. 80)
H_2O (gas) water	$7.45+0.002T$ $7.30+0.00246T$	45.13 45.13 ± 0.03	I (p. 36) II (p. 105) III (p. 80)

[1] I = Kelley *et al.* (1941)
II = Kelley (1950)
III = Kelley (1960)

siderable effect on the free energy values since it is incorporated into the aT term of equation (1).

Recalculation of the entropy for the reaction using the accepted value of $S°_{298}=16.75$ cal/deg-mole for liquid water (Giauque and Stout, 1936; Kelley, 1960) yields $\Delta S°_{298}=25.5+(2\times16.75)-46.4=12.6$ cal/deg.

Hence, equation (2) becomes

$$\Delta S°_T = -135.84 + 65.17 \log T - 0.043\, T \tag{3}$$

Using (Kelley *et al*, 1941, p. 44),

$$\Delta H°_T = -2495 + 28.30\, T - 0.0215\, T^2 \tag{4}$$

the free energy expression becomes

$$\Delta G°_T = -2495 + 164.14\, T - 65.17\, T \log T + 0.0215\, T^2 \tag{5}$$

This equation gives 319°K (46°C) as the gypsum-anhydrite equilibrium temperature, an increase of 6°C over the value obtained from the expression of Kelley *et al* (1941) (Equation (1)).

The free energy expression can be further modified by employing the revised heat capacity of anhydrite given by Kelley (1960, p. 46). The following relationships for the reaction are then obtained:

$$C_p = 31.02 - 0.0524\, T$$

and

$$\Delta H°_T = \Delta H°_0 + 31.02\, T - 0.0262\, T^2 \tag{6}$$

Substituting the mean value, $\Delta H^\circ_{298}=4030$ cal[1] (Kelley *et al* 1941), of the heat of solution measurements in equation (7):

$$\Delta H^\circ_0 = -2890 \text{ cals}$$

so that

$$\Delta H^\circ_T = -2890 + 31.02\,T - 0.0262\,T^2 \qquad (7)$$

Using

$$\Delta S^\circ_{298} = 25.5 + (2 \times 16.75) - 46.4 = 12.6 \text{ cal/deg. in}$$

$$\Delta S^\circ_T = \Delta S^\circ_0 + 31.02 \ln T - 0.0524\,T$$

we obtain

$$\Delta S^\circ_T = -148.55 + 31.02 \ln T - 0.0524\,T \qquad (8)$$

From equations (7) and (8) it follows that

$$\Delta G^\circ_T = -2890 + 179.57\,T + 0.0262\,T^2 - 71.44\,T \log T \qquad (9)$$

This equation gives T(equil.)=46°C, demonstrating that the equilibrium temperature is insensitive to small variations in the heat capacity of anhydrite.

If the uncertainties of measurement assigned to each one of the thermodynamic values (Table 6) used in the derivation of equation (9) are assembled, then the confidence to be placed in this equation can be assessed. From the maximum and minimum possible values of each property, except the heat capacity, we obtain two limiting free energy equations:

$$\Delta G^\circ_T = -2870 + 180.43\,T + 0.0262\,T^2 - 71.44\,T \log T \qquad (10)$$

and

$$\Delta G^\circ_T = -2910 + 178.71\,T + 0.0262\,T^2 - 71.44\,T \log T \qquad (11)$$

Equation (10), designed to give a maximum temperature, was derived using $\Delta H^\circ_{298}=4030+20=4050$ cal and $\Delta S^\circ_{298}=25.1+(2\times16.72)-46.8=11.74$ cal/deg. The equivalent values for equation (11), which gives a minimum temperature, are $\Delta H^\circ_{298}=4030-20=4010$ cal and $\Delta S^\circ_{298}=25.9+(2\times16.78)-46.0=13.46$ cal/deg.

The equilibrium temperatures given by equations (10) and (11) are 68°C and 25°C respectively. It is clear that the available thermochemical data can fix the gypsum-anhydrite transition point at no better than 46±22°C!

Calculation of the effect of dissolved salts on the gypsum-anhydrite transition temperature at atmospheric pressure. For the conversion of gypsum to anhydrite in the presence of any aqueous solution containing dissolved salts, the reaction may be written

$$CaSO_4 \cdot 2H_2O = CaSO_4 + 2H_2O_{(\text{liq; soln.})}$$

A simplified equilibrium constant for this reaction can be applied if the compositions of the solid phases remain unchanged (pure liquid H_2O and the pure solids at 1 atmosphere being taken as the standard states):

$$(K_a)_{p=1,T} = a^2_{H_2O}$$

[1] Kelley *et al* (1941, p. 15) give ±20 cals. as the uncertainty in this value.

Now, for any chemical reaction

$$\Delta G_T = \Delta G^\circ_T + RT \ln K_a$$

Therefore, for the dehydration of gypsum to anhydrite

$$\Delta G_T = \Delta G^\circ_T + 2RT \ln a_{H_2O} \tag{12}$$

It follows from this equation that a lowering of the activity of H_2O of the solution (e.g., by increasing the salinity) would decrease the free energy of reaction. The effect would be to lower the dehydration temperature. To evaluate this quantitatively it is necessary to know ΔG°_T (reaction) and the a_{H_2O} of the solutions in which the reaction occurs.

An expression for ΔG°_T (reaction) as a function of temperature has been derived (equation 9 above):

$$\Delta G^\circ_T = -2890 + 179.57\,T + 0.0262\,T^2 - 71.44\,T \log T \tag{9}$$

Therefore, the change in equilibrium temperature with change in a_{H_2O} of the co-existing solution can be determined from

$$\Delta G_T = -2890 + 179.57\,T + 0.0262\,T^2 - 71.44\,T \log T + 2RT \ln a_{H_2O} \tag{13}$$

An expression similar to (13) but based on the free energy equation of Kelley *et al* (1941) (equation 1), was derived by MacDonald (1953, p. 889) using a slightly different thermodynamic treatment:

$$\Delta G_T = -2495 + 163.89\,T + 0.0215\,T^2 - 65.17\,T \log T + 2\,RT\,2.303 \log p/p^\circ \tag{14}$$

From this, MacDonald determined the transition temperature as a function of concentration of sodium chloride.

Kelley *et al* (1941, Fig. 8, p. 41) also had considered the effect of activity of H_2O on the gypsum-anhydrite transition temperature. They presented the results in diagrammatic form only and did not give the equation used in the calculation. This, however, is most certain to be the equation given by MacDonald, who used their data and produced exactly equivalent results.

Equation (13) gives 20°C and equation (14) 15°C for the transition temperature in the presence of halite in the system $CaSO_4-NaCl-H_2O$ ($a_{H_2O}=0.75$). The uncertainties in these temperatures will remain in the order of ±22°C, the uncertainty range for the solution of equation (9).

References

Alexander, G. B., W. M. Heston and H. K. Idler (1954) The solubility of amorphous silica in water. *J. Phys. Chem.* 58, 453–455.

Ans, J.D' (1933) *Die Lösungsgleichgewichte der Systeme der Salze ozeanischer Salzablagerungen.* Kaliforschungsanstalt, Berlin.

——— D. Bredtscheider, H. Eick and H. E. Freund (1955) Untersuchungen über die Calciumsulfate. *Kali Steinsalz*, no. 9, 17–38.

——— and P. Höfer (1937) Über das System $CaSO_4$-H_3PO_4-H_2O. *Angew. Chem.* 50, 101–104.

Arons, A. B. and C. F. Kientzler (1954) Vapor pressure of sea-salt solutions. *Trans. Amer. Geophys. Union* 35, 722–728.

Bäckström, H. L. J. (1921) Über die Affinität der Aragonit—Calcit—Umwandlung. *Z. Phys. Chem.* 97, 179–228.

Bock, E. (1961) On the solubility of anhydrous calcium sulphate and of gypsum in concen-

trated solutions of sodium chloride at 25°C, 30°C, 40°C, and 50°C. *Can. Jour. Chem.* **39**, 1746–1751.

BORCHERT, H. AND E. BAIER (1953) Zur Metamorphose ozeaner Gipsablagerungen. *Neues. Jahrb. Mineral. Abh.* **86**, 103–154.

BRAMKAMP, R. A. AND R. W. POWERS (1955) Two Persian Gulf lagoons (abstract). *J. Sediment. Petrol.* **25**, 139–140.

BUNDY, W. M. (1956) Petrology of gypsum-anhydrite deposits in southwestern Indiana. *J. Sediment. Petrol.* **26**, 240–252.

CONLEY, R. F. AND W. M. BUNDY (1958) Mechanism of gypsification. *Geochim. Cosmochim. Acta* **15**, 57–72.

CURTIS, R., G. EVANS, D. J. J. KINSMAN AND D. J. SHEARMAN (1963) Association of dolomite and anhydrite in Recent sediments of the Persian Gulf. *Nature*, **197**, 679–680.

DEER, W. A., R. A. HOWIE AND J. ZUSSMAN (1962) *Rock-Forming Minerals*. v. 5. John Wiley and Sons, New York. 371 p.

DELLWIG, L. F. (1955) Origin of the Salina salt of Michigan. *J. Sediment. Petrol.* **25**, 83–110.

FYFE, W. S., F. J. TURNER AND J. VERHOOGEN (1958) Metamorphic reactions and metamorphic facies. *Geol. Soc. Amer. Mem.* **73**, 259 p.

GIAUQUE, W. F. AND J. W. STOUT (1936) The entropy of water and the Third Law of Thermodynamics. The heat capacity of ice from 15° to 273°K. *J. Amer. Chem. Soc.* **58**, 1144–1150.

GOLDMAN, M. I. (1952) Deformation, metamorphism, and mineralization in gypsum-anhydrite cap-rock, Sulphur Salt Dome, Louisiana. *Geol. Soc. Amer. Mem.* **50**, 169 p.

HARDIE, L. A. (1965) Phase equilibria involving minerals of the system $CaSO_4$-Na_2SO_4-H_2O. Ph.D. Thesis, The Johns Hopkins University, Baltimore, Maryland.

HARNED, H. S. AND B. B. OWEN (1958) The physical chemistry of electrolytic solutions, 3rd ed. Reinhold Publishing Co., New York. 803 p.

HILL, A. E. (1934) Ternary systems, XIX. Calcium sulfate, potassium sulfate and water. *J. Amer. Chem. Soc.* **56**, 1071.

——— (1937) The transition temperature of gypsum to anhydrite. *J. Amer. Chem. Soc.* **59**, 2242–2244.

——— AND WILLS, J. H. (1938) Ternary Systems XXIV. Calcium Sulfate, Sodium Sulfate and Water. *J. Amer. Chem. Soc.* **60**, 1647–1655.

HODGMAN, C. D. (1953) *Handbook of Chemistry and Physics*. 35th Edition. Chemical Rubber Publishing Co., Cleveland. 3163 p.

HOFF, J. H. VAN'T, E. F. ARMSTRONG, W. HINRICHSEN, F. WEIGERT AND G. JUST (1903) Gips und Anhydrit. *Z. Phys. Chem.* **45**, 257–306.

HULETT, G. A. AND L. E. ALLEN (1902) The solubility of gypsum. *J. Amer. Chem. Soc.* **24**, 667–679.

HUNT, C. B., T. W. ROBINSON, W. A. BOWLES AND A. L. WASHBURN (1966) Hydrologic basin Death Valley California. *U.S. Geol. Surv. Prof. Pap.* **494-B**, 138 p.

International Critical Tables (1928) v. III and IV. McGraw-Hill Book Co., New York.

KABLUKOV, I. A. AND K. I. ZAGWOSDKIN (1935) Dampfspannungen der Phosphorsäurelösungen. *Z. Anorg. Chem.* **224**, 815–820.

KELLEY, K. K. (1950) Contributions to the data on theoretical metallurgy. XI. Entropies of inorganic substances. Revision (1948) of data and methods of calculation. *U.S. Bur. Mines Bull.* **477**.

——— (1960) Contributions to the data on theoretical metallurgy, XIII. High-temperature heat-content, heat capacity, and entropy data for the elements and inorganic compounds. *U.S. Bur. Mines Bull.* **584**.

——— J. C. Southard and C. T. Anderson (1941) Thermodynamic properties of gypsum and its dehydration products. *U.S. Bur. Mines Tech. Pap.* 625.

Kinsman, D. J. J. (1965) Dolomitization and evaporite development, including anhydrite in lagoonal sediments, Persian Gulf. (abstract). *Geol. Soc. Amer. Spec. Pap.* 82, 108–109.

Krauskopf, K. B. (1956) Dissolution and precipitation of silica at low temperatures. *Geochim. Cosmochim. Acta*, 10, 1–26.

MacDonald, G. J. F. (1953) Anhydrite-gypsum equilibrium relations. *Amer. J. Sci.* 251, 884–898.

Madgin, W. M. and D. A. Swales (1956) Solubilities in the system $CaSO_4$-NaCl-H_2O at 25° and 35°. *J. Appl. Chem.* 6, 482–487.

Marignac, C. (1874) Sur la solubilite du sulfate de chaux. *Ann. Chim. phys.*, 1, 274–282.

Marsal, Dietrich (1952) Der Einfluss des Druckes auf das System $CaSO_4$-H_2O. *Heidelberger Beit. Mineral Petrol.* 3, 289–296.

Masson, P. H. (1955) An occurrence of gypsum in Southwest Texas. *J. Sediment. Petrol.* 25, 72–79.

Moiola, R. J. and E. D. Glover (1965) Recent anhydrite from Clayton Playa, Nevada. *Amer. Mineral.* 50, 2063–2069.

Morris, R. C. and P. A. Dickey (1951) Modern evaporite deposition in Peru. *Amer. Ass. Petrol. Geol. Bull.* 41, 2467–2474.

Murray, R. C. (1964) Origin and diagenesis of gypsum and anhydrite. *J. Sediment. Petrol.* 34, 512–523.

Ogniben, L. (1955) Inverse graded bedding in primary gypsum of chemical deposition. *J. Sediment. Petrol.* 25, 273–281.

Ostroff, A. G. (1964) Conversion of gypsum to anhydrite in aqueous salt solutions. *Geochim. Cosmochim. Acta.* 28, 1363–1372.

Partridge, E. P. and A. H. White (1929) The solubility of calcium sulfate from 0° to 200°C. *J. Amer. Chem. Soc.* 51, 360–370.

Phleger, F. B. and G. C. Ewing (1962) Sedimentology and oceanography of coastal lagoons in Baja California, Mexico. *Geol. Soc. Amer. Bull.* 73, 145–182.

Posnjak, Eugen (1938) The system $CaSO_4$-H_2O. *Amer. J. Sci.* 35A, 247–272.

Posnjak, Eugen (1940) Deposition of calcium sulfate from sea water. *Amer. J. Sci.* 238, 559–568.

Raupenstrauch, G. C. (1886) Über die Bestimmung der Löslichkeit einiger Salze in Wasser bei verschiedenen Temperaturen. *Sitzungsber. Akad. Wiss. Wien* 92II, 463–491.

Schaller, W. T. and E. P. Henderson (1932) Mineralogy of drill cores from the potash field of New Mexico and Texas. *U.S. Geol Surv. Bull.* 833, p. 124.

Seidell, A. (1958) *Solubilities. Inorganic and Metal-organic Compounds.* v. 1, 4th ed. by W. F. Linke, van Nostrand Co., Princeton, 1487 p.

Stewart, F. H. (1953) Early gypsum in the Permian evaporites of North-eastern England. *Proc. Engl. Geol. Ass.* 64, 33–39.

Stewart, F. H. (1963) Marine evaporites. Chap. Y *in* M. Fleischer, (ed.) *Data of Geochemistry.* 6th ed. *U.S. Geol. Surv. Prof. Pap.* 440-Y, p. 52.

Sund, J. O. (1959) Origin of the New Brunswick gypsum deposits. *Can. Mining Met. Bull.* 52, 707–712.

Swanson, H. E., R. K. Fuyat and G. M. Ugrinnic (1955) Standard X-ray diffraction powder patterns. *Nat. Bur. Stand. (U.S.) Circ.* 539, 4, 67.

Toriumi, T. and R. Hara (1934) On the transition of calcium sulfate in water and in concentrated sea water. *J. Chem. Soc. Japan* 55, 1051–1059 (in Japanese).

——— T. KUWAHARA AND R. HARA (1938) On the calcium sulfate in sea water II. Solubilities of calcium sulphate hemihydrate in sea water of various concentrations at 65°–150°. *Technol. Rep. Tohoku Imp. Univ.* **12**, 560–571.

WELCHER, F. J. (1962) *Standard methods of chemical analysis*, vol. 2, part A, 6th ed. Van Nostrand Co., Princeton, 1282 p.

WELLS, A. J. (1962) Recent dolomite in the Persian Gulf. *Nature*, **194**, 274–275.

WINCHELL, A. N. (1933) *Elements of Optical Mineralogy. Part II. Descriptions of Minerals*, 3rd ed. John Wiley and Sons, New York.

WOOSTER, W. A. (1936) On the crystal structure of gypsum, $CaSO_4 \cdot 2H_2O$. *Z. Kristallogr.* **94**, 375.

WRAY, J. L. AND F. DANIELS (1957) Precipitation of calcite and aragonite. *J. Amer. Chem. Soc.* **79**, 2031–2034.

ZEN, E-AN (1962) Phase-equilibrium studies of the system $CaSO_4$-NaCl-H_2O at low temperatures and 1 atmosphere pressure (abstr.). *Geol. Soc. Amer. Spec. Pap.* **68**, 306.

——— (1965) Solubility measurements in the system $CaSO_4$-NaCl-H_2O at 35°, 50° and 70° and one atmosphere pressure. *J. Petrol.* **6**, 124–164.

Manuscript received, March 19, 1966; accepted for publication, August 19, 1966.

Attachment B-12

JOURNAL OF SEDIMENTARY PETROLOGY, VOL. 34, NO. 3, PP. 512–523
FIGS. 1–11, SEPTEMBER, 1964

ORIGIN AND DIAGENESIS OF GYPSUM AND ANHYDRITE[1]

R. C. MURRAY[2]

ABSTRACT

Despite data on the stability of anhydrite at high earth surface temperatures, the observation of Recent gypsum and the evidence for formation and preservation of metastable gypsum suggest that this form may be the common if not universal original calcium sulfate mineral. Gypsum beds can be produced by two mechanisms: (1) Precipitation and sedimentation in a standing body of water subjected to evaporation. Such deposits are original sedimentary facies, contemporaneous with other sedimentary facies. (2) Growth of abundant crystals by displacement of unconsolidated sediment or weathered rocks, which results in beds of gypsum which later is replaced by nodular anhydrite. These nodular anhydrite beds represent a diagenetic facies and postdate the host material. The distinction between sedimented and nodular is important in the interpretation of any given evaporite deposit.

These primary deposits act as a source of calcium sulfate for subsurface growth of replacement and void-filling anhydrite. The latter two secondary types of anhydrite can be distinguished in reflected light, since a dark color is imparted to replacement anhydrite by included material.

From observations in Recent sediments, older outcrops, and the subsurface, there appears to be a characteristic cycle in the diagenesis of gypsum-anhydrite minerals: surface or near-surface gypsum is replaced by anhydrite as a result of burial and is in turn replaced by gypsum if the anhydrite is thereafter brought close to the surface.

ORIGIN OF PRIMARY DEPOSITS

Sedimentary deposits of the calcium sulfate minerals (gypsum and anhydrite) are common throughout much of the geologic record. They are commonly associated with carbonate rocks, especially dolomite and ferruginous clastics. The object of this paper is to examine the evidence regarding which mineralogic form is the primary depositional product and to trace the diagenetic changes that accompany burial and re-exposure of these deposits. This has been the subject of much discussion in the literature with many authors favoring anhydrite as the original form.

Physical Evidence

In general, gypsum is found near the surface and in Recent sediments, whereas anhydrite is the common form of the subsurface. Indeed, it is not uncommon in large gypsum quarries to encounter interbedded anhydrite and gypsum followed by isolated gypsum patches and finally pure anhydrite with depth. Many authors, for example, Sund (1959), argue convincingly for the replacement of anhydrite by gypsum under near-surface conditions. The evidence for this replacement may be observed in all deep quarries and shallow cores where some anhydrite is still preserved. Although the transition commonly takes place within a few hundred feet of the present surface, the replacement of anhydrite by gypsum has been observed as deep as 3500 feet in the Permian San Andres Formation, Dune field, Crane County, Texas (fig. 1).

Bundy (1956) suggested that the gypsum may be the predominant or only form of calcium sulfate precipitated from sea water. Such a generalization is naturally at variance with interpretations of a primary origin of anhydrite. However, studies of Recent evaporite deposits—for examples, Fisk (1959), Morris and Dickey (1957), Phleger and Ewing (1962), Masson (1955), Talmage and Wootton (1937), and Wells (1962)—have emphasized the observations that gypsum is the common if not universal form present. It has generally been impossible to determine the specific composition and temperature of the solution at the time the gypsum was precipitated. However, gypsum is forming today in some of the hottest parts of the surface of the earth.[3] Recently, Curtis and others (1963) have reported Recent anhydrite above the free water level in the supratidal flats along the Trucial Coast of the Persian Gulf.

Stewart (1953) observed pseudomorphs of anhydrite after gypsum in the Permian evaporites of northeastern England. These pseudomorphs could only be seen when weathered sur-

[1] Manuscript received July 22, 1963.

[2] Shell Development Company (A Division of Shell Oil Company), Exploration and Production Research Division, Houston, Texas (Publication No. 354).

[3] Professor F. H. Stewart has correctly reminded the author that the argument of near universal Recent gypsum may not be applicable to deep water evaporites of the past which do not have Recent analogues. However, MacDonald (1953) suggests that increasing hydrostatic pressure favors gypsum.

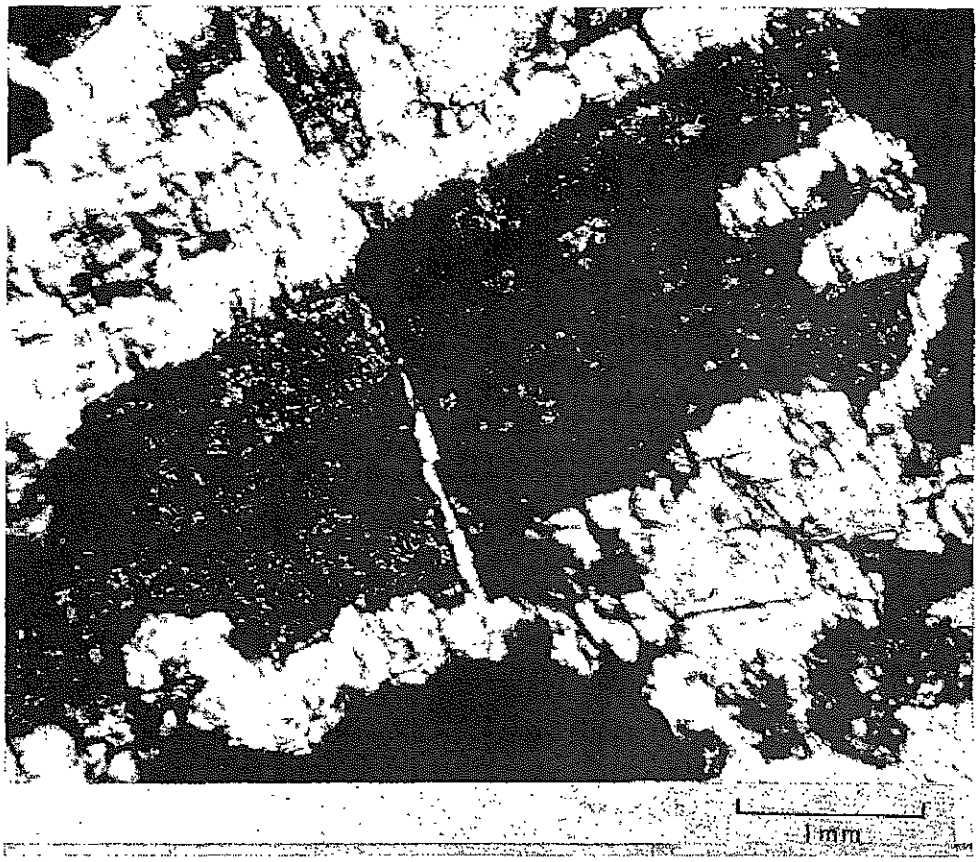

FIG. 1.—Gypsum replacing replacement anhydrite; San Anydres Formation, 3500 feet below the present surface. Gypsum (white) rims and indents a core of subhedral anhydrite. The anhydrite had originally replaced fine sucrose dolomite.

faces of the core were studied. Some of the original crystal outlines were flattened, and in extreme cases the structures were barely detectable. This direct type of observation has seldom been made in massive evaporite beds. The reason must, in part, be ascribed to imperfection of preservation. However, this example is primafacie evidence of the metagypsum origin of these anhydrite beds.

These general observations suggest the generalization that a common diagenetic cycle exists in the calcium sulfate minerals—deposition of gypsum followed, during burial, by replacement of gypsum by anhydrite followed in turn, during uplift and erosion of overlying strata, by replacement of anhydrite by gypsum (fig. 2). Henderson (1954) argued that gypsum in the Stanford Range has never been buried to sufficient depth for replacement of gypsum by anhydrite. If his interpretation based on delicate preservation of textures is correct, these ancient deposits have never passed through the complete cycle.

Chemical Evidence

The physical-chemical environment that favors primary precipitation of gypsum or anhydrite or replacement of one mineral by the other has received much study since the early work of Van't Hoff in the early 1900's. Posnjak (1938) produced data on the stability of gypsum and anhydrite as a function of temperature. These data were obtained only by dissolution. The intersection of the solubility curves for the two minerals defines a temperature above which anhydrite is less soluble than gypsum and thus presumably more stable. The temperature of intersection for distilled water was 42°C; thus, anhydrite should be favored above this temperature. From his earlier work Posnjak recognized that solubility determinations in different concentrations of sea salt solutions could be helpful in interpreting the conditions of deposition of the two minerals from concentrated sea water. He made solubility determinations in solutions of sea salts at 30°C (Posnjak, 1940) and showed that an increase in salt concentration would lower the temperature of equal solubility. He concluded that sedimentary marine deposits of pure anhydrite either must have been partly derived from originally deposited gypsum or must have been formed near or above 42°C. However, from stability considerations some anhydrite could have been formed below 42°C.

During his experiments Posnjak observed that

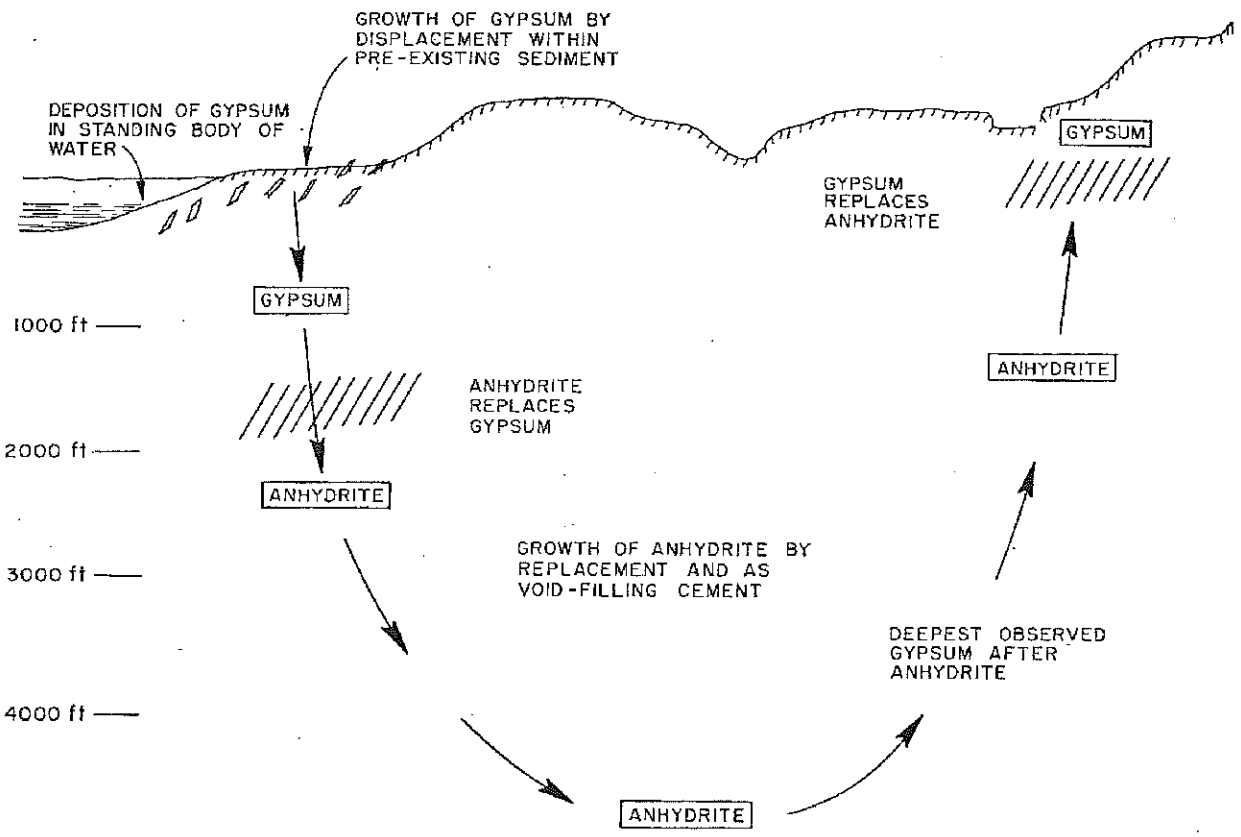

FIG. 2.—Schematic diagram illustrating gypsum-anhydrite-gypsum diagenetic cycle.

gypsum was very persistent and crystallized easily even in its metastable state. Indeed, evaporation of sea water in the temperature range 60°–80°C produces gypsum rather than anhydrite as a final product. This suggests that factors other than the solubilities of the two minerals may be involved in determining the conditions under which one or the other will be formed.

MacDonald (1953) approached the problem thermodynamically in order to study the effect of concentrated salt solutions and pressure on the gypsum-anhydrite transition temperature. From previously determined thermodynamic properties he calculated a transition temperature of 40°C for the reaction $CaSO_4 \cdot 2H_2O \rightleftarrows CaSO_4 + 2H_2O$ in pure water. This value corresponds closely with Posnjak's experimental data.

He also demonstrated the effect of pressure on the reaction in pure water. Under hydrostatic conditions the transition curve had a positive slope, indicating that an increase of total pressure would increase the transition temperature and would favor the formation or preservation of gypsum.

From further thermodynamic calculations, MacDonald (1953) produced a graph showing the transition temperature as a function of the concentration of NaCl, which was compared with sea water by corresponding chlorinities. This graph shows the transition temperature decreasing with an increased concentration of salts; thus, theoretically, one could determine the transition temperature of gypsum-anhydrite at any concentration of sea water. With an estimated concentration of 3.35 times that of normal sea water as the saturation point of $CaSO_4$ in the evaporation of sea water, a transition temperature of 34°C was determined. Therefore, if deposition is an equilibrium process, gypsum will be the stable phase and will precipitate out of sea water first at all temperatures less than 34°C, and anhydrite will precipitate out first at all temperatures greater than 34°C.

Henderson (1954) presented additional data on relative solubility of gypsum and anhydrite in salt solutions and concluded that gypsum should be stable to a maximum depth of 2000 feet.

Conley and Bundy (1958) studied the mechanisms involved in converting anhydrite to gypsum. By experimental work they further substantiated Posnjak's observations concerning the persistence and ease of crystallization of gypsum in its metastable state. They also determined

that the reaction of gypsum going to anhydrite plus water is very slow or nonexistent below 42°C. Further, in contrast with Posnjak's and MacDonald's work showing that salt solutions lower the temperature at which anhydrite becomes more stable, they showed that some salts activate rather than inhibit the hydration process in the temperature range studied. In other words, these salts promote the conversion of anhydrite to gypsum, even under conditions theoretically favoring the formation of anhydrite. The best activators were found to be sodium and potassium sulphate.

From their data, Conley and Bundy postulated that it is highly improbable that anhydrite is ever precipitated primarily from sea water because (1) gypsum crystallizes relatively easily in its metastable state, and (2) as soon as crystallites of anhydrite would begin to form in sea water, the activating constituents in the sea water would bring about an almost immediate conversion to gypsum at temperatures below 42°C. They conclude that the thermodynamic applications which predict the formation of anhydrite from gypsum in concentrated salt solutions are incomplete in that they do not incorporate the effect of $CaSO_4$ activators which influence the reaction kinetics.

Despite the evidence from solubility and thermodynamic calculations that anhydrite is more stable in concentrated salt solutions below 42°C, the observation of common if not universal occurrence of Recent gypsum in brine and the influence of kinetic factors in allowing formation and preservation of metastable gypsum suggest that the primary deposit may almost always be gypsum.

Thus, there is a body of evidence that suggests that under most surface conditions gypsum should be the sedimentary product. Very high temperatures might locally cause formation of some anhydrite at the surface in the presence of gypsum. Indeed, this is happening today on the supratidal flats of the Trucial Coast. However, formation and preservation of gypsum may occur for kinetic reasons when surface temperatures are sufficiently high to make anhydrite the stable phase. With burial, gypsum should be replaced by anhydrite. The minimum depth for the transition should be a temperature of 42°C corrected for the pressure effect at the depth of the transition. Because the rate of the change of gypsum to anhydite with respect to the rate of subsidence is unknown, this value must remain a minimum depth. Theoretical values for the depth of this transition range around 2000 feet. However, the author is not familiar with any study of gypsum-to-anhydrite transformation in a formation undergoing initial burial. In the deeper subsurface, anhydrite is the almost universal form.

Environments of Formation

Studies of anhydrite in carbonate rocks and in association with carbonate and clastic rocks suggest that a threefold distinction can be made on the basis of the mode of formation. This distinction involves the recognition of (1) bedded anhydrite, (2) pore-filling anhydrite, and (3) replacement anhydrite. The anhydrite beds which represent the sedimentary unit of primary formation and thus generally metagypsum are the obvious source of material for formation of the two secondary types.

From the previous discussion it is apparent that most of the sedimentary units of anhydrite observed in the subsurface are metagypsum. This may be true despite the fact that independent evidence of this replacement in individual examples is relatively rare. The original condition of precipitation involved concentration through evaporation of water, commonly sea water or ground water that has moved through preexisting evaporite deposits. Such deposits may be of two general types, each with its own significance with respect to paleoenvironment. Although an individual formation may exhibit both types, a distinction between (1) sedimented and (2) nodular fabrics can commonly be recognized.

The sedimented or laminated anhydrite or gypsum beds of which much of the Castile formation (King, 1947) and the Pleistocene Lisan formation of the Dead Sea are composed represents precipitation and sedimentation in a standing body of water. The concentration of the evaporating brine may be maintained within the field of $CaSO_4$ precipitation by limited flow of new sea water into the body of water and reflux of the heavy brine out through the inlet (King, 1947) or through the underlying sediments and rocks (Adams and Rhodes, 1960; Deffeyes, Lucia, and Weyl, 1964). Such evaporite beds commonly show continuous laminations (fig. 3) and sedimentary structures and should be essentially devoid of uniformly distributed marine fossils. They represent a depositional sedimentary facies, time-contemporaneous with other facies. These other facies may be clastic sediments or even carbonate. The latter is more difficult because extensive carbonate deposition which depends on organic production is not possible in concentrated brines.

Nodular anhydrites or gypsum, although they occur in thick units relatively free of carbonate and clastic material, present a different problem

of genesis. All gradations exist, from isolated nodules in fossiliferous limestone or dolomite to thick beds of clustered nodules with only a thin matrix or sheath of limestone, dolomite, or siliceous clastic material. The crystal fabric of the anhydrite in nodules is similar to that of the sedimented anhydrite. Both exhibit a tightly interlocking fabric of needlelike to tabular crystals commonly preferentially oriented parallel or subparallel to bedding (fig. 4). This preferred fabric may change to an orientation subparallel to the nodule surface near the boundary.

Nodules of anhydrite commonly exist in fossiliferous limestones and fossiliferous limestone replaced by dolomite. However, because of general lack of foreign inclusions or ghosts and the draping of the host rock around the nodule, they do not appear to have formed by replacement of carbonate rock. The similarity of nodule shapes observed in rocks of different age and lithology and the absence of nonfilled vugs of similar shape and size argue against gypsum cementation of large vugs. The thin sheath or matrix of carbonate rock commonly observed between closely spaced nodules excludes the vug origin and suggests a displacement or compactional origin where one nodule has been squeezed against another. These anhydrite nodules appear to exist simply as ovoid masses within carbonate rocks whose origin is inconsistent with an evaporite environment.

Gypsum crystals similar to those found today on the shores of Lake Lucero near White Sands, New Mexico offer an explanation for the anhydrite nodule origin (fig. 5). These crystals have grown within the Recent alluvial sediments. During growth the crystals physically push aside the silt, sand, and gravel and form clear or nearly clear selenite crystals. When these sediments are buried, the gypsum will be replaced by anhydrite. If compaction of the sediment accompanies this change, draping of sediment both over and under the nodule will result. If the gypsum crystals grew in carbonate sediment, and they do today in most of the arid climate carbonate supratidal flats, the same relations should hold, and the product would be anhydrite nodules within, but not necessarily related by original depositional environment to the carbonate host rocks (figs. 6 and 7). Small gypsum crystals should produce the small pellet-like anhydrite nodules. The larger crystals should produce the larger anhydrite nodules.

The formation of selenite crystals and rosettes by displacement of soft sediments or weathered rocks appears to take place by at least two mechanisms: (1) Evaporation of ground water in the vadose or capillary zone (Talmage and Wootton, 1937). Crystals of this origin are indicative of subaerial exposure of the top of the host rock or sediment. (2) Evaporation of water on a playa or other standing body of water and down-

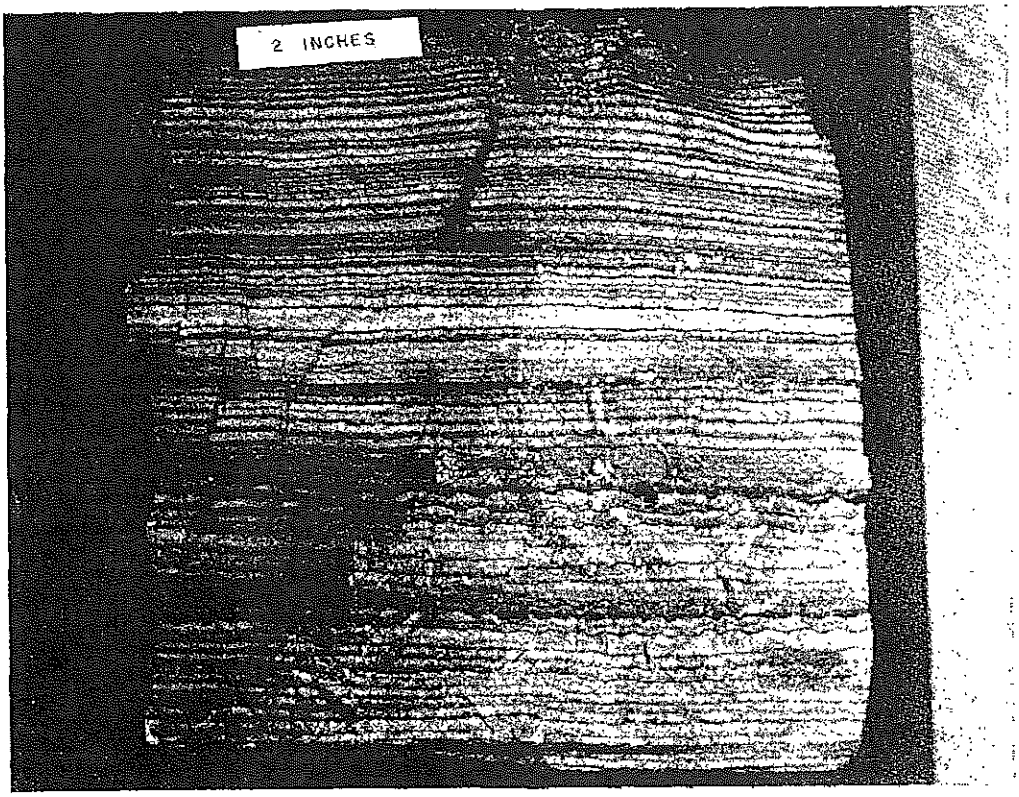

FIG. 3.—Laminated gypsum and calcite; Castile Formation, Permian, West Texas.

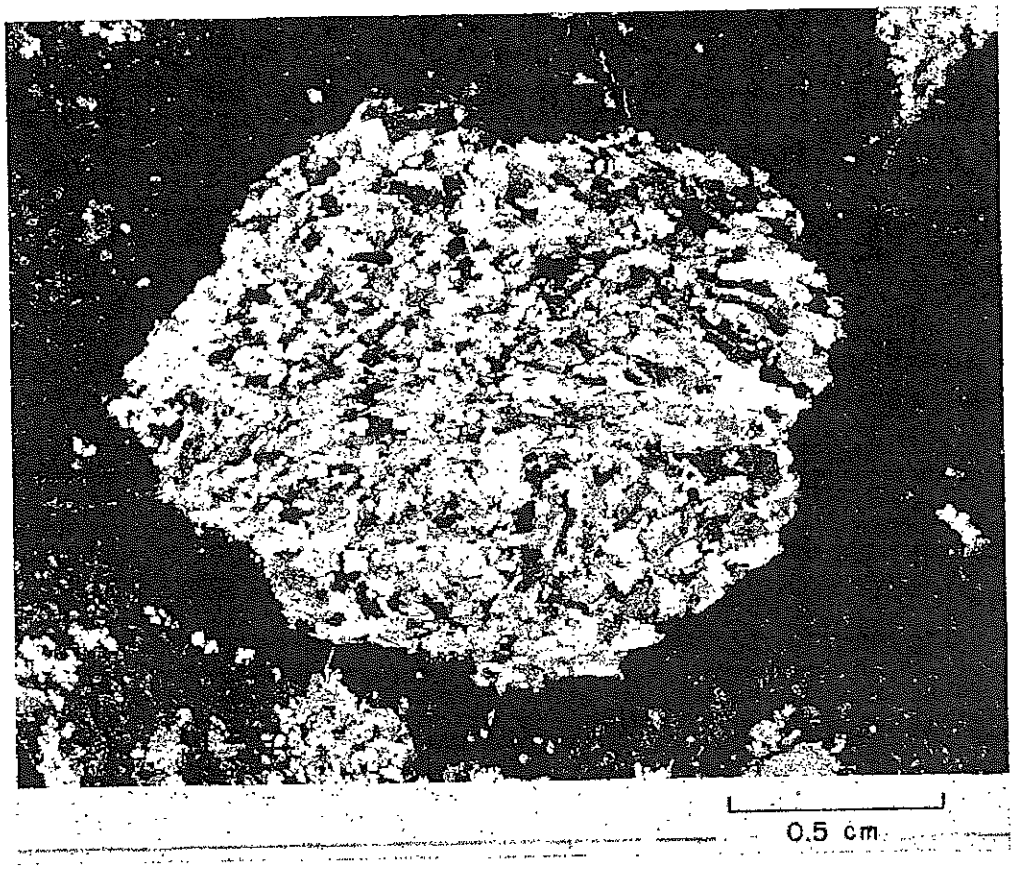

FIG. 4.—Small anhydrite nodule; transmitted light. Note the orientation of the individual anhydrite crystals subparallel to the bedding. The host San Andres dolomite is draped around the nodule.

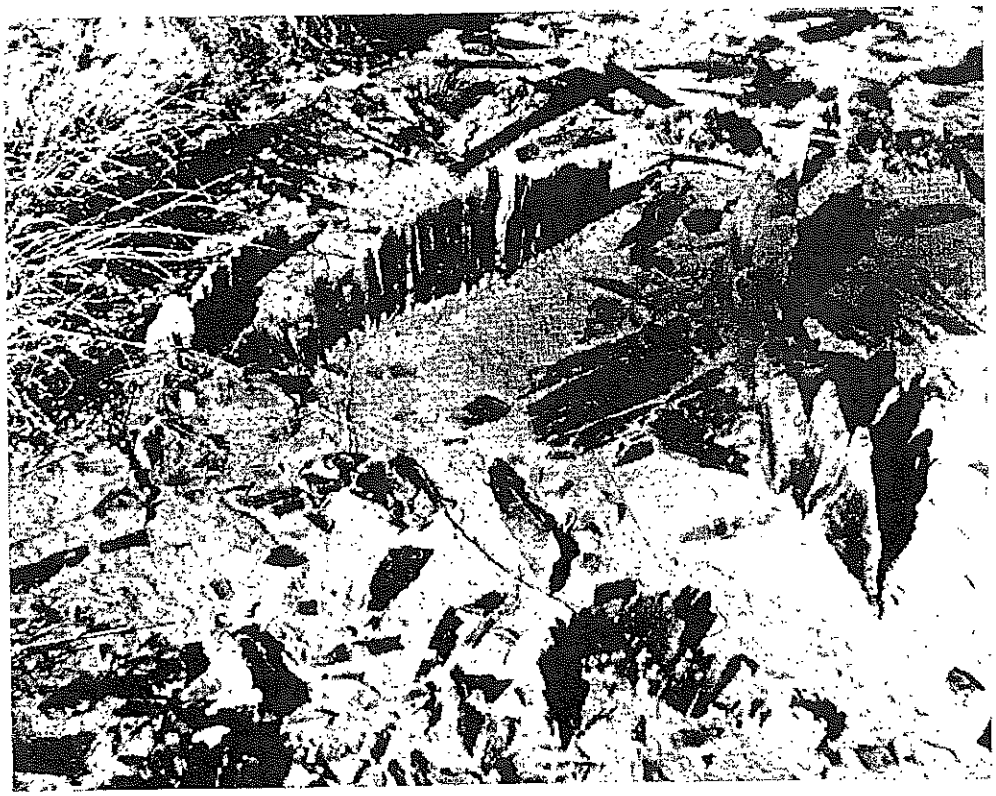

FIG. 5.—Surface of valley fill sediments west of Lake Lucero, New Mexico. The clear gypsum crystals have grown within the sand and silt by displacement. The tops of some crystals have been exposed by erosion.

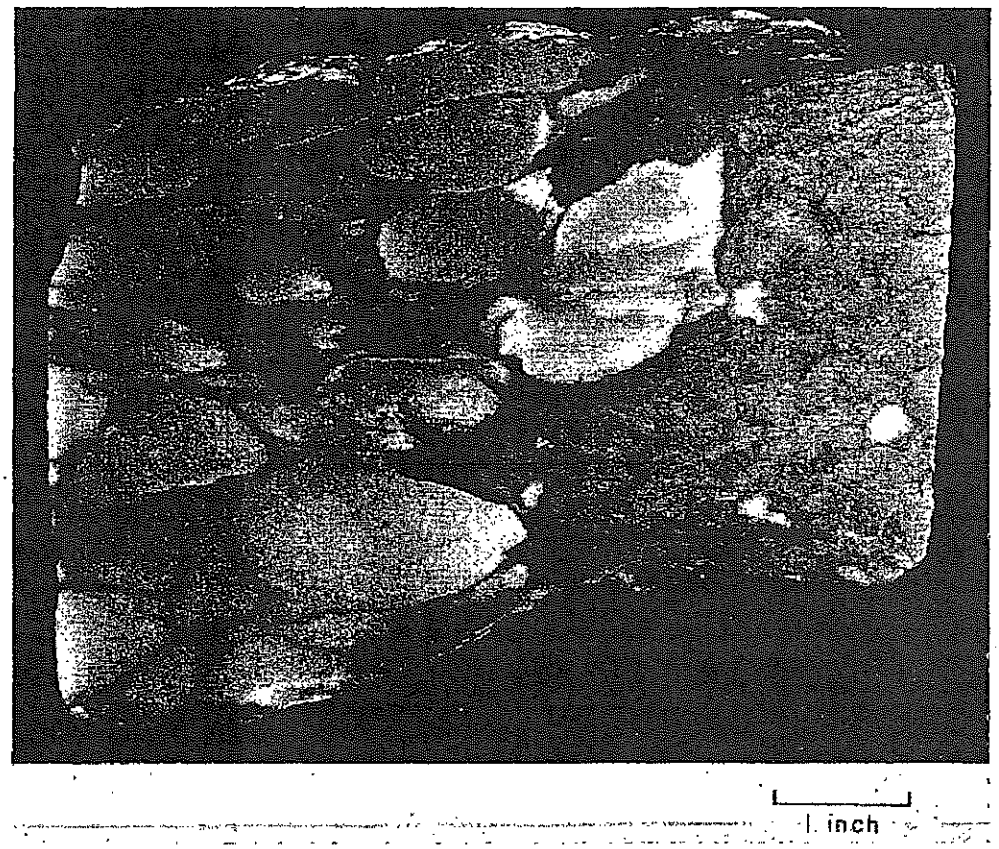

FIG. 6.—Bed of nodular anhydrite grading into fossiliferous sucrose dolomite; Clear Fork Formation, West Texas.

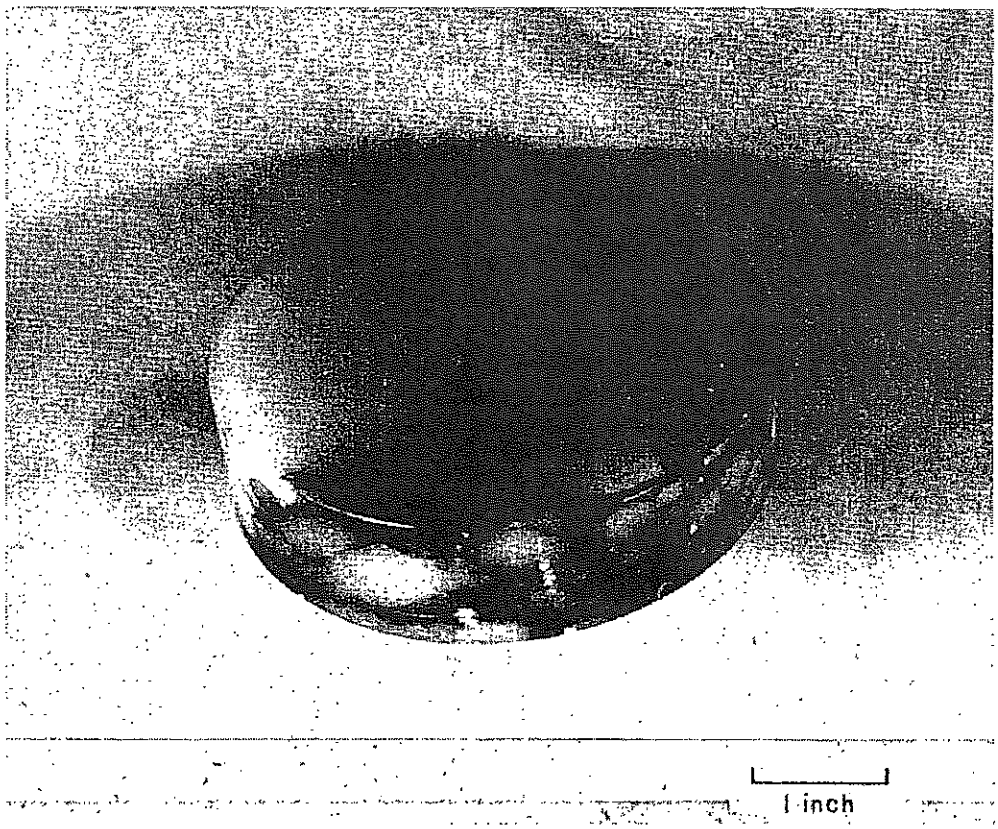

FIG. 7.—Bed of nodular anhydrite showing thin sheath of original sediment between pure anhydrite nodules; Madison Formation, Montana.

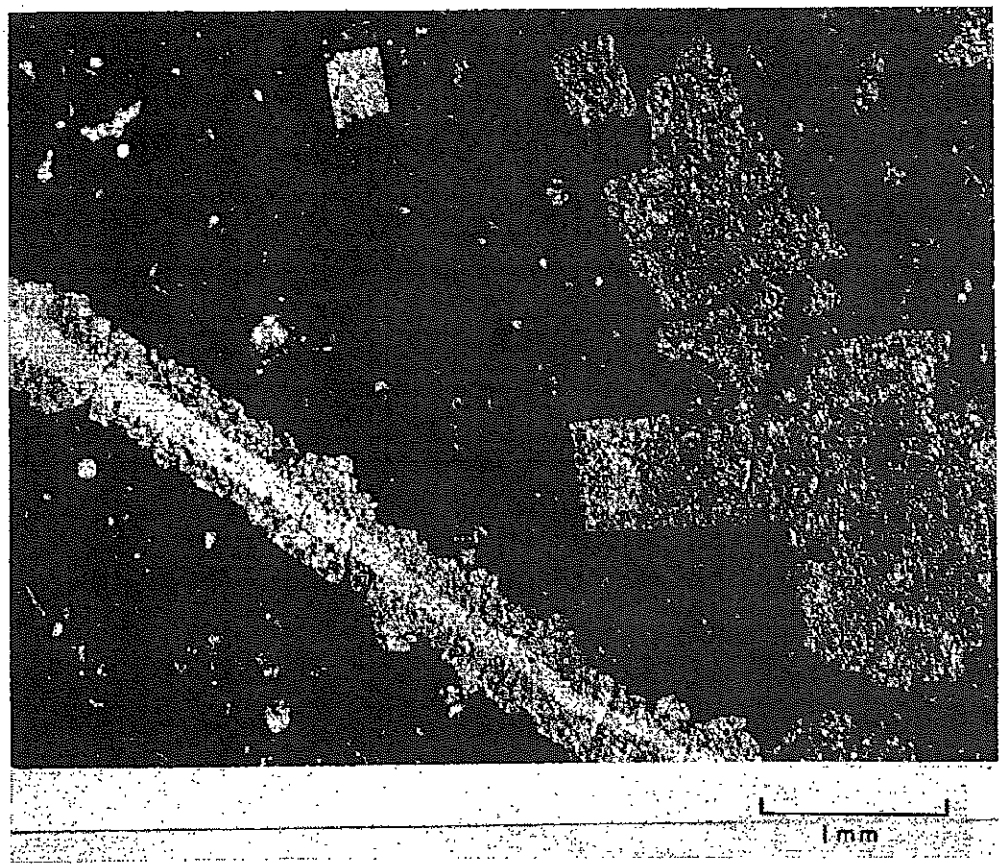

FIG. 8.—Replacement and void-filling anhydrite. The large blocky crystals have grown by replacement of limestone. The fracture in the lower left has been filled with clear anhydrite crystals. These crystals have developed overgrowths by replacement of the limestone wall rock. The same observation may commonly be made in a carbonate sand where anhydrite fills the interparticle space and continues growth by replacement of the particles.

ward movement of the dense hypersaline water into sediment below, with resulting formation of the gypsum crystals. Crystals of this origin are forming in the Laguna Madre tital flats (Masson, 1955). With either mechanism the presence of the anhydrite nodules is not necessarily indicative of hypersaline water during deposition of the host rock. Thus, the apparent inconsistency of coexisting marine organisms and rocks and hypersaline conditions is satisfied If the host rock existed at an unconformity that exposed sediments or weathered rocks of different age, the nodular bedded anhydrite would appear to be time-transgressive.

Recently, Kerr and Thomson (1963) have observed pseudomorphs of anhydrite nodules after gypsum crystals, indicating that the gypsum crystal form is not always destroyed in producing anhydrite nodules and presenting primafacie evidence of a metagypsum origin of the anhydrite. Using the Recent analogy of the Laguna Madre gypsum, they point out the association of tidal-flat sediments with nodular anhydrite and suggest that this environment of intermittent inundation with sea water offers an ideal environment for formation of nodular evaporites.

The nodular anhydrite beds thus represent growth of gypsum by displacement of soft sediment after deposition of the host material and must be considered an early diagenetic facies rather than a depositional facies. Many of the bedded evaporites in the geologic record contain thick sections of the nodular form. Indeed, most of the examples of Recent evaporites occur on supratidal flats and shallow lakes on supratidal flats rather than in large, deeper-standing bodies of water.

Thus, the conclusion may be drawn that nodular anhydrite is indicative of subaerial exposure of soft sediments with evaporation of $CaSO_4$-bearing water taking place within the sediment. Such conditions commonly exist today on the supratidal flats in arid climates or in desert playas. In the former the source of water is commonly the sea and transport into the supratidal sediments may take place during a large storm or by seepage through the sediments. In the latter the source of the water may be ground water that has passed through older evaporites and

SPECTROCHEMICAL ANALYSIS OF THE THREE TYPES OF ANHYDRITE*
(Weight Percent)

Metallic Elements	East Poplar Charles Formation			Wasson San Andres Formation			Sturgeon Lake Leduc Formation	
	Murphy #43 5791 Ft Replacement	Murphy #10 5634 Ft Pore-Filling	Murphy #10 5633 Ft Bedded	Roberts #1 4945 Ft Replacement	Roberts #1 4945 Ft Pore-Filling	Roberts #1 4944 Ft Nodules	SB-1-12 8346 Ft Pore-Filling	SB-1-12 8342 Ft Bedded
Aluminum	0.01	0.003	0.003	0.02	0.002	0.003	0.001	0.002
Antimony	0.0	0.0	0.0	0.0	0.0	0.0	0.0	0.0
Arsenic	0.	0.	0.	0.	0.	0.	0.	0.
Barium	0.002	0.001	0.001	0.002	0.0006	0.0003	0.00003	0.0008
Beryllium	0.000	0.000	0.000	0.000	0.000	0.000	0.000	0.000
Bismuth	0.00	0.00	0.00	0.00	0.00	0.00	0.00	0.00
Boron	0.0	0.0	0.0	0.0	0.0	0.0	0.0	0.0
Cadmium	0.0	0.0	0.0	0.0	0.0	0.0	0.0	0.0
Calcium	26.	30.	30.	33.	28.	29.	28.	29.
Chromium	0.000	0.000	0.000	0.000	0.005	0.000	0.000	0.000
Cobalt	0.00	0.00	0.00	0.00	0.00	0.00	0.00	0.00
Columbium	0.0	0.0	0.0	0.0	0.0	0.0	0.0	0.0
Copper	0.000	0.000	0.000	0.000	0.004	0.006	0.003	0.000
Gallium	0.00	0.00	0.00	0.00	0.00	0.00	0.00	0.00
Germanium	0.00	0.00	0.00	0.0	0.0	0.0	0.0	0.0
Gold	0.0	0.0	0.0	0.0	0.0	0.0	0.0	0.0
Indium	0.00	0.00	0.00	0.00	0.00	0.00	0.00	0.00
Iron	0.06	0.03	0.03	0.09	0.1	0.04	0.02	0.02
Lead	0.00	0.00	0.00	0.00	0.00	0.00	0.00	0.00
Magnesium	0.3	0.007	0.008	0.8	0.02	0.004	0.006	0.000
Manganese	0.000	0.000	0.000	0.000	0.000	0.000	0.000	0.000
Molybdenum	0.000	0.000	0.000	0.000	0.01	0.000	0.000	0.000
Nickel	0.09	0.09	0.09	0.1	0.08	0.09	0.07	0.1
Palladium	0.00	0.00	0.00	0.00	0.00	0.00	0.00	0.00
Potassium	1.	0.8	1.	0.0	0.0	0.0	0.0	0.0
Silicon	0.3	0.1	0.1	1.	0.2	0.1	0.06	0.08
Silver	0.000	0.000	0.000	0.000	0.000	0.000	0.000	0.000
Sodium	0.2	0.2	0.2	0.0	0.0	0.0	0.0	0.0
Strontium	0.3	0.5	0.2	0.3	0.1	0.1	0.1	0.2
Tantalum	0.	0.	0.	0.	0.	0.	0.	0.
Tin	0.00	0.00	0.00	0.00	0.00	0.00	0.00	0.00
Titanium	0.01	0.01	0.01	0.03	0.00	0.00	0.00	0.00
Tungsten	0.	0.	0.	0.	0.	0.	0.	0.
Vanadium	0.000	0.000	0.000	0.000	0.000	0.000	0.000	0.000
Zinc	0.0	0.0	0.0	0.0	0.0	0.0	0.0	0.0
Zirconium	0.0	0.0	0.0	0.0	0.0	0.0	0.0	0.0
Phosphorous	0.	0.	0.	0.	0.	0.	0.	0.
Mercury	0.	0.	0.	0.	0.	0.	0.	0.

*Ca may be in error as much as ± 8-10 percent absolute. Normal error of the other elements is ± 50 percent of the value reported.

FIG. 9.—Spectrochemical analysis of the three types of anhydrite.

thus represents a reconstructed water. Because nodules may form below standing bodies of water in earlier sediments and because shallow bodies of water may temporarily exist as lakes or supratidal flats or desert playas, both sedimented and nodular anhydrite may exist together. The relative abundance and distribution of the two types often permits the recognition of the environment of formation.

In addition, beds of both the sedimented and nodular calcium sulfate deposits probably act as the source material for many of the examples of pore-filling and replacement anhydrite observed in the subsurface. That is, they offer a source of $CaSO_4$ available for dissolution and reprecipitation in void space or growth by replacement in pre-existing rocks.

ANHYDRITE PETROLOGY

Void-filling Anhydrite

Free growth of anhydrite or gypsum takes place within previously existing voids and thus occurs in space formerly occupied by water. Several types of voids can be generated in carbonate rocks (Murray, 1960): interparticle space in carbonate or terrigenous clastic sand, intercrystalline space in dolomite, primary cavities in fossils, dissolution vugs or fractures. Anhydrite growing within such voids has little opportunity to include pre-existing rock and thus forms clear crystals. These crystals may occur as relatively large clear individuals that fill the pre-existing space or in larger spaces as clusters of clear tabular crystals. However, void-filling anhydrite in carbonate rocks commonly continues to grow by replacement into the rock margin of the pre-existing void (fig. 8).

Replacement Anhydrite

Replacement anhydrite crystals grow within the rock and occupy space previously occupied by other minerals and fine pore space. Bioclastic particles appear to be the most commonly replaced material. This process probably takes

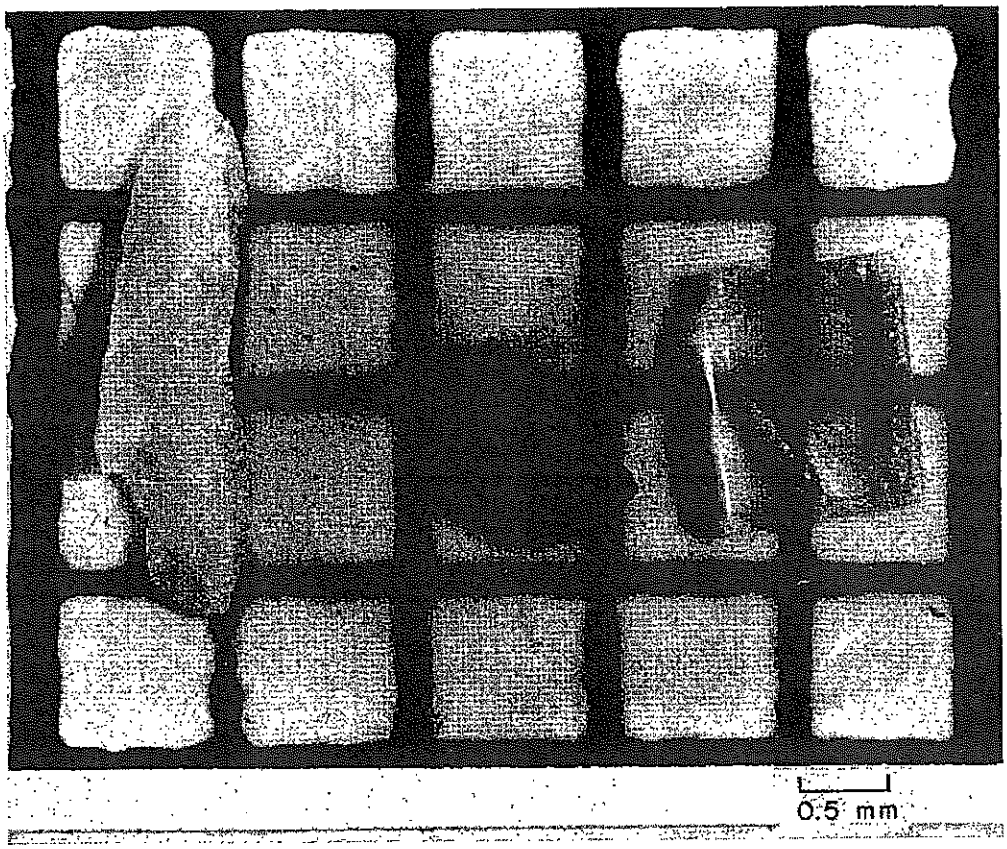

FIG. 10.—Anhydrite types in reflected light; Mississippian Charles Formation, Montana. Left—Nodular anhydrite from a thick anhydrite unit. Center—Replacement anhydrite from limestone 3 feet under the anhydrite bed. Right—Void-filling anhydrite from limestone 3 feet under anhydrite bed.

place by simultaneous dissolution of the parent rock and precipitation of the anhydrite, as demonstrated by the in-situ distribution of inclusion produced relict patterns. Dissolution is often incomplete, and the anhydrite continues to grow around the more resistant relict calcite, dolomite, and noncarbonate clastic grains, attempting to maintain its rectangular habit, but often the final shape is partially controlled by the shape of the material being replaced. These leftover particles remain within the replacement anhydrite crystal and, if they are large enough, can easily be seen when the anhydrite crystal is turned to extinction. Because of this imperfect replacement, resulting in the inclusion of relict particles within the anhydrite crystal, these crystals are usually cloudy to brown in reflected light. The color, of course, depends on the amount, distribution, and nature of the relict material.

Chemical analyses by emission spectrograph were made of anhydrite samples representing two sets of the three anhydrite types (fig. 9). These samples were prepared by removing all the surrounding carbonate rock with dilute hydrochloric acid. Within the limits of accuracy, the bedded nodular and the pore-filling anhydrites appear quite similar in trace element content. However, the replacement anhydrite from the San Andres dolomite and Charles limestone examples contains excess magnesium, silicon, and aluminum. This undoubtedly represents relicts of nonreplaced dolomite, quartz, and clay minerals within the replacement anhydrite crystals and confirms the nature of the relicts and the cause of the cloudy to brown color. Further confirmation was obtained by X-ray analysis of the three Charles anhydrites. The bedded and pore-filling anhydrite showed only anhydrite, whereas the replacement sample contained between 5 and 10 percent calcite and some quartz.

The three anhydrite types can be distinguished in reflected light because of the textural differences and the presence of inclusions in replacement anhydrite.

Bedded anhydrite is commonly granular to massive and translucent to opaque and may be white or light colored, depending on contained impurities (figs. 10 and 11). Pore- or vug-filling anhydrite commonly occurs as clear single crystals with well-defined cleavage (figs. 10 and 11). Rock-replacement anhydrite, because it often fails to digest completely the rock being replaced, appears as cloudy to brown single crystals (figs.

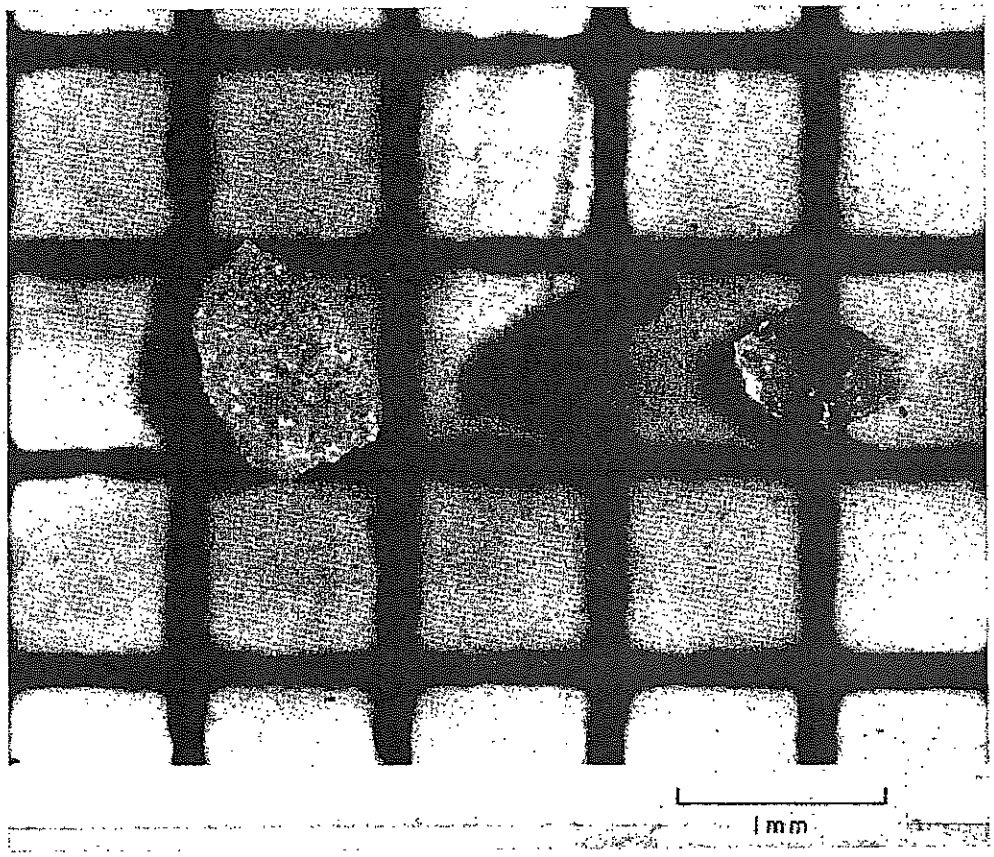

FIG. 11.—Anhydrite types in reflected light; Permian San Andres Dolomite West Texas. Left—Nodular anhydrite. Center—Replacement anhydrite from dolomite. Right—Void-filling anhydrite from dolomite.

10 and 11). Brown metasomatic anhydrite has been reported by Fuller (1956), and the presence of abundant inclusions has been noted by the author in all examples of replacement anhydrite studied.

Relationships of Anhydrite to Porosity

Bedded anhydrite seldom contains pore space in the subsurface. It is presumed that this anhydrite acts as a source of material for the two secondary anhydrite types. Commonly, void-filling and replacement anhydrite is concentrated near, and in association with, bedded anhydrite. In addition, the bedded anhydrite often appears to act as a barrier for further movement of hydrocarbons and thus may act as a seal for a hydrocarbon accumulation.

Replacement anhydrite in itself neither creates nor destroys porosity unless, as is quite common, earlier interparticle, intercrystalline, or vuggy void spaces are engulfed by a solid replacement crystal. However, replacement anhydrite is commonly dissolved later to produce anhydrite mold vugs (Murray, 1960).

CONCLUSIONS

The available evidence suggests that a common diagenetic cycle exists in the $CaSO_4$ minerals. The original material is commonly if not universally gypsum deposited either by precipitation in standing bodies of water or by growth of displacement gypsum crystals in pre-existing sediment or weathered rock. By either mechanism, beds of calcium sulfate minerals may be produced. With burial the gypsum is replaced by anhydrite, and with uplift and removal of overburden the anhydrite is replaced by gypsum. Pre-existing void space in rocks may be filled with anhydrite or gypsum and pre-existing carbonate rock is commonly replaced by anhydrite. The distinction between bedded, void-filling, and replacement anhydrite can be made in reflected light because of differences in texture between bedded and void-filling anhydrite and because of the abundance of included material in replacement anhydrite.

ACKNOWLEDGMENTS

The author is most appreciative for the assistance and comments generously given by his colleagues during this study and preparation of the manuscript, especially F. J. Lucia, J. W. Rasmussen, T. W. Donnelly, R. T. Buffler, and A. L. Diehl.

REFERENCES

ADAMS, J. E., AND RHODES, M. L. (1960), Dolomitization refluxion: Bull. Amer. Assoc. Petroleum Geol., v. 44, 1912–1920.

BUNDY, W. M. (1956), Petrology of gypsum-anhydrite deposits in southwestern Indiana: J. Sed. Petrology, v. 26, 240–252.

CONLEY, R. F., AND BUNDY, W. M. (1958), Mechanism of gypsification: Geochimica et Cosmochimica Acta, v. 15, 57–72.

CURTIS, R., EVANS, G., KINSMAN, D. J. J., AND SHEARMAN, D. J. (1963), Association of dolomite and anhydrite in Recent sediments of the Persian Gulf: Nature, v. 197, 679–680.

DEFFEYES, K. S., LUCIA, F. J., AND WEYL, P. K. (1964), Dolomitization: Observations on the Island of Bonaire, Netherlands Antilles: Science, vol. 143, no. 3607, 678–679.

FISK, H. N. (1959), Padre Island and the Laguna Madre flats, Coastal South Texas: Natl. Acad. Sci.-Natl. Res. Coun., 2nd Coastal Geog. Conf., pp. 103–151.

FULLER, J. G. C. M. (1956), Mississippian rocks and oilfields in southeastern Saskatchewan: Saskatchewan Dept. of Min. Resources, Report 19.

HENDERSON, G. G. L. (1959), Geology of the Stanford Range of the Rocky Mountains: British Columbia Dept. of Mines, Bull. 35.

KERR, S. D., AND THOMSON, A. (1963), Origin of nodular and bedded anhydrite in Permian shelf sediments, Texas and New Mexico: Bull. Amer. Assoc. Petroleum Geol., vol. 47, no. 9, 1726–1732.

KING, R. H. (1947), Sedimentation in Permian Castile sea: Bull. Amer. Assoc. Petroleum Geol., vol. 31, 470–477.

MACDONALD, G. J. F. (1953), Anhydrite-gypsum equilibrium relations: Amer. J. Sci., v. 235-A, 247–272.

MASSON, P. H. (1955), An occurrence of gypsum in Southwest Texas: J. Sed. Petrology, v. 25, 72–79.

MORRIS, R. C., AND DICKEY, P. A. (1957), Modern evaporite deposition in Peru: Bull. Amer. Assoc. Petroleum Geol., v. 41, 2467–2474.

MURRAY, R. C. (1960), Origin of porosity in carbonate rocks: J. Sed. Petrology, v. 30, 59–84.

PHLEGER, F. B., AND EWING, G. C. (1962), Sedimentology and oceanography of coastal lagoons in Baja California, Mexico: Geol. Soc. Amer. Bull., v. 73, 145–182.

POSNJAK, E. (1938), The system, $CaSO_4$-H_2O: Amer. J. Sci., v. 235-A, 247–272.

——— (1940), Deposition of calcium sulfate from sea water, Amer. J. Sci., v. 238, 559–568.

STEWART, F. H. (1953), Early gypsum in the Permian evaporites of northeastern England: Proc. Geol. Assoc., v. 64, 33–39.

SUND, J. O. (1959), Origin of the New Brunswick gypsum deposits: Canadian Mining and Met. Bull., v. 52, No. 571, 707–712.

TALMAGE, S. B., AND WOOTTON, T. P. (1937), The non-metallic mineral resources of New Mexico and their economic features: New Mexico Bur. of Mines and Min. Resources, Bull. 12, 159 pp.

WELLS, A. (1962), Recent dolomite in the Persian Gulf: Nature, v. 194, 274.

Attachment B-13

If inorganic precipitation were involved, the Florida Bay area, an ideal insulation basin, should then have the greatest needle abundance, but as Ginsburg (1953) has already pointed out, this is not the case. Only in the Bahamas, where some definite precipitates are known to accompany the needle occurrences (Illing, 1954), is there any legitimate reason to attribute at least some needles to chemical precipitation.

The discovery of algally-secreted needles establishes an endemic biogenic source for aragonite needles in sediments for the first time. The concordant distribution and abundance relations between the critical algae and sedimentary needle occurrences in the examples cited answers in large part the question raised here initially. The post-mortem role of the calcifications of many algae which have not been reported or reported only in small amounts in bioclastic debris, is actually important in the sedimentary record. Single needles and calcification fragments can now be shown to be deposited in the clay to sand size fraction.

Representatives of algal genera, with aragonite-secreting species in the west Atlantic, are also distributed widely in subtropical and tropical seas elsewhere. Cursory examination of congeneric species showed aragonite needles in *Udotea orientalis* from the Philippines, *Udotea argentea* from New Caledonia, *Udotea (Flabellaria) desfontainii* from Tripoli in the Mediterranean, and from several unidentified species of *Halimeda* from Kayangle atoll, Palau. Sediment samples collected by the writer in the Kayangle lagoon contain aragonite needles. Therefore, wherever aragonite needle-secreting algae occur within equatorial shoal waters, bounded by the 15°C isotherms for the coldest month of the year, quiet water sediments should contain aragonite needles. Another implication is that fossil calcilutites attributed to physiochemical precipitation or mechanically reduced skeletal carbonates may have been partially or largely derived from algally-secreted aragonite needles from ancestral algae.

Acknowledgment is made to Dr. [illegible] Bernatowicz for identification of Bermuda algae, Dr. E. Y. Dawson for specimens and literature data, and Dr. P. H. Monaghan from Humble Oil and Refining Company for needle bearing bottom samples from the Bahamas. Research was supported by a grant from the California Research Corporation.

REFERENCES

CHAVE, K. E., 1954, Aspects of the biogeochemistry of magnesium. 2: Calcareous sediments and rocks: Jour. Geol., 62, pp. 587–594.

CLOUD, P. E., JR. AND BARNES, V. E. 1948, Paleoecology of the early Ordovician Sea in Central Texas: Rpt. Committee Treatise Marine Ecol. and Paleont. No. 8, p. 37.

GEE, H., 1932, Preliminary experiments in precipitation by removal of carbon dioxide under aseptic conditions: Bull. Scripps Inst. Oceanog. Tech. Ser. 3, p. 180.

GINSBURG, R. N., 1953, Carbonate sediments: API Proj. 51, Rpt. 8, SIO Ref., pp. 26–95.

ILLING, L. V., 1954, Bahama calcareous sands: Am. Assoc. Petroleum Geologists Bull., 38, 1–95.

PIA, J., 1926, Pflanzen als Gesteinsbildner, Borntraeger, Berlin, 104 pp.

REVELLE, R., 1932, Report on precipitate obtained by removal of carbon dioxide from sea water: Bull. Scripps Inst. Oceanog., Tech. Ser. 3, p. 188.

VAUGHAN, T. W., 1917, Chemical and organic deposits of the sea: Geol. Soc. America Bull., p. 933.

——, 1924, Present status of studies on the causes of the precipitation of finely divided calcium carbonate: Nat. Res. Council, Prt. Committee Sedim., p. 53.

WILLIAMS, H., 1933, Geology of Tahiti, Moorea, and Maiao: Bernice P. Bishop Mus. Bull., p. 79.

JOURNAL OF SEDIMENTARY PETROLOGY, VOL. 25, NO. 4, PP. 273–281
FIGS. 1–6, DECEMBER, 1955

INVERSE GRADED BEDDING IN PRIMARY GYPSUM OF CHEMICAL DEPOSITION

L. OGNIBEN
Montecatini S. A. (Settore Miniere), Milan, Italy

ABSTRACT

The Gypsum formation of the Sulphur series of Sicily shows thick gypsum beds, mostly made up of basal zones of primary gypsum with rhythmic structure and of thicker upper zones of secondary gypsum. The latter is characterized by swelling structures due to transformation from anhydrite.

The rhythmic primary gypsum is bedded in two to three mm thick laminae, which present a structure of inverse graded crystalline mosaic with the finer grain sizes at the base and the bigger ones at the top.

Some slightly reworked types of primary gypsum show loss of the grading and uniform grain size. Some rhythmites show a grading from finer to bigger sizes, ending in the deposition of anhydrite crystals which have been transformed to gypsum during the deposition of the following lamina, thus deforming it.

The inverse size grading is referred to a seasonal concentration increase by evaporation, possibly together with an average temperature increase. The return to the initial sizes at the base of each lamina is attributed to a rainy, perhaps cold season, which interrupts the evaporation and consequently the chemical deposition.

STRATIGRAPHIC POSITION OF THE PRIMARY GYPSUM IN SICILY AND ITS SIGNIFICANCE

The Upper Miocene Sulphur series of Sicily has been described in previous papers (Ogniben, 1953; 1954a; 1954b). From top to bottom it is: (1) Trubi formation (Globigerina marl and marly limestone); (2) Gypsum formation (interbedded gypsum, marl, and clay); (3) Basal limestone formation (evaporitic limestone interbedded with minor marl); (4) Tripoli formation (interbedded diatomite and diatomitic marl). It includes other minor more discontinuous members among which are the well known sulphur sedimentary deposits interbedded between Basal limestone and Gypsum formations and important halite and potassium-magnesium salt deposits within the Gypsum formation. It is a typical "arid restricted basin" association, related to a phase of regression and separation of the Mediterranean area from the oceans.

In marginal areas of the "arid restricted basin" the Gypsum formation shows the "sulphiferous facies" with prevalence of gypsum and minor interbedded marls and clays. It reaches 100 meters maximum total thickness and contains the sulphur deposits at its base. From Mt. Etna to Sciacca, in a median area of the basin, the "saliferous facies" which attains maximum thickness of about 1000 meters, with very abundant marls and clays and interbedded saline deposits, is shown.

Gypsum occurs in beds from one to some tens of meters thick which are mostly made up of secondary gypsum by transformation from anhydrite, and by a thin basal zone of primary gypsum of chemical deposition (fig. 1). The latter is a dense microcrystalline white-grayish rhythmic rock, or rhythmite (Sander, 1936), of waxy appearance, distinctly divided into thin laminae, and often fissile. Its local name is balatino.

The selenitic secondary gypsum of the "sulphiferous facies" has already been described (Ogniben, 1954c). It makes up the greatest part of the thick gypsum beds as selenite in swallow tail (100) twins a few centimeters long with a

FIG. 1.—Thick beds of secondary selenitic gypsum divided by interbedded marl. Note the thin zone of primary gypsum at the base of the upper bed. Grottacalda, Enna, Sicily.

preferred orientation according to the Mottura's Rule, i.e. with the twinning plane and the c axis perpendicular or subperpendicular to the bedding plane, and with a constant polarity of the twins concave angle toward the top of the beds, and of the apex toward the bottom. Swelling structures of the upper surface of the beds and deformation of the overlying marls make the transformation from anhydrite evident. This event seems to have been paradiagenetic as is indicated also by the present study.

The alabastrine secondary gypsum of the "saliferous facies" is a white saccharoidal rock with irregular knotlike swelling structures, and seems to have originated by recent transformation of anhydrite caused by the approach of the external erosion surface.

In both facies, at the base of the formation some beds can be entirely made up by primary rhythmic gypsum, and at the top some beds can be wholly made of secondary gypsum; but in most beds the typical association is a thin basal zone of primary gypsum with a much thicker upper part of secondary gypsum (fig. 2). The sequence, marl—primary rhythmic gypsum—secondary gypsum—marl, is thus polar from bottom to top, always repeating itself in the same order.

This cyclical sequence bears a precise significance. The interbedded marls, so common in evaporitic formations, were originated by periods of terrigenous supply, and therefore of strong water inflow, which interrupted or overshadowed the chemical deposition. When the latter started again, gypsum, now visible as rhythmite, always precipitated first, after which deposition of anhydrite, now visible as secondary gypsum, took place.

The next following phase of terrigenous supply caused dilution of the basin water, and the successive chemical deposition took place as gypsum again, thence passing to anhydrite, and so on.

Transition from gypsum to anhydrite in calcium sulphate deposition by evaporation is caused by increase of concentration and temperature (Posnjak, 1940). Deposition of gypsum from sea water at 30° takes place when concentration has reached 3.35 times the normal salinity, and deposition of anhydrite takes place after having reached 4.8 times the normal salinity. These conditions are not greatly modified at temperatures even 10°–15° lower. At 42° anhydrite always will be deposited whatever the type of calcium sulfate solution may be.

In geological environments variation of concentration must be more determinant than that of temperature, since average temperatures much over the above mentioned 30° could have hardly lasted for such a long time as that required by the formation of the gypsum layers. A slow salinity variation is easily understood if a balance between inflow of water and loss by evaporation is admitted. In this way the water concentration can be maintained for a long time in the field of less solubility of gypsum, slowly increasing until it reaches the field of less solubility of anhydrite, still longer permanence in this field.

The possibility of such an equilibrium must be accepted since it is documented by its products. Only a continuous inflow of sea water can have carried to these vast basins the enormous quantities of evaporitic minerals we find to-day in the corresponding formations. So only

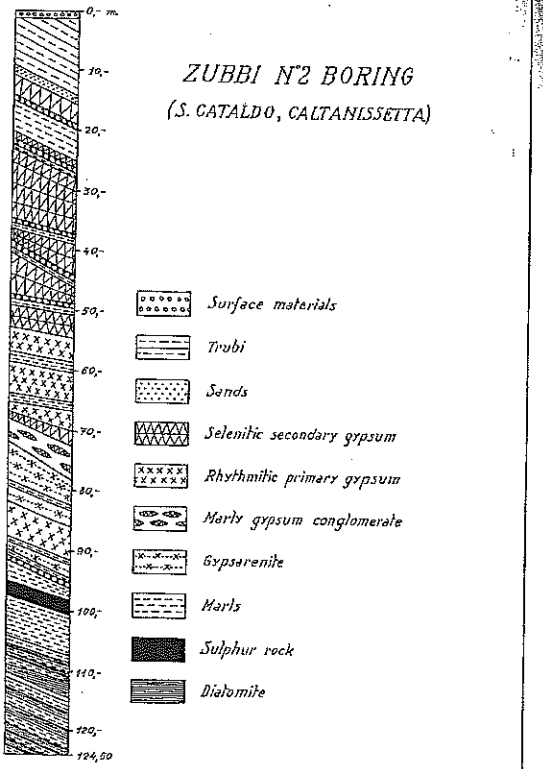

FIG. 2.—Typical sequence of primary and secondary gypsum beds interbedded with marl and clastic gypsum. The Gypsum formation passes upward into the Trubi, downward into the Tripoli formation (diatomite). The Basal limestone formation is lacking. S. Cataldo, Caltanissetta, Sicily.

correspondence between inflow and loss by evaporation could have maintained the water concentration of the various basins in the deposition field of a single mineral for such a long time, without allowing the successive precipitation of the whole sequence of evaporation minerals in a short time.

The chance of such a nice balance is all the more evident because the inflow of water is originated, and thus ruled, by the loss by evaporation. Since during the the gypsum deposition there was no deposition of all other salts carried by the water flowing into the basin, a slow increase of salinity took place. After a while, this led the concentration into the field of anhydrite deposition which lasted until the next period of terrigenous supply and of water dilution. This explains the sequence of terrigenous marl, primary gypsum (rhythmite), and anhydrite (secondary gypsum).

The absence of swelling structures shows that the rhythmite was directly deposited as gypsum rather than as anhydrite. Thus, the investigation of an originary structure of chemical deposition, not yet fully known as such, is granted, since the evaporites thus far investigated are wholly recrystallized like the saline deposits, or were subjected to transformations and to very strong tectonic disturbances like the Permian evaporites of the saline domes of the United States and of Germany. Udden (1924) describes an anhydrite rhythmite of the Castile formation of Texas, probably of primary deposition, which resembles the gypsum rhythmite studied here, but he does not fully analyze its microstructure.

MICROSTRUCTURE OF THE RHYTHMIC PRIMARY GYPSUM

Under the microscope the gypsum shows bedding laminae one to five mm, but mostly two to three mm thick. They are frequently made evident by very thin intercalations of marly pelite, but especially by the inverse grading of the gypsum grains. These form a polygonal mosaic with euhedral tendency, showing a grain size of 0.01 mm at the base of the laminae, gradually increasing to average sizes of 0.15–0.2 mm at the top (fig. 3). Common are rhomboidal sections of prismatic grains and less common lamellar sections of tabular ones with the longest diameter lying in the bedding plane. However, nearly isodiametric irregularly polygonal grains are most abundant.

The grains show a more or less strong preferred orientation, easily observed with the gypsum plate, generally having

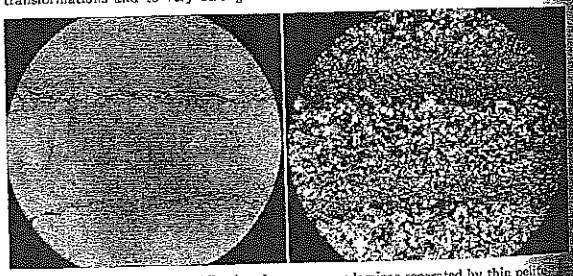

FIG. 3.—Inverse graded bedding in primary gypsum laminae separated by thin pelitic streaks. Parallel and crossed nicols, ×10.

γ^1 perpendicular to the bedding plane, but in some specimens γ^1 is parallel to the bedding plane. Since there are no traces of recrystallization, the preferred orientation must be ascribed to a mechanical effect of elongated or flat grains settling down with their longest diameter parallel to the deposition surface. The prevailing isodiametric polygonal grains, also following the preferred orientation rule, must therefore be derived from original elongated forms, later blunted and made isodiametric by solution phenomena due to rock compaction. This manner of compaction by solution is typical for gypsum rocks, and can be seen very well in the gypsarenites of the Sulphur series containing microfossils and other grains less soluble than gypsum.

The marly pelite of the thin intercalations between the graded gypsum laminae or between single gypsum grains results in carbonate grains generally of a size about 0.001 mm, and in argillaceous matter of still finer size. It is, therefore, normal marl like that interbedded between the big gypsum layers. Very small foraminifera, *Globigerina* and *Bulimina*, with diameters about 0.05 mm, are sometimes associated with it.

Another widespread accessory component is chalcedonic silica in either simple fibro-radiating aggregates or showing several aggregation centers with diameters up to 0.1–0.2 mm (fig. 4). They evidently are authigenic by replacement of gypsum caused by siliceous solution coming from neighboring formations like the underlying Tripoli formation. The latter is essentially composed of opaline silica which is supposed to be the original form of most chalcedonic silica (Pettijohn, 1949).

The chalcedonic spherulites often clearly show their aggregation centers lying in a former intergranular border between gypsum grains, sometimes with small grains of quartz or of another silica form in the center.

Rare accessory components of these gypsum rhythmites are very small granules of pyrite showing diameters from 0.01 to 0.05 mm.

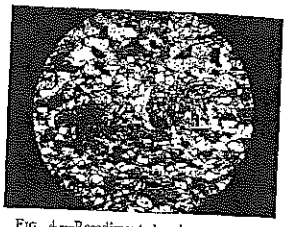

FIG. 4.—Resedimented primary gypsum, with authigenic chalcedonic aggregates. Crossed nicols, ×27.

RESEDIMENTED PRIMARY GYPSUM

In the strata of rhythmic gypsum non-rhythmic zones, sometimes extending over the entire stratum, can be observed. Under the microscope their chief characteristics are absence of grading and uniform grain size, varying in different strata from 0.02 mm to 0.05–0.1 mm (fig. 4). There is a greater amount of marly pelite in the non-rhythmic zones than in the rhythmic layers, but it is scattered among the grains instead of being concentrated in thin streaks between the laminae. The bedding plane is evident by the parallelism of the elongated or flat grains.

Detrital minerals, which are rare in the rhythmic gypsum, are frequent. Among them are angular fragments of calcareous aggregates, detrital quartz, detrital rounded glauconite in sizes up to 0.05 mm, and lamellae of brown clay minerals of medium birefringence or of greenish chloritic minerals of very low birefringence. Common are *Globigerina* and *Bulimina* of small size (0.05–0.1 mm) and authigenic fibro-radiating aggregates of chalcedony (fig. 4) often originating from central fragments of detrital silica, analogous to those of the rhythmites.

The reworking significance of this

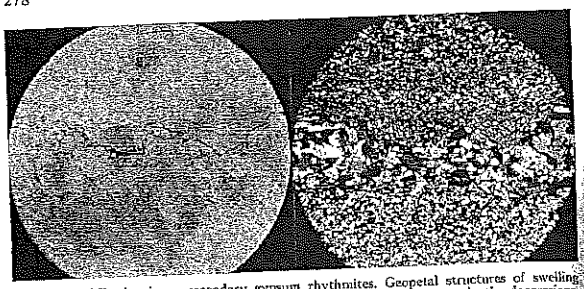

FIG. 5.—Mixed primary-secondary gypsum rhythmites. Geopetal structures of swelling at the upper surface of the laminae, and of filling by small size gypsum in the depressions. Parallel and crossed nicols, ×10.

structure is made clear first by the disappearance of the rhythmic grading. In addition, there are the frequency of foraminifera, the occurrence of noticeable amounts of psammitic detrital materials, and of terrigenous pelite in larger amount than in the rhythmic gypsum. The study of other rocks of the Gypsum formation shows that organic remains associated with gypsum always bear a detrital significance, as does the rounded glauconite in the whole Sulphur series.

The homogenous grain size is due to sorting by transportation. There are resedimented primary gypsum layers with a 0.02 mm grain size, evidently originated by the accumulation of the small basal grains of the rhythmic laminae. More often the primary resedimented gypsum rocks show a 0.05–0.1 mm grain size, clearly caused by accumulation of the top gypsum of the rhythmic laminae.

In resedimented primary gypsum there is no readily visible preferred orientation as in the rhythmites. Therefore, it has been destroyed by the reworking and must be considered a characteristic of the very first sedimentation process.

RHYTHMITES WITH ASSOCIATED PRIMARY AND SECONDARY GYPSUM

A third structural type is megascopically visible by the occurrence of rows of gypsum crystals one mm or more in size between the dense rhythmic laminae. This type is widespread in the Gypsum formation, and it can be found in layers up to several meters thick, all or partly substituting for the normal rhythmic gypsum.

Under the microscope isolated crystals or groups of crystals, averaging 1–2 mm in size, can be observed at the top of the inverse graded laminae, while all other normal or accessory components of the rock are like those of the normal rhythmites. The major size crystals more or less continuously follow the top boundary of the laminae in form of upward arching structures. The corresponding depressions between them are marked by very thin interbedded pelitic streaks. The basal zone of the smallest size gypsum of each overlying lamina exactly mirrors the undulated surface of each underlying lamina, thus showing that it shared in the deformation. Small size gypsum then fills the depressions of this basal zone with a very clear geopetal sedimentary picture (fig. 5), thus allowing the following small size gypsum to be deposited on a flat surface and to continue upward the normal inverse graded lamina.

The upper surface swellings of the underlying lamina seem, therefore, to have formed during the deposition of the first small size gypsum of each overlying lamina in such a manner that a part of the gypsum was deformed, a part filled the resulting depressions, while the remaining portion of the lamina did not undergo any deformation.

Many big gypsum crystals are variously oriented (100) twins and many of them follow the previously mentioned Mottura's Rule, i.e. they are subperpendicular to the bedding and present the concave angle upward and the apex downward. Their length sometimes exceeds the thickness of the containing lamina, stretching out into the overlying and sometimes into the underlying lamina, deforming the small size gypsum sediment.

The position of these crystals, perpendicular to the bedding, is sufficient proof of their epigenetic origin. In addition, at their borders a crystalloblastic cribrose structure is to be observed which is indicative of their growth within the sediment. Often serrated ruptures perpendicular to the crystal elongation are also observed, with small displacement of the single pieces and resulting formation of a superindividual (fig. 6).

This crystalloclastesis, together with the deformation of the embedding sediment, the elongation of the crystal perpendicular to the bedding, and the crystalloblastic structures, clearly shows that a crystal neoformation took place with mechanical strains due to volume increase, i.e. to the transformation from anhydrite.

A gypsum deposition like that of the normal rhythmic layers must, therefore, have taken place ending with deposition of some anhydrite grains of bigger size than the gypsum ones on each lamina top. During the successive deposition of the small size gypsum belonging to the overlying lamina, the anhydrite grains underwent a transformation into big size gypsum, swelling and thus partly deforming the embedding sediment.

These mixed primary-secondary gypsum rhythmites often show a trend toward anhedral forms and a size increase of the primary gypsum grains, i.e. a trend toward the "Sammelkristallisation" of the German authors.

The significance of the mixed primary-secondary gypsum rhythmic deposition is that of a cyclical oscillation about the anhydrite-gypsum transition point. The phenomenon could have been a temperature oscillation, but more likely consisted of a concentration oscillation. The normal rhythmites, therefore, represent oscillations (graded bedding!) within the field of less solubility of gypsum with slow gradual increase of salinity until it reaches the field of anhydrite deposition (now represented by the thick layers of secondary gypsum); i.e. with slow displacement of concentration in a nice oscillating equilibrium between water evaporation and inflow from outside of the basin. In a like manner the mixed primary-secondary gypsum demonstrates a long salinity oscillation about

FIG. 6.—Cataclastic twinned superindividual, showing elongation perpendicular to the bedding (Mottura's Rule), and crystalloblastic structure at its borders. Crossed nicols, ×10.

the gypsum-anhydrite transition point. This is a particular case, wherein the oscillating concentration remained predominantly either in the gypsum stability field, or in the anhydrite one.

SIGNIFICANCE OF GRADED BEDDING

Graded bedding has been known for a long time, but it has found ample treatment only in two classical papers, one by Bailey (1930) who stressed its connection with the geosynclinal detrital deposits and the other by Kuenen and Migliorini (1950) who related it to redeposition of detrital sediments by turbidity currents.

No descriptions have been found of graded bedding of sediments other than detrital. Inverse graded bedding has been referred to by Kuenen and Migliorini (1950), always in relation to detrital materials caused by variations in transport competency.

In the Gypsum formation of Sicily there are also detrital gypsum sediments, originated by reworking of the chemical deposits, but they are typical littoral formations, lenticular in form and with bedding of the current type. True psammitic ("gypsarenites") and psephitic gypsum rocks of this kind are widespread. What can be inferred on the geological environment of the Sicilian evaporites does not agree with the various possibilities of detrital graded bedding according to Kuenen and Migliorini (1950). The evaporitic basins were small and irregular, receiving very little terrigenous supply, and showing a tendency to become dry and miss many members of the deposition sequence.

The mixed primary-secondary gypsum rhythmites seem to demonstrate that the grain size increase of the sediments was connected with a concentration increase of the basin water since the deposition of the big size gypsum crystals ended in the deposition of anhydrite crystals. Afterwards, basin water dilution again caused deposition of very small gypsum crystals and at the same time it caused transformation of anhydrite into gypsum, thus straining the newly formed sediment.

The parallel change of the crystalline size of gypsum and of the saline concentration is very interesting, because it would be possible to control it experimentally. A relationship between grain size and temperature could not have been expressed so simply since it ought to have recorded strong daily variations, not only seasonal ones. However, it is possible that an average temperature effect has contributed to the grain size increase.

The variation of concentration expressed in the graded bedding, and thus also the laminae deposition rhythm, seems to have been nothing else than seasonal. The chemical deposition would correspond to an arid and eventually warm season; the interruption of deposition, the small terrigenous deposit of the thin pelitic streaks, and the dilution of the basin water would correspond to a rainy and eventually a cold season. No independent inflow of sea water is possible as a cause of the deposition rhythm since it was controlled by water evaporation, and this in turn by the seasons.

The passages between the evaporitic basin and the oceans may have been more or less wide. The only necessary condition was a restricted circulation which permitted inflow of normal sea water at the surface to balance the loss by evaporation and prevented outflow of concentrated water in depth. In this way a slow concentration in the whole basin was inevitable, and was only interrupted by major geological events.

The present study thus explains the depositional environment of the Gypsum formation of Sicily as a region of basins of little depth. The rhythmic sedimentation structure was generally preserved, but sometimes subject to reworking. The average environmental temperatures were about the same as Posnjak's (1938, 1940, i.e. about 30°, with ample oscillations possible.

According to all the considerations mentioned above, the single laminae seem to correspond to annual deposits, i.e. varves, like all the mm-rhythmites (Sander, 1936, with the previous literature). An average thickness of two to three mm can be calculated for each lamina, from about two mm (2.2–2.3 mm) for normal rhythmites, to about three mm for mixed primary-secondary gypsum rhythmites.

For the thin basal primary gypsum zones, 20–50 cm, of the main gypsum beds, a depositional time from 100 to 200 years may be therefore calculated. For the bulky beds of independent primary gypsum, which often can be seen at the base of the Gypsum formation, a maximum thickness up to 14.5 m has been measured. Its depositional time, therefore, may have lasted about 7000 years.

The arrangement of primary and secondary gypsum in thick layers interbedded with marl layers was probably controlled by tectonic phenomena related to the rhythm of subsidence.

REFERENCES

Bailey, E. B., 1930, New light on sedimentation and tectonics: Geol. Mag., v. 67, pp. 77–92.

Kuenen, Ph. H., and Migliorini, C. I., 1950, Turbidity currents as a cause of graded bedding: Jour. Geology, v. 58, pp. 91–127.

Ogniben, L., 1953, Argille scagliose ed Argille brecciate in Sicilia: Boll. Serv. Geol. d'Italia, v. 75, fasc. 1, pp. 281–289.

———, 1954a, Das petrographische Gefügebild der Brekzientone Siziliens und ihre geologische Bedeutung: Neues Jb. Mineral., Mh. 1954, 1/2, pp. 18–28.

———, 1954b, Le argille brecciate siciliane: Mem. Ist. Geol. e. Min. Padova, v. 18, pp. 1–92.

———, 1954c, La Regola di Mottura di orientazione del gesso: Per. Mineral., Anno 23, pp. 53–65.

Pettijohn, F. J., 1949, Sedimentary rocks. Harper and Bros., New York, 526 pp.

Posnjak, E., 1938, The system, $CaSO_4$—H_2O: Am. Jour. Sci., 5th ser., v. 35 A, pp. 247–272.

———, 1940, Deposition of calcium sulfate from sea water: Am. Jour. Sci., v. 238, pp. 559–568.

Sander, B., 1936, Beiträge zur Kenntnis der Anlagerungsgefüge. (Rhytmische Kalke und Dolomite aus der Trias): Zschr. f. Krist., Min. u. Petr. Abt. B, Min. u. Petr. Mitt., N.F., Bd. 48, H. 1–2, pp. 27–139, H. 3–4, pp. 141–209.

Udden, G. A., 1924, Laminated anhydrite in Texas: Geol. Soc. America Bull., v. 35, pp. 347–354.

Attachment B-14

COBISS: 1.01

DAMAGE TO THE HISTORIC TOWN OF STAUFEN (GERMANY) CAUSED BY GEOTHERMAL DRILLINGS THROUGH ANHYDRITE-BEARING FORMATIONS

ŠKODA V ZGODOVINSKEM MESTU STAUFEN (NEMČIJA) POVZROČENA Z GEOTERMALNIM VRTANJEM SKOZI ANHIDRITNE FORMACIJE

Ingo SASS[1] & Ulrich BURBAUM[2]

Abstract UDC 504.6:550.822(430)

Ingo Sass & Ulrich Burbaum: Damage to the historic town of Staufen (Germany) caused by geothermal drillings through anhydrite-bearing formations

Shallow geothermal systems for the heating and cooling of buildings will play an important role in the future renewable energy supply. Especially in dense settlements the geothermal energy utilization for facility heating and cooling is very promising. Therefore, it is important to analyse the damage to Staufen im Breisgau (Germany). In September of 2007, seven geothermal borehole heat exchanger (BHE) drillings were performed in a small square directly adjacent to the 16th century town hall in the centre of the town. These led to enormous structural damage to buildings as a function of four different geological parameters: artesian groundwater, two interacting karst formations, strong tectonization, and a swellable anhydrite formation. Some weeks after termination of the well construction, uplift started, and recently (March 2010) reached a magnitude of approximately 26 cm. Actually, some 250 buildings (March 2010) are involved; showing cracks, tilting, and other effects of the differential swelling movements beneath the foundations. Surface uplifts with rate up to 10 mm/month have been determined using high-resolution spaceborne radar data and radarinterferometric techniques. These amplitudes correlate with data from benchmarks of terrestrial geodetic surveyng. Besides the uplift due to the swelling processes, future problems could arise from the fact that the gypsum formed from the swelled anhydrite is soluble in water. Thus, sinkholes and other karst related phenomena may occur.

Keywords: Anhydrite swelling, borehole heat exchangers, borehole heat exchanger drillings, damage to buildings, gypsum karst.

Povzetek UDK 504.6:550.822(430)

Ingo Sass & Ulrich Burbaum: Škoda v zgodovinskem mestu Staufen (Nemčija) povzročena z geotermalnim vrtanjem skozi anhidritne formacije

Plitvi geotermalni sistemi za ogrevanje in ohlajanje zgradb bodo v prihodnje igrali pomembno vlogo pri oskrbi z obnovljivo energijo. Zlasti v gosto poseljenih naseljih je koriščenje geotermalne energije mnogo obetajoče za ogrevanje in hlajenje. Zato je pomembno analizirati škodo povzročeno v Staufnu, Breisgau (Nemčija). Septembra 2007 je bilo v centru mesta, na manjšem trgu v neposredni bližini mestne hiše iz 16. stoletja, izvedeno vrtanje sedmih geotermalnih vrtin za toplotno izmenjavo (VTI). Vrtanje je povzročilo ogromno škode na stavbah, saj je vplivalo na štiri različne geološke parametre: na arteško podtalnico, medsebojno vplivanje kraških formacij, močno tektonizacijo in na nabrekanje anhidritnih formacij. Nekaj tednov po zaključku izdelave vrtin se je pričelo dvigovanje in je marca 2010 doseglo premike do približno 26 cm. Dejansko je bilo do marca 2010 poškodovanih okoli 250 stavb, kjer so opazne razpoke, nagibi in druge posledice različnih premikov pri nabrekanju pod temelji. Površinski premiki s stopnjo do 10 mm/mesec so bili določeni z interferometričnimi tehnikami in obdelavo podatkov visokoločljivega satelitskega radarja. Te razsežnosti so v korelaciji z oznakami relativnih višin izmerjenimi s terestičnimi geodetskimi meritvami. Poleg dvigovanja, ki ga je povzročilo nabrekanje, lahko v prihodnosti nastanejo dodatni problemi z raztapljanjem iz anhidrita nastale sadre. Tako lahko pride do nastanka udora in drugih pojavov, ki so povezani s korozijo.

Ključne besede: nabrekanje anhidrita, vrtin za toplotno izmenjavo, škoda na poslopjih, sadreni kras.

[1] Technische Universität Darmstadt, Institut für Angewandte Geowissenschaften, Schnittspahnstraße 9, 64287 Darmstadt, e-mail: sass@geo.tu-darmstadt.de

[2] CDM Consult GmbH, Motorstraße 5, 70499 Stuttgart

Received/Prejeto: 26.2.2010

DAMAGE SYMPTOMS

Staufen im Breisgau (Staufen) is located in the southwestern Germany on the western flank of the Upper Rhine Valley graben (Fig. 1). The drilling of seven shallow borehole heat exchangers (BHE) at the City of Staufen triggered a series of events in completely different domains that have caused a very problematic situation. The complicated process is not completely investigated today. Since the installation of the BHE in September 2007, the subsoil in the inner city shows an uplift of up to approximately 10 mm/month (LGRB 2009). The current cumulative value (as of March 2010) is approximately 26 cm. The geothermal wells were drilled up to 140 m depth, and were intended to supply the town hall with geothermal energy for heating and cooling purposes.

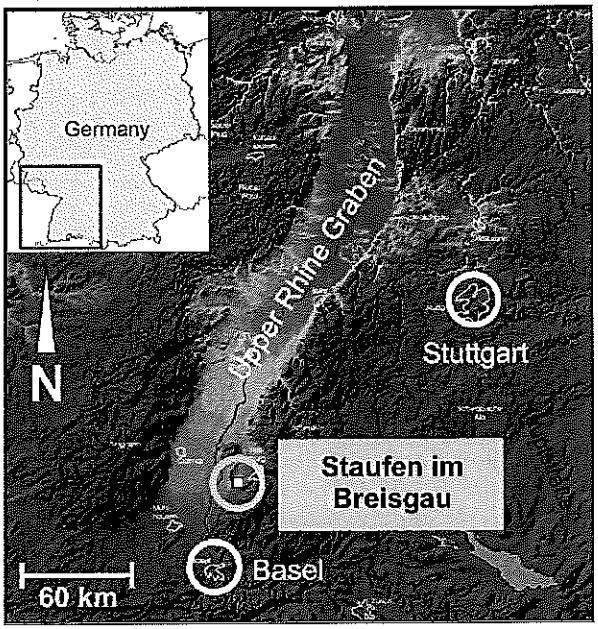

Fig. 1: Staufen im Breisgau.

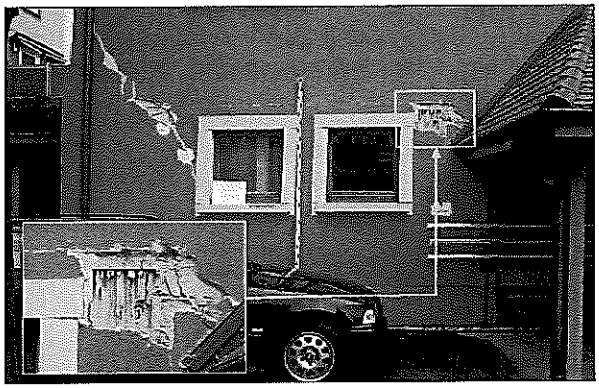

Fig. 2: Uplift cracks in building Kirchstraße, inner courtyard, distance to the well field approx. 20 m to the east. Destruction of the supporting masonry, March 2009 (Photo: U. Burbaum).

The differential uplift affects buildings as well as infrastructure by inducing stresses which exceed the tension and shear strengths of the structural components, producing tension and shear cracks (Figs. 2 and 3). In addition, the deformations also cause tilting, which in turn puts compressive stress on bearing elements. The uniaxial compressive strength of construction components is locally exceeded, and they fail. Damages to the local infrastructure (Fig. 4) are severe. For example, gas and water utilities require expansion bends (Fig. 5) to prevent future desasters. The damage patterns are dependent upon the tectonic setting, the lithologic conditions, hydrogeological heterogeneity, and the BHE drilling geometry as well as varying BHE construction quality.

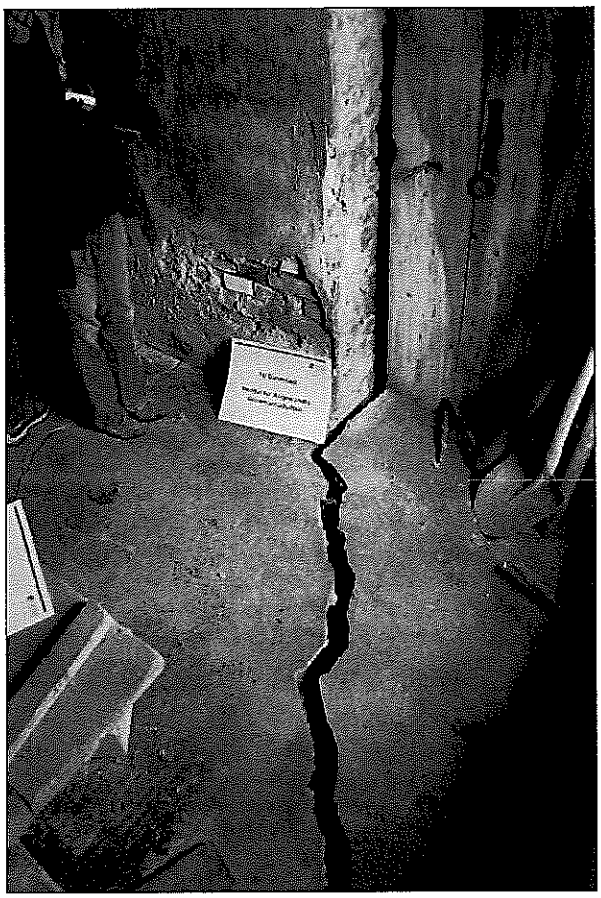

Fig. 3: Tension crack in a baseplate, building Jägergasse, distance to the well field approx. 70 m to the northeast, March 2009 (Photo: U. Burbaum).

Apertures of cracks typically range up to some centimeters, with some more than 10 cm. To date (March 2010) approximately 250 houses are seriously affected, and the number is still increasing (although this num-

Fig. 4: Crack in the street "Jägergasse", distance to the wellfield approx. 80 m to the NE, March 2009 (Photo: U. Burbaum).

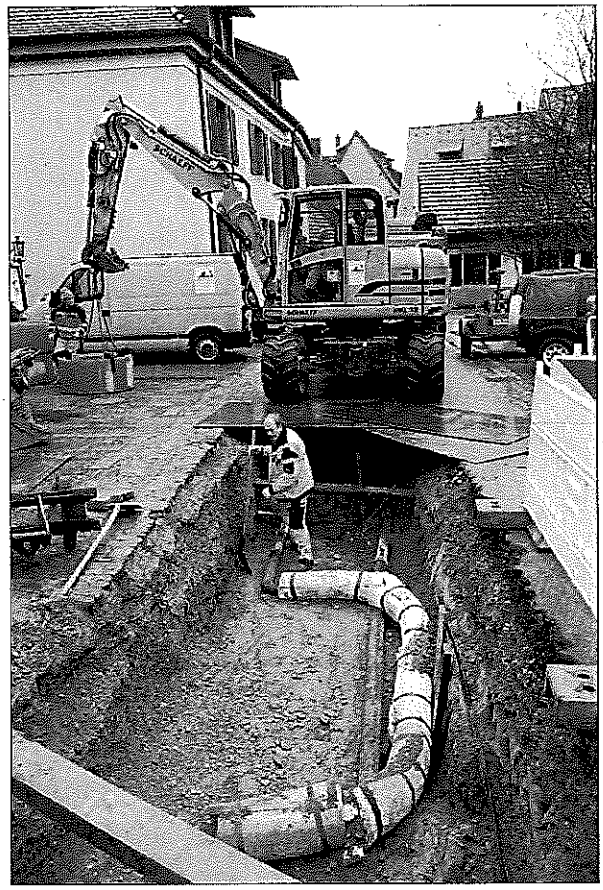

Fig. 5: Installation of an expansion bend in a PE-HD gas pipe, Meiergasse, distance to the well field approx. 80 m in northnortheast direction, March 2009 (Photo: U. Burbaum).

ber may include cracks formed in objects that could not verifiably be linked to the uplifting process). Therefore, it appears that the area of damage is growing, and that the uplift in vertical as well as in radial extension around the well field persists and damages rises.

The financial damage, and the best point of time for reconstruction of buildings and infrastructure, are not determinable since the swelling persists and is quantitatively not predictable to date. Thus, an economic basis for the claim settlement does not exist. A method to quantify the restoration and compensation costs must be developed in the near future.

GEOLOGY AND ANHYDRITE SWELLING

The location of Staufen on the western flank of the Upper Rhine Valley graben (Fig. 6) is affected by complex and partially unexplored tectonic conditions (Landesvermessungsamt Baden-Württemberg 1996). Fig. 7 shows a NW-SE geologic cross-section in the area of the inner city (after Schreiner 1991, as cited in a report by the Landesanstalt für Umweltschutz Baden-Württemberg 2005). Small scale features of shearing, compressive and extensive tectonic movements are typical, and produce multi-phase fracture systems (Geyer & Gwinner 1991).

Thus, the quantitative determination of the groundwater movement and its flow paths is difficult. However, it is most likely that the fracture system can provide various hydraulic connections. Drilling risks should therefore be categorized as high since drill holes could collapse, or other problems may occur.

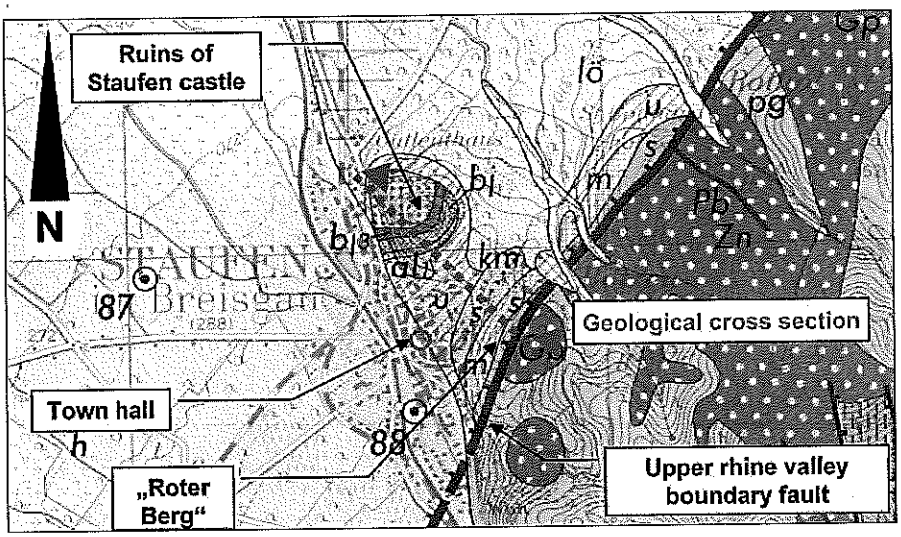

Fig. 6: Modified detail image of the geological map of Freiburg, M 1:50.000. (Landesvermessungsamt Baden-Württemberg 1996).

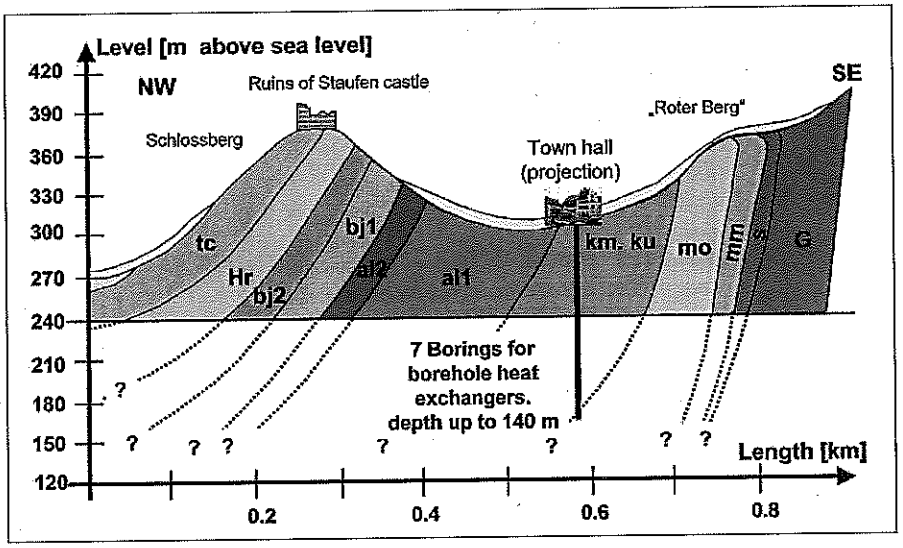

Fig. 7: Geological cross section NW-SE (modified after Schreiner, A. 1991, cited in: Landesanstalt für Umweltschutz Baden-Württemberg 2005).

tc = Tertiary conglomerate, Hr = Hauptrogenstein, bj2 = Bajocian 2, bj1 = Bajocian 1, al2 = Aalenian 2, al1 = Aalenian 1: Opalinus clay, km = Middle Keuper, ku = Lower Keuper, mo = Upper Muschelkalk, mm = Middle Muschelkalk, s = Buntsandstein, G = Granite.

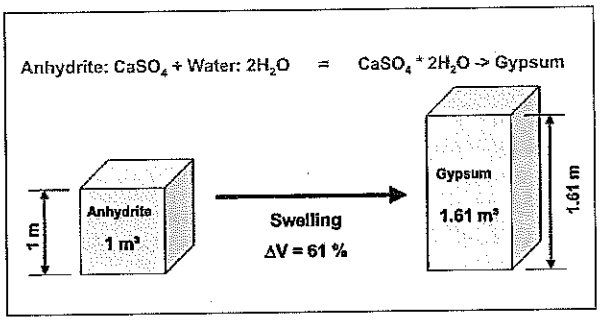

Fig. 8: Swelling process of anhydrite into gypsum.

Complicated groundwater conditions, and local occurrence of artesian groundwaters, are typical at the Rhine Valley flanks. For this reason, the guidelines for the utilization of shallow geothermal energy (LGRB 2005) of Baden-Wuerttemberg assigns geothermal well drillings into the highest case; group D. This group permits geothermal drillings only after individual examinations, and only under certain technical and regulatory conditions.

The general stratification in the vicinity of the town hall (Figs. 6 and 7) can be taken from the geological map (Landesvermessungsamt Baden-Württemberg 1996; Landesvermessungsamt Baden-Württemberg 1999), which proved to be quite appropriate. Basically, thin-bedded strata of Jurassic age cover some meters of Schilfsandstein (Stuttgart Formation) and Gipskeuper (Grabfeld Formation). The Gipskeuper reaches a thickness of about 100 to 150 m (Geyer & Gwinner 1991) throughout the southwest of Baden-Württemberg.

In Staufen, wells proved a thickness of about 100 m. The geothermal probes presumably reached their final depths in the Lettenkeuper (Erfurt Formation). The underlying Muschelkalk has not been drilled yet (according to known well logs, Gemeinde Staufen 2007). One research drilling later reached the Muschelkalk in Summer 2009. However, the Lettenkeuper has only some meters thickness and due to the structural fracturing, the hydraulic head of the Muschelkalk is probably connected to the drill site. Due to the petrographic patterns and the strong tectonics, the Lettenkeuper has to be regarded as an aquifer-aquitard intercalation. The hydrogeological map (LGRB 1977) shows limestone, and dolomite, respectively, in the vicinity of Staufen. This could be Muschelkalk (Landes-

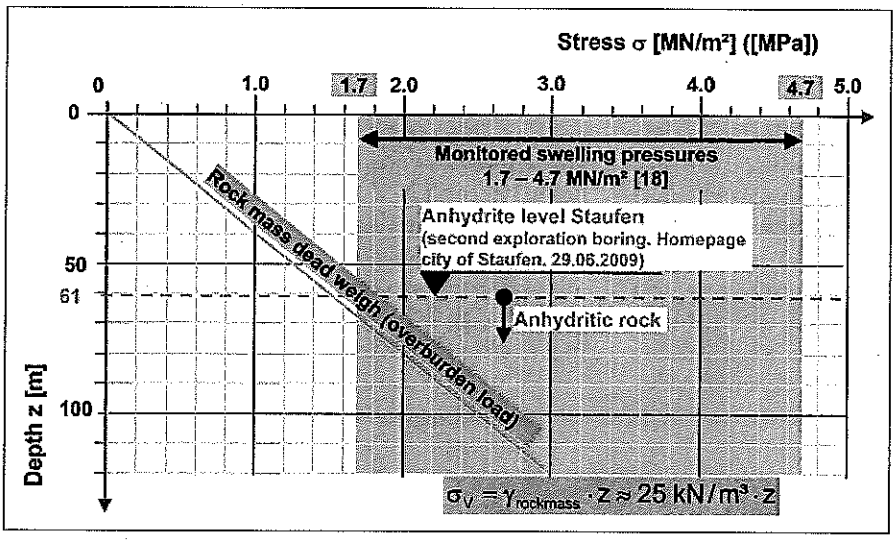

Fig. 9: Swelling pressure (modified from Steiner 1989, 1993, 2007).

vermessungsamt Baden-Württemberg 1996; LGRB 1977; Wagenplast 2005). The aquifers in the Muschelkalk have, due to their location and their catchment areas on the higher ground in the outlying hills, the potential to be artesian in the inner city districts of Staufen (Fig. 7).

When anhydrite and water interact, anhydrite recrystallizes as gypsum. This process involves swelling in the formation, with an increase of volume up to 60% (Fig. 8). Swelling processes in anhydrite have been described often (Chiesi *et al.* 2010; Steiner 1989, 1993, 2007). If swelling is prevented due to confining conditions, immense swelling pressures may occur. In some tunnel projects in anhydrite rock, swelling pressures from 1.7 up to 4.7 MPa were monitored (Steiner 1989, 1993, 2007). Swelling could be avoided only if sufficient overburden rock mass is present. The relationship between necessary overburden rock mass and possible swelling pressure is shown in Fig. 9. The dead weight of rock mass related to its depth is compared to the swelling pressure monitored by Steiner (Steiner 1989, 1993, 2007). The anhydrite rock in Staufen is located at about 60 m depth (see below). Thus, the overburden rock mass is insufficient to prevent swelling.

BOREHOLE HEAT EXCHANGER SYSTEMS

Worldwide, several systems for borehole heat exchangers (BHE) are established. The capacity of a borehole heat exchanger is essentially determined by the thermal properties of the surrounding ground and the backfilling in the annular space between exchanger pipes and borehole lining. The heat transport from the surrounding ground to the pipes is dominated by groundwater. For a good heat transport, the borehole backfill should be as permeable as possible (unsealed BHE systems, Fig. 10, left side). If groundwater is present, it is thermally most efficient to use no backfill. However, regulations in Germany require a complete grouting of the annular space.

A great advantage of sealed systems (Fig. 9 right side) is the protection of

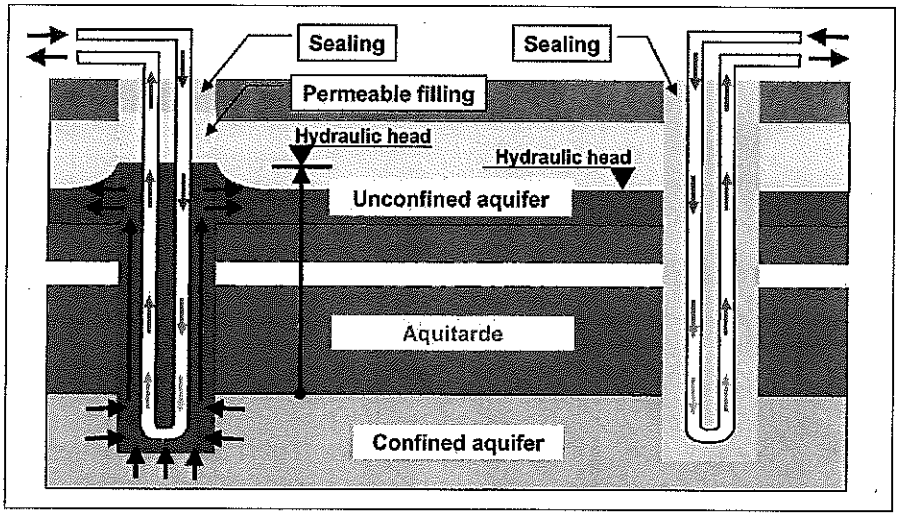

Fig. 10: Filling of borings for borehole heat exchangers.
Left: Unsealed BHE, Right: Sealed BHE

groundwater resources. Using ungrouted BHE systems, heat exchanger fluids (if they contain antifreeze agents like monoehtyleneglycol) may contaminate groundwater in case of a leakage from the pipes. Furthermore, layered aquifers are kept from communicating with each other. Additionally, surface contaminants may infiltrate downward into groundwater resources in unsealed BHE systems.

Therefore, in some countries authorities require a sealing by use of an impermeable backfill. National rules in this particular matter vary widely. However, from a hydrogeological perspective, the sealing of BHE is indispensible and the thermal capacity of borehole heat exchangers is then somewhat decreased. But the reduced performance of such a BHE is an acceptable trade-off.

For this reason, in Germany, the joining of two aquifers is forbidden. Each borehole of a heat exchanger has to be sealed by a cementbased backfill, which can be thermally enhanced to reduce the negative impact on the BHE performance. The backfill grout must be durable for long-term use according to groundwater quality, and it must be grouted from the borehole bottom to the top to provide a proper seal.

BOREHOLE HEAT EXCHANGER INSTALLATION IN STAUFEN

The drilling, cementing and casing operations on all seven double-U-tube geothermal probes (S1 to S7 in chronological order) were performed between 03.09.2007 and 21.09.2007 (Figs. 10, 11 and 12, Tab. 1) (Report 2007b). Distances between wells are at least 4.5 to 10 m. It is noticeable that the drill logs of S2 report a final depth of 105 m, while the planned and the authorized depth was 140 m (Gemeinde Staufen 2007; Landratsamt Breisgau-Hochschwarzwald 2007, Report 2007a). Presumably, the borehole collapsed below a depth of 105 m. S1 also collapsed from 135 to 140 m before installation of the heat exchanger pipes. Collapsed borehole sections cannot be grouted successfully.

Tab. 1: Data of borings (Report 2007b).

Boring	*Length (drilled) [m]*	*Length (completed) [m]*	*Diameter*
S1	140	135	0-14 m : 161 mm 14-135 m: 135 mm
S2	140	105	0-14 m : 161 mm 14-105 m: 135 mm
S3 – S7	140	140	0-14 m : 161 mm 14-140 m: 135 mm

Wells were drilled with a roller bit, and pressurized air was used as the drilling fluid. The surface casings extended to a depth of up to 14 m (Report 2007b).

Well S1 reportedly penetrated artesian groundwater at a depth of 32 m. The piezometric level at the wellhead was at about 0.5 m above ground surface (Report 2007b). All other wells did not encounter artesian conditions (according to residents and the administration of Staufen). It can be concluded that the hydraulic potential of the Muschelkalk karst aquifer was connected

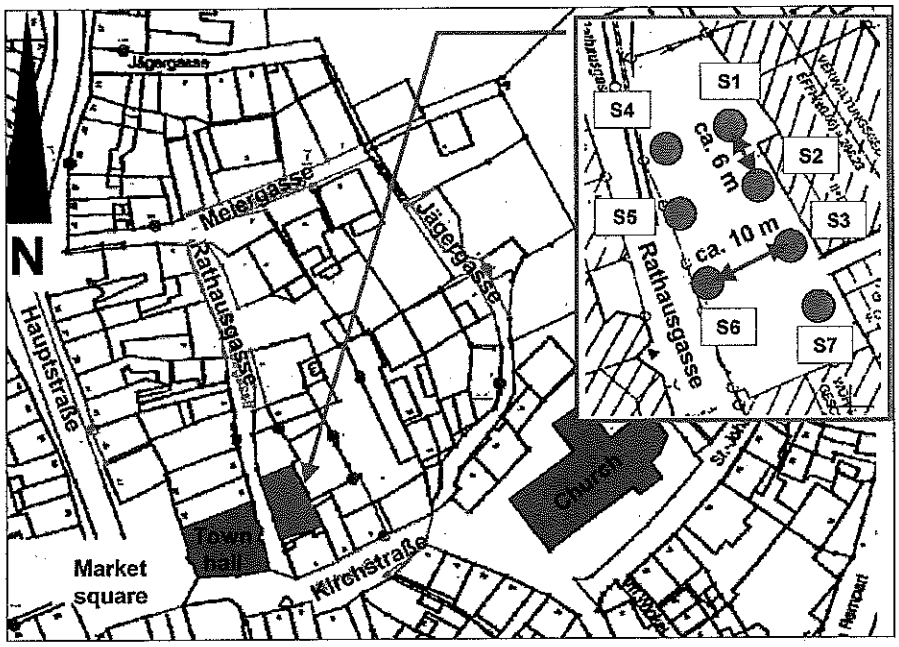

Fig. 11: Site sketch of well locations with interspaces at the city of Staufen town centre.

to the borehole S1 via fractures penetrating the Lettenkeuper layers. However, drilling contractor well logs show artesian conditions in all wells. Information on artesian control during drilling operations are missing in the well logs.

A water-suspended mixture of powdered clay and cement was used as backfilling grout. The amount of injected grout materials are shown in Tab. 2 (Report 2007b). Noticeable is well S2 which had a grout take much larger than predicted.

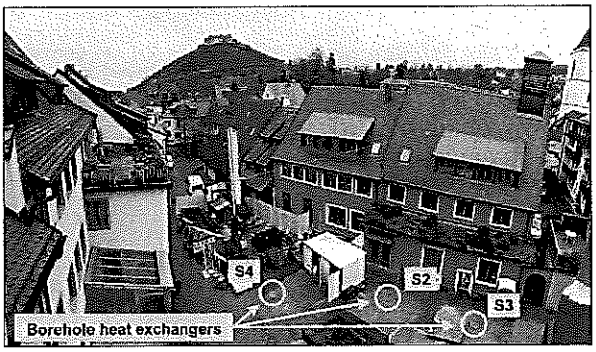

Fig. 12: Borehole heat exchanger field at Rathausgasse with drill rig for the first exploration boring for determining the cause of damage (March 2009). Photo taken from the tower of the town hall by U. Burbaum.

Tab. 2: Volume of sealing material in boreholes S1-S7 (Report 2007b).

Boring	*Gross volume (target) [m³]*	*Injected amount according to logs (actual) [m³]*	*Difference [m³]*
S1	2.01	2.23	0.22
S2	1.59	2.00	– 0.41
S3 - S7	2.09	2.00	– 0.09

Well S1 was drilled to its planned depth, but the borehole could not be cemented and backfilled for the last 5 m due to cave-ins. It is uncertain whether the filled excavations are all sealed-off. Due to the fact that the drilling operations were performed with only a short surficial casing, groundwater could ascend through the fracture system into the anhydrite- and possibly corrensite-bearing zones of the Gipskeuper, which is located below the gypsum level. Based on later surveys, it is likely that a fault was penetrated. Later observations (see below) suggest the swelling process was possibly triggered with the first well drilling operation.

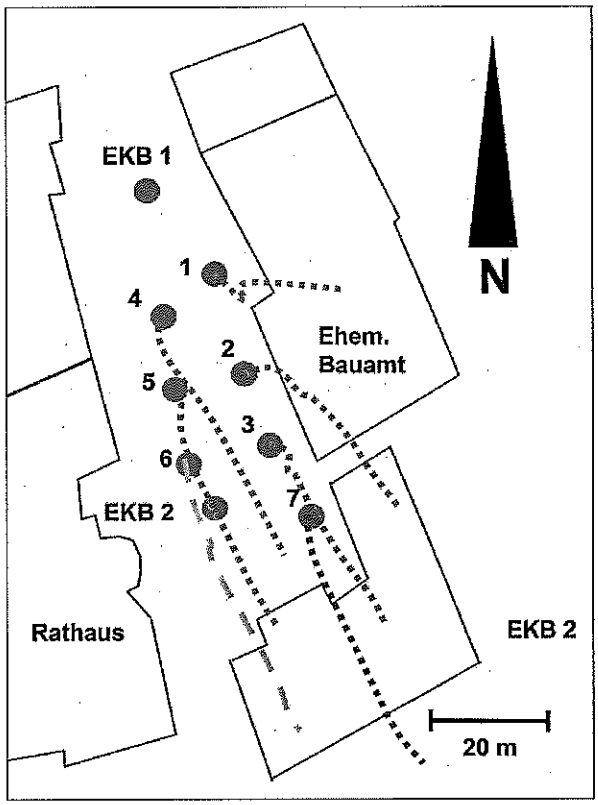

Fig. 13: Deviation of drillings.

The second well (S2) presumably penetrated the same fault or another related fault at about 105 m depth, as suggested by cave-ins prior to the installation of the geothermal probe at 140 to 105 m. These flow paths were probably not sealed off completely during the drilling operation.

An investigation of the inclination of the drillings shows a great horizontal deviation of all drillings up to some 20 m (LGRB 2010). This is shown in Fig. 13. The main deviation occurs in a depth of approx. 60 to 70 m. The depth correlates with the lower end of the temporary drilling casings.

UPLIFT IN THE URBAN AREA OF STAUFEN

In November 2007, only 6 to 8 weeks after finishing the installation of the BHE, the first cracks were noticed in buildings. Cracks were quite small at first, and were not linked to the drilling operations. From 12/2007 to 01/2008 cracks were marked with gypsum markers (Fig. 14).

Soon so many buildings were affected that geodetic leveling measurements were performed (Schad 2008), and revealed an extensive uplift of the town centre of Staufen.

The distribution of the uplift has been monitored since the 22.07.2008 by high-resolution, satellite-aided radar data (Petrat & Al-Enezi 2006). The procedure is based on radar interferometry, which has the advantage of an extensive monitoring of ground movement under

Fig. 14: Gypsum markers on a crack, building Rathausgasse 3, with logs of the fracture spacing since December 2007 (Photo from March 2009 by I. Sass & U. Burbaum).

ideal conditions. Radar interferometry is used in mining and oil and gas production (Petrat & Al-Enezi 2006). Small scale and complex ground and building movements can be monitored and measured quite well using the high (better than 1 m) resolution satellite data. High-resolution satellite images are provided through the radar satellite TerraSAR-X, which has been commercially active since 2008. TerraSAR-X has a comparatively short circulation time of 11 days (by comparison to conventional radar satellite systems), which allows a reliable temporally-variable monitoring of the ground movements. Data shown in Fig. 15 are withdrawn from Petrat (Petrat & Al-Enezi 2006; Sass *et al.* 2009). TerraSAR-X operates at a wavelength of 3.1 cm. The movement of the buildings was monitored in the so called StripMap mode, totaling nine data sets. Phase differences can be determined by comparing individual data sets, and are shown in interferograms. Differences are generally determined by analyzing the topography and ground movement that occurred between two succeeding data sets (satellite passes). After a revision of the topographic phase, each interferogram shows movement-related phase fractions, which can be converted into ground movement by assuming a movement direction. The data commonly contains atmospheric phases, which can be reduced by adequate stacking or by integrating multiple succeeding data sets. Data analysis suggests a considerable ground

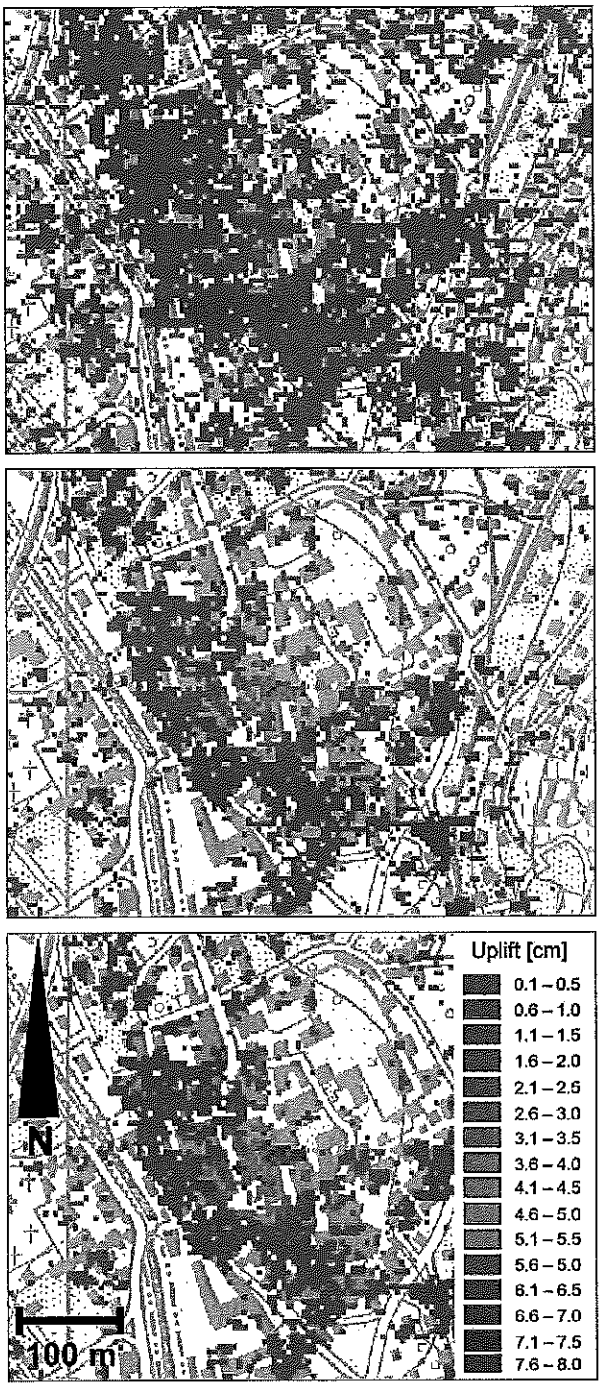

Fig. 15: Analysis of satellite-based ground level uplift monitoring by radar interferometry, a) July 2008 to 29. October 2008, b) July 2008 to 3. January 2009, c) July 2008 to 25. January 2009.

movement in the town centre of Staufen. An example of the chronological development of the ground movement, which was calculated by integrating individual interferograms is given in Fig. 15a–c. Missing areas in individual images are caused by a loss in coherence due to changes

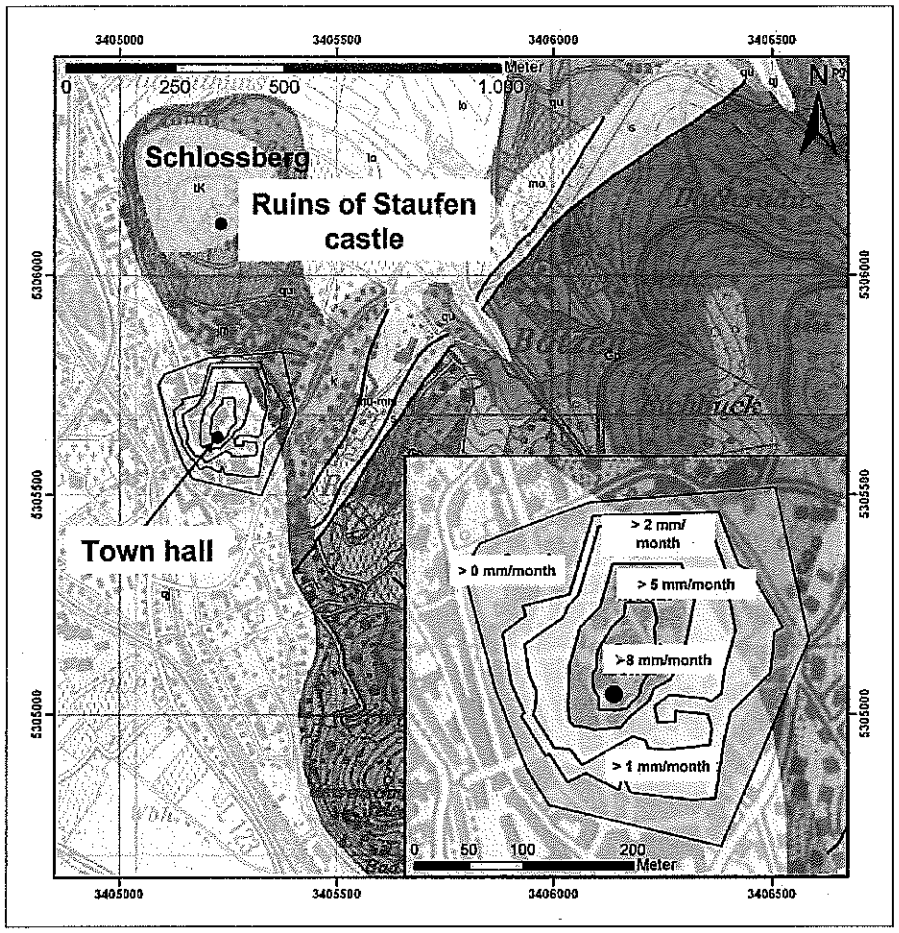

Fig. 16: Uplift rates in the city centre (LGRB 2009) plotted over the geological map Blatt 8112, Staufen im Breisgau, M 1:25.000.

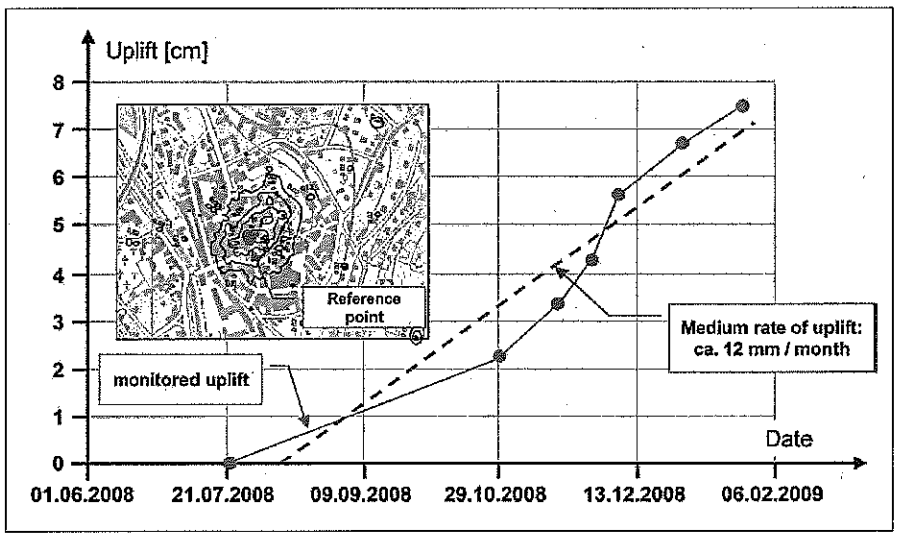

Fig. 17: Chronological development of the uplift of the town centre.

in vegetation on the surface. Longer time ranges cause higher losses. The movement information was interpolated to achieve a better interpretation. Interpolations were used to calculate contour lines, which have been plotted over the available uplift results (Fig. 16). The time-uplift relationship for a selected location is plotted in Fig. 17. The calculated uplift rate is approx. 12 mm per month. This value correlates well with the geodetic leveling measurements (Schad 2008).

In general, results of the geodetic surveillance and satellite-based radar images (Fig. 15a-c) of the uplifted zone show an elliptical dome with a NNE-SSW axis (Fig. 16). This position coincides well with the bedding of the Jurassic, Keuper and Muschelkalk series.

MAPPING OF DAMAGES AND GEOLOGY

Concepts for the technical restoration of the City of Staufen require detailed data on the complex geological situation. There are no outcrops in the damage area. Since the Grabfeld-Formation (Gipskeuper) is a subject to easy weathering, outcrops within this stratum are also not available. Structural geology data can only be achieved by analogue studies of the surrounding outcrops of younger or older beds with respect to the Middle and Upper Keuper. Three very small outcrops of the Muschelkalk and the Tertiary could be investigated. Fig. 18 shows related jointing rose diagrams for the outcrop locations. The major directions can be mapped in the historic city centre of Staufen by categorizing the cracks on the outside walls of the buildings (Fig. 18).

Investigations into the intensity of damages to buildings were carried out. Four categories of damage were chosen:

- open fissures (width: centimeter),
- open fissures (width: millimeters),
- fissures smaller than one millimeter,
- no fissures.

Some buildings or parts of the buildings could not be evaluated. Most of the fissures were smaller than one millimeter. Some buildings have fissures of some millimeters width. More than four buildings have fissures of some centimeters width.

The zone of the most damaged buildings is consistent with the main orientation of geological fault structures, which is NNW-SSE and WSW-ENE (Fig. 18).

The orientation of building damages corresponds to the orientation of the discontinuities (Figs. 18 and 19) that were obtained by a field study in October 2009. It can be concluded that groundwater not only flows through drillings but now through discontinuities, too. The swelling process therefore cannot be stopped by sealing the BHE-Drillings. A larger area remediation approach must be found.

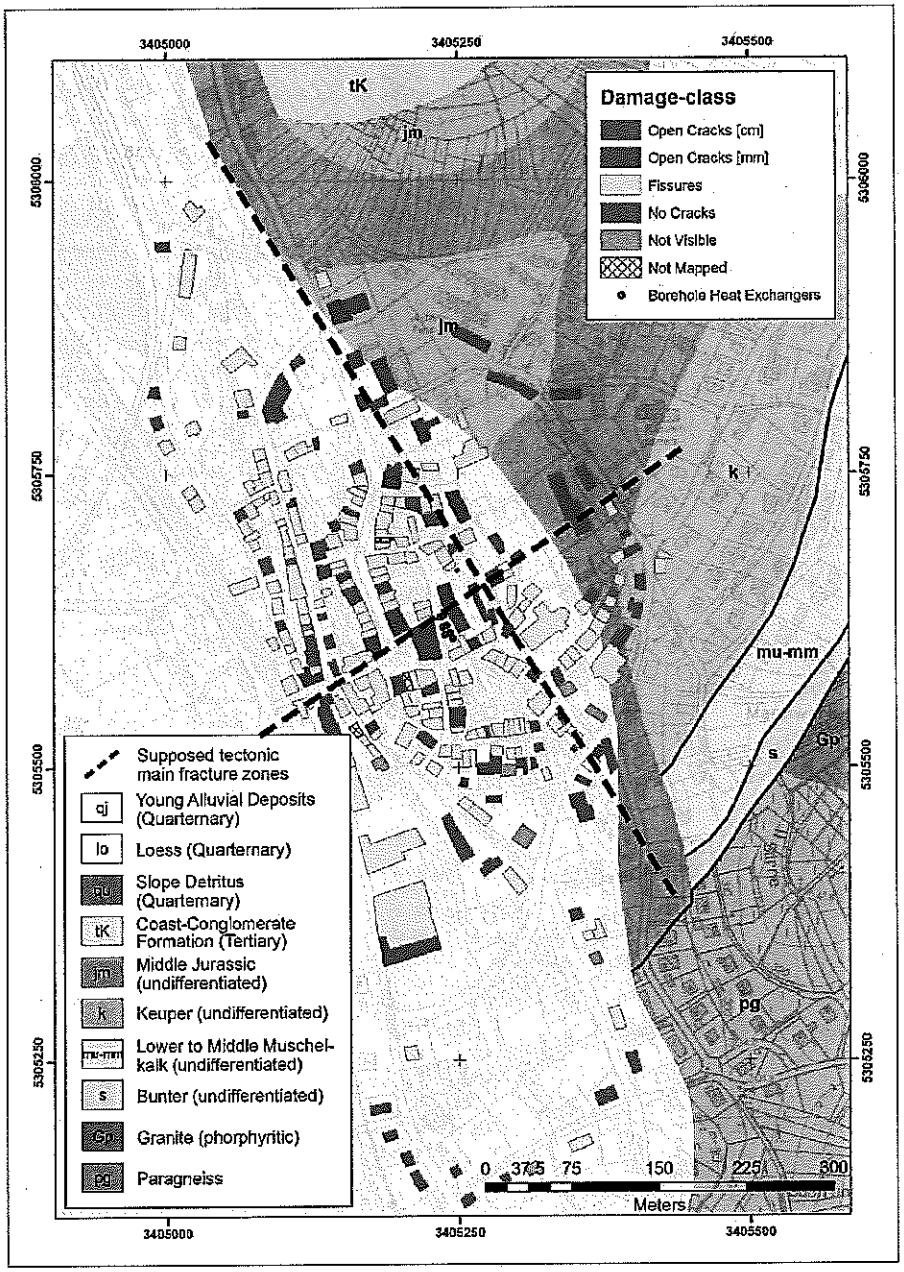

Fig. 18: Mapping of damages and geology.

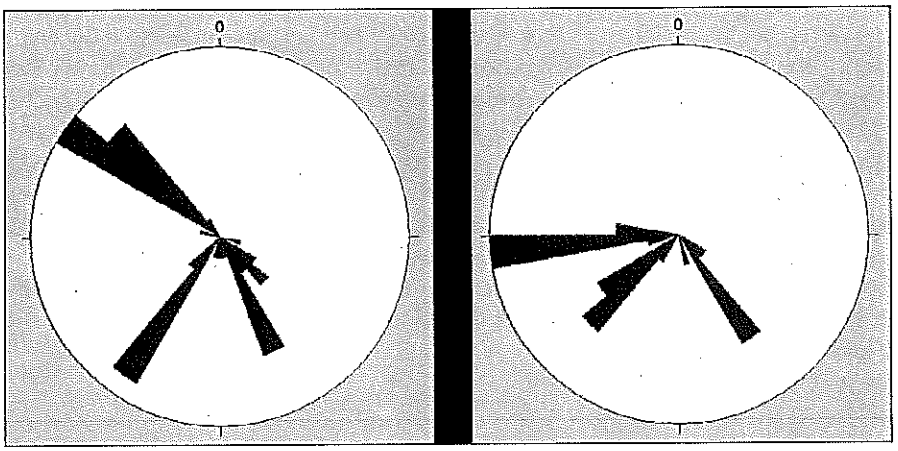

Fig. 19: Rose diagrams of outcrops. Left: Upper Muschelkalk, Right: Hauptrogenstein.

CONCLUSIONS

In total, four geological circumstances probably came into interaction due to an unsuitable drilling process, which resulted in the uplift caused by swelling: I) artesian groundwater in the karst section of the Gipskeuper, II) high anhydrite concentrations in that formation below, III) strong tectonization due to the position on the graben shoulder and IV) good connectivity to the Muschelkalk aquifer with a high hydraulic potential with respect to the Black Forest.

The uplift of the ground surface is obviously linked to large-scale swelling processes in the Gipskeuper. Furthermore, additional swelling of clay minerals (e.g., Corrensite) possibly occurs due to the contact with water. The contact with water has been rendered possible by hydraulic connections between the affected rocks and confined groundwater. These hydraulic connections were initiated by the geothermal drillings:

1. The chronological coherence between the drillings and the appearance of the cracks is a strong evidence for the causal coherence.

2. The contour lines of the uplift are elliptical around the well field (Figs. 15 and 16), which is an indication that the contact between water and Gipskeuper is located in the centre of the ellipse.

The natural causes discussed in Schad (2008), which explain the hydraulic pathways within and into the Gipskeuper strata by geological zones of weakness that opened up due to earthquakes, can be excluded, as damage symptoms and the damage history are not consistent with this hypothesis. Furthermore, there were no seismic events in the time period in question.

In 2007, only earthquakes with a magnitude up to 2.6 on the Richter scale were registered in the area (LGBR 2007a, b). This magnitude is in no case able to produce such displacements.

The first step towards a complete tectonic and hydraulic investigation in and around the BHE field is done (LGRB 2010) but this is insufficient to supply a temporal and geometrical prognosis of the uplift. It is quite certain that the uplift will continue until the inflow of water into the swelling strata ceases, or until the entire hydraulically-accessible anhydrite has reacted to gypsum.

At this point, the rehabilitation concept of the geothermal well field has to fit in. Under supervision of the state geological survey (LGRB) the grouting of the BHE was begun in late 2009. A new method to perforate the BHE pipes from inside was applied to inject sealing grout into backfill failures (LGRB 2010). At the end of March 2010 about 14 m^3 of grout were injected into the BHE field. The rate of uplift seemed to slow down in the centre of the swelling area. However, the number of damaged buildings still increases. This remedial measure was assisted by an ongoing groundwater withdrawal of about 2 l/s from the investigation well EKB 2, which leads to a drawdown of more than 100 m.

Furthermore, gypsum is dissolving due to the continuous groundwater contact. This gives rise to recent karstification. Fine cavities will arise and will be distributed according to the distribution of the anhydrite and gypsum in the rock. These cavities will be closed due to the vertical stress of the overlying rocks, with subsidence of the ground surface as the consequence. If these fine distributed cavities get linked with each other, subsidence of the buildings into sinkholes may occur. A sinkhole event some tens of meters west of the town hall was reported 17 years ago. Therefore, this scenario is very

likely. The recent decrease of the uplift rate could also be related to the beginning of karst formation or to the hydraulic drawdown. Further observations and investigations will be necessary to clarify this uncertainty.

The reconstruction of the City of Staufen is not expedient until the uplift ceases. In the short-term, only actions that serve the security and preserve the building substance and infrastructure should take place.

Sealing the geothermal wells currently seems to be the only option the stop the water inflow. This approach has to be carried out by the state geological survey. It is doubtful that this will affect the uplift in the entire 250 to 200 m elliptical dome.

In March 2009, a first boring to investigate the damage has been aborted, with the Lettenkeuper (Lower Keuper, Erfurt Formation) penetrated at only 16 m depth. In fact, it was expected at about 120 to 130 m. A survey proved a tectonic fault in the geothermal well field. A second investigation boring was finished in February 2010. The current level of information suggests that BHE well S1 penetrated an artesian aquifer.

A first step to a geological model has been developed, but more information is now required.

ACKNOWLEDGEMENT

The authors gratefully thank Timothy D. Bechtel (Lancaster, PA, USA) for proofreading and language corrections. Furthermore we acknowledge the thoughtful comments of the editor Nico Goldscheider (Munich) and Annette E. Götz (Darmstadt) for critical comments.

REFERENCES

Chiesi, M., De Waele, J. & P. Forti, 2010: Origin and evolution of a salty gypsum/anhydrite karst spring: the case of Poiano (Northern Apennines, Italy).- Hydrogeology Journal, DOI 10.1007/s10040-010-0576-2.

Gemeinde Staufen, 2007: *Bohranzeige über Bohrarbeiten für die Errichtung einer erdgekoppelten Erdwärmepumpe auf dem Grundstück Flurstücks-Nr. 44.*- Gemarkung Staufen, Gemeinde Staufen, Landratsamt Breisgau-Hochschwarzwald, Fa. Systherma, 28.03.2007.

Geyer, O. F. & M. P. Gwinner, 1991: *Geologie von Baden-Württemberg.*- Schweizerbart, pp. 482, Stuttgart.

Goldscheider, N. & T. Bechtel, 2009: Editors' message: The housing crisis from underground - damage to a historic town by geothermal drillings through anhydrite, Staufen, Germany.- Hydrogeology Journal, 17, 3, 491–493.

Landesvermessungsamt Baden-Württemberg, 1999: *Geologische Karte von Baden-Württemberg, Blatt 8112: Staufen im Breisgau, M 1:25.000.*- Freiburg im Breisgau.

Landesvermessungsamt Baden-Württemberg, 1996: *Geologische Karte von Baden-Württemberg: Freiburg im Breisgau und Umgebung mit Erläuterungen, M 1:50.000.*- Freiburg im Breisgau.

Landesanstalt für Umweltschutz Baden-Württemberg, 2005: *Geotope im Regierungsbezirk Freiburg, 1. ed..*- Landesanstalt für Umwelt, Messungen und Naturschutz Baden-Württemberg, Karlsruhe.

Landratsamt Breisgau-Hochschwarzwald, 2007: *Wasserrechtliche Erlaubnis für den Einbau von zwölf Erdsonden zum Betrieb einer Erdsonden-Wärmepumpenanlage auf Flst.-Nr. 44 der Gemarkung Staufen.*- Landratsamt Breisgau-Hochschwarzwald, Freiburg.

LGRB Landesamt für Geologie, Bergbau und Rohstoffe Baden-Württemberg, 1977: *Hydrogelogische Karte von Baden-Württemberg, Oberrheingebiet Bereich Kaiserstuhl – Markgräflerland.*- Geologisch-Hydrologische Karte, Freiburg i. Br. Umweltministerium Baden-Württemberg, Stuttgart.

LGRB Landesamt für Geologie, Bergbau und Rohstoffe Baden-Württemberg, 2005: *Leitfaden zur Nutzung von Erdwärme mit Erdwärmesonden.*- Umweltministerium Baden-Württemberg, Stuttgart.

LGRB Landesamt für Geologie, Bergbau und Rohstoffe Baden-Württemberg, 2007: *Erdbebendienst: Epizentren von Erdbeben im Jahr 2007.*- Umweltministerium Baden-Württemberg, Stuttgart.

LGRB Landesamt für Geologie, Bergbau und Rohstoffe Baden-Württemberg, 2007: *Erdbebendienst: Seismisches Bulletin Baden-Württemberg.*- Umweltministerium Baden-Württemberg, Stuttgart.

LGRB Landesamt für Geologie, Bergbau und Rohstoffe Baden-Württemberg (2009): *Stadt Staufen TK 8112, Hebungsgeschwindigkeit, 05.10.2008 - 09.12.2008.*- Umweltministerium Baden-Württemberg, Stuttgart.

LGRB Landesamt für Geologie, Bergbau und Rohstoffe, Baden-Württemberg, 2010: *Sachstandsbericht zur Erkundung und Sanierung des Schadensfalls Staufen, 22.02.2010.*- Umweltministerium Baden-Württemberg, Stuttgart.

Petrat, L. & A. Al-Enezi, 2006: Monitoring Oil Field Induced Subsidence using Satellite-Based Radar-interferometry.- In: *GEO 2006 – 7th Middle East Geoscience Conference in Manama*, 27th–29th March 2006, Bahrain.

Rauh, F., Spaun, G. & K. Thuro, 2006: Assessment of swelling potential of anhydrite in tunnelling projects.- In: Culshaw, M. et al. (eds.) *IAEG Engineering geology for tomorrow's cities, Proceedings 10th IAEG International Congress*, 6th–10th September 2006, Nottinham, England.

Rauh, F, 2009: *Untersuchungen zum Quellverhalten von Anhydrit und Tongesteinen im Tunnelbau.*- Münchener Geowissenschaftliche Abhandlungen, Reihe B. Nr. 1, pp. 110, München.

Report, 2007a: *Bohrprojekt Stadt Staufen mit 12 Bohrungen bis 140 m Tiefe/Länge, Gemeinde Staufen im Breisgau, Gemarkung Staufen, Flst.-Nr. 44.*- Anzeigenbestätigung der Bohranzeige, eingereicht durch Stadt Staufen, 28.03.2007.

Report, 2007b: *Fertigstellungsbericht Erdwärmesonden der Fa. Wälder Bau Bohrtechnik GmbH, Projekt Staufen i. Br. mit Lageplänen, Bohrprotokolle, Schichtenverzeichnissen, Verpressprotokollen, Druckprüfungsprotokollen.*- Fa. Wälder Bau Bohrtechnik GmbH, Schwarzenberg

Sass, I., Burbaum, U. & L. Petrat, 2009: Staufen im Breisgau: Artesisches Grundwasser, Anhydrit und Karst im Konflikt mit geothermischen Bohrungen.- In: Schwerter, R. (ed.) *17. Tagung für Ingenieurgeologie und Forum Junge Ingenieurgeologen*, 6th–9th May 2009, FDGG, 49, Zittau.

Schad, H., 2008: *Sachverständigengutachten der Materialprüfungsanstalt der Universität Stuttgart.*- Fachbereich/Abteilung Geotechnik vom 19.09.2008.

Schreiner, A., 1991: Geologie und Landschaft.- In: Hoppe, A. & Hrsgb. Das Markgräflerland (eds.) *Entwicklung und Nutzen einer Landschaft.*- Ber. natforsch. Ges. Freiburg 81, 11–24, Freiburg, 1991, cited in Landesanstalt für Umweltschutz Baden-Württemberg, 2005: Geotope im Regierungsbezirk Freiburg, 1. ed.

Steiner, W., 1989: *Wisenbergtunnel.*- Sonderdruck aus Tagungsbericht D037 der Fachgruppe für Untertagbau des SIA, 69–80.

Steiner, W., 1993: Swelling Rock in Tunnels: Rock Characterization, Effect of Horizontal Stresses and Construction Procedures.- International Journal of Rock Mechanics and Mining Sciences & Geomechanics Abstracts, 30, 4, 361–380.

Steiner, W., 2007: Einfluss der Horizontalspannungen auf das Quellverhalten von Gipskeuper.- Felsbau, 25,1, 15–22.

Wagenplast, P., 2005: *Ingenieurgelogische Gefahren in Baden-Württemberg.*- Information des LGRB, pp. 79. 46, Freiburg i. Br.

Attachment B-15

Available online at www.sciencedirect.com

SCIENCE DIRECT®

Cement and Concrete Research 35 (2005) 623–630

CEMENT AND CONCRETE RESEARCH

Hydration of anhydrite of gypsum ($CaSO_4$.II) in a ball mill

T. Sievert, A. Wolter*, N.B. Singh

Institute for Nonmetallic Materials, Technical University, Zhentnerstrasse 2a, Clausthal Zellerfeld 38678, Germany

Received 6 May 2003; accepted 13 February 2004

Abstract

The hydration of an anhydrite of gypsum ($CaSO_4$.II) in a ball mill was studied as a function of time and temperature. The amount of gypsum formed at different intervals of time was determined by weight loss method and powder X-ray diffraction technique. Specific surface area at different time intervals was determined by LASER granulometric method. The results showed that the maximum rate of formation of gypsum was at a longer time than the time for the development of maximum specific surface area. In the presence of activators, the time for maximum rate of gypsum formation and maximum specific surface area shifted towards lower hydration time. Morphological changes during the course of hydration have been studied by the scanning electron microscopic (SEM) technique. A mechanism of hydration has been proposed.

Keywords: Anhydrite; Hydration; Kinetics; Sulfate, Modeling

1. Introduction

Various forms of calcium sulphate hydrate have been reviewed by Hand [1]. Depending on the temperature, calcium sulphate exists as anhydrite ($CaSO_4$), subhydrate ([2]; $CaSO_4.xH_2O$, $0<x\leq 0.8$) and dihydrate ($CaSO_4.2H_2O$). The $CaSO_4$.II phase of anhydrite is the one that is thermodynamically stable up to 1180 °C and occurs naturally as the mineral anhydrite. It may also be produced by high-temperature (≈ 600 °C) calcinations of natural or by-product gypsum. Under ambient conditions, CaSO4.II reacts very slowly with water, and, hence, the name dead burnt gypsum is also given to this mineral.

The ability of anhydrite to react with water, converting itself into gypsum, is the basis of its use as a construction material. However, this process, known as setting, is very slow. The reactivity can be enhanced considerably by grinding the anhydrite to fine powders and also adding certain activators.

Murat et al. [3] found that the hydration kinetics of pure synthetic orthorhombic anhydrite depends on the temperature of preparation, mechanical activation by grinding and the nature of foreign cations in the solution used as chemical activators. They considered the hydration as dissolution–nucleation–growth process, in which nucleation was the more concerned step.

According to Ottemann [4], the strength development in the anhydrite binder depends on the degree of drying and hydration. Riedel et al. [5] are also of the opinion that strength depends on the degree of hydration. On the other hand, El Hajjouji and Murat [6] disagree with the findings of Ottemann [4] and consider that the pore size, which is influenced by the size of the resulting gypsum crystals, is responsible for the strength of the hardened material. According to them, the size of the resulting gypsum crystals is dependent on the type of activator cation used.

Israel [7] found that there is a direct relationship between the amount of gypsum and flexural tensile strength of the hydrating anhydrite. Depending on the activators, the morphologies are changed. This changes the strength in a different way.

Singh [8] found that in the presence of an activator K_2SO_4, the hydration of anhydrite to gypsum is enhanced considerably, and the morphology of the crystallizing gypsum is changed. This was explained in terms of the formation of a double salt at the surface of anhydrite.

* Corresponding author. Tel.: +49-5323-72-2029; fax: +49-5323-72-3669.

E-mail address: a.wolter@tu-clausthal.de (A. Wolter).

0008-8846/$ – see front matter © 2004 Elsevier Ltd. All rights reserved.
doi:10.1016/j.cemconres.2004.02.010

It appears that controversies exist regarding the mechanism of hydration and requires further investigations. In addition, most of the studies have been made in pastes only. In the present investigation, the hydration of anhydrite of gypsum has been studied in a ball mill, and a mechanism of hydration has been proposed.

2. Experimental

2.1. Materials

Natural anhydrite was obtained from the south Hercynian region of Germany. It consists of 93.7% anhydrite, 4.4% gypsum and 1.9% $CaCO_3$. The particle size was less than 90 μm. The density of the material was 2.31 g/cm^3.

H_2SO_4 (pH 1), 5% $MgSO_4.7H_2O$ and a dilute solution of calcium hydroxide were used as activators. To prepare the calcium hydroxide solution, a saturated solution was made at 20 °C and then diluted to 50%.

2.2. Methods

The hydration of anhydrite was studied at room temperature in a laboratory ball mill with a water–solid ratio of 1.32. Hydrations were stopped at different intervals of time, with isopropyl alcohol. The amount of gypsum formed was determined by the powder X-ray diffraction technique, as well as by weight loss method, at 40 and then 350 °C [9]. It is found that the results obtained by the two methods are in good agreement [10].

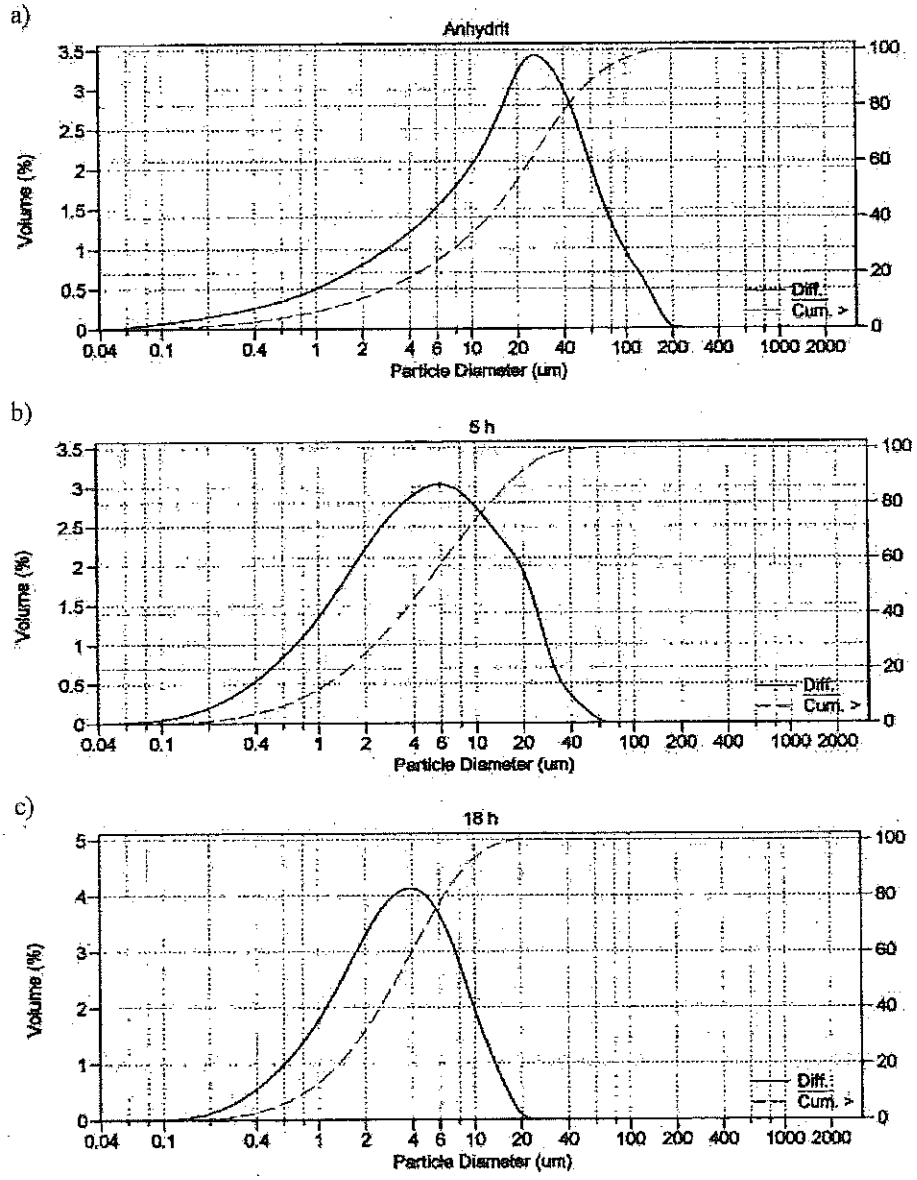

Fig. 1. Variation of percent cumulative and differential volume with particle size.

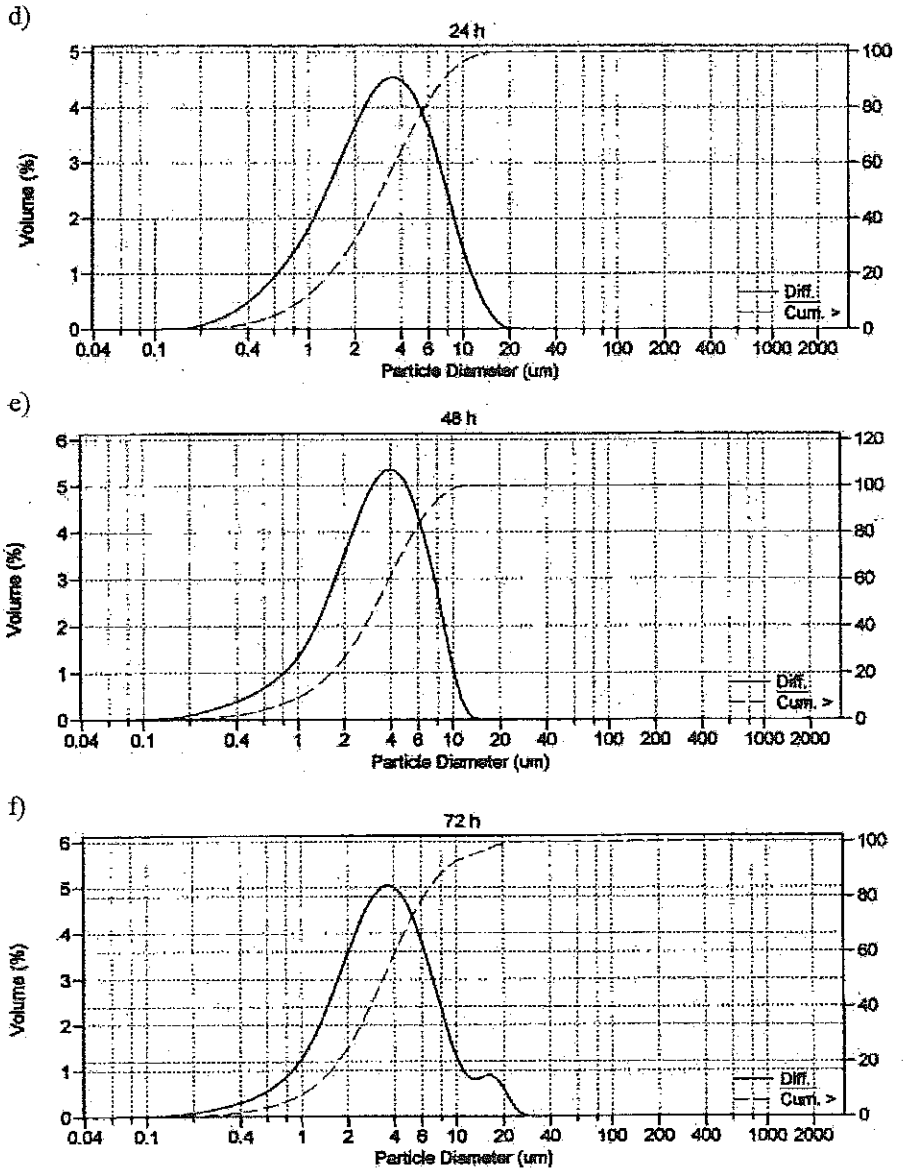

Fig. 1 (*continued*).

Particle size distribution and specific surface areas at different intervals of time were determined by LASER granulometric method [10] by using the Coulter LS-230 instrument.

The experiments were also performed at different temperatures (10, 20 and 40 °C) and in presence of activators.

Scanning electron microscopic (SEM) pictures of some hydrated anhydrites were also recorded.

3. Results and discussion

The particle size distributions in the hydrating anhydrite, at different intervals of time, are shown in Fig. 1. The percent cumulative volume and differential volume are plotted as a function of particle size (log scale). As the time progressed, the particle size decreased due to constant hit by the balls, and the curves for the differential volume became sharp, with a peak at lower particle sizes. At 72 h of hydration, a second small peak also appears, which may be due to the agglomeration of smaller particles or the recrystallization of gypsum. From the particle size distribution, the specific surface areas were calculated and are given in Figs. 2–5.

The variation of the amount of gypsum formed and the specific surface area developed during the hydration of anhydrite with hydration time are given in Fig. 2. The amount of gypsum first increases slowly and then appears at a faster rate (Fig. 2a). The rate of formation of gypsum with hydration time is shown in Fig. 2b. The curve shows that the rate first increases slowly and then

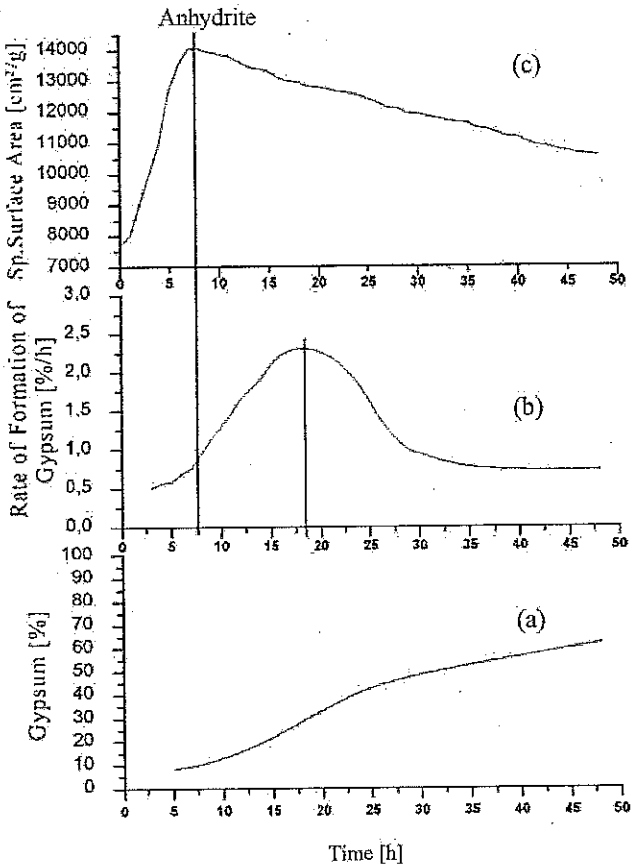

Fig. 2. Variation of (a) percent gypsum formed, (b) rate of formation of gypsum and (c) specific surface area with time in the hydrating anhydrite.

rapidly, with a maximum at about 18 h of hydration. After the maximum, the rate of formation of gypsum decreases and ultimately becomes constant. The variation of specific surface area with hydration time is given in Fig. 2c. The surface area increases continuously with time, reaches a maximum value at about 7.5 h of hydration and then decreases. The figures indicate that the time for the maximum rate of gypsum formation does not coincide with the time for maximum specific surface area. The maximum specific surface area is obtained at a shorter time, whereas the rate of formation of maximum gypsum is obtained at a longer time of hydration with anhydrite.

The hydration studies were also carried out in the presence of different activators such as H_2SO_4 (pH 1), 5% $MgSO_4.7H_2O$ and calcium hydroxide solution (50% dilution of the saturated solution of calcium hydroxide), and the results are presented in Figs. 3–5. Similar results are obtained without activator. The maximum rate of gypsum formation and the maximum value of specific surface area shifted to lower hydration times as compared with that without activator (Fig. 2).

The effect of temperature (10, 20 and 40 °C) on the formation of gypsum and the development of specific surface area in the hydrating anhydrite were also studied. The gypsum formed increased with time at all the temperatures, but the values are always lower at 40 °C (Fig. 6). The amounts of gypsum formed at 10 and 20 °C are almost similar. The solubilities of gypsum and anhydrite in water, at 40 °C, are the same and, hence, at this temperature, they exist in equilibrium. This may be one of the reasons for the lower values of gypsum in hydrating anhydrite at 40 °C. On the other hand, the variation of specific surface area at different temperatures follow the reverse sequence (Fig. 7); that is, the values are highest at 40 °C. The results show that the lower the amount of gypsum formed, the higher the specific surface area.

SEM pictures of anhydrite hydrated for 5 and 18 h in the absence and presence of H_2SO_4 (pH 1) are given in Fig. 8. The figures show that there is very little morphological change with hydration time and in the presence of H_2SO_4. This suggests that the hydration properties of anhydrite are not controlled by the morphology of hydration products.

From the results, the following mechanism can be proposed for the conversion of anhydrite into gypsum during hydration in a ball mill. As soon as anhydrite comes into contact with water, a part of it is dissolved, making the solution saturated with respect to Ca^{2+} and SO_4^{2-} ions.

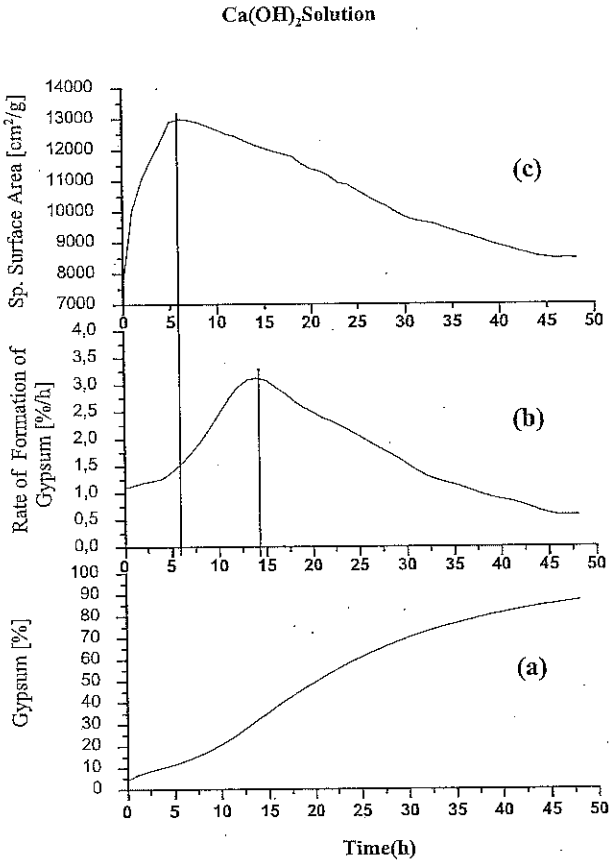

Fig. 3. Variation of (a) percent gypsum formed, (b) rate of formation of gypsum and (c) specific surface area with time in the hydrating anhydrite, in presence of calcium hydroxide solution.

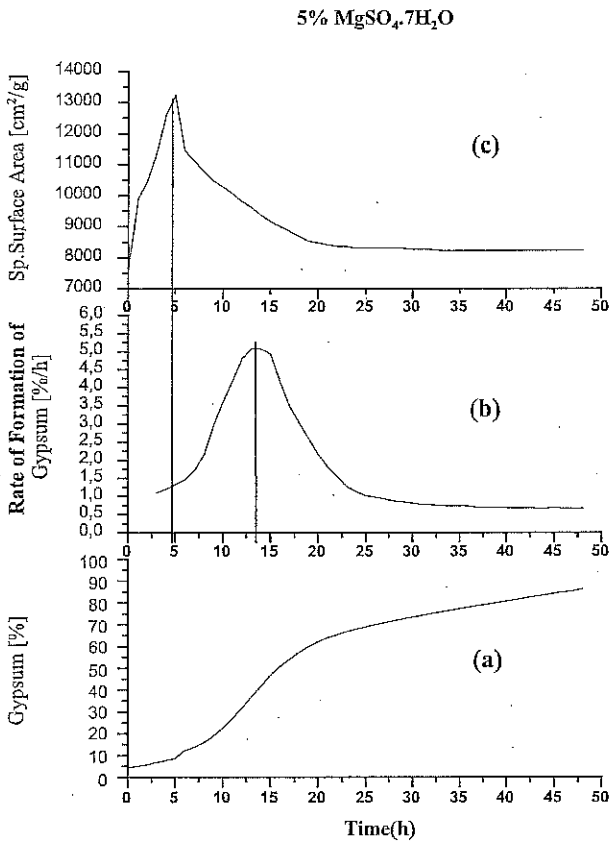

Fig. 4. Variation of (a) percent gypsum formed, (b) rate of formation of gypsum and (c) specific surface area with time in the hydrating anhydrite, in presence of 5% $MgSO_4.7H_2O$ solution.

These ions, which are hydrated in the solution, rapidly get adsorbed at the surface of anhydrite, giving a higher surface area. The thickness of the adsorbed layer increases with time. The Ca^{2+} and SO_4^{2-} ions of anhydrite have a tendency to go into solution, whereas water molecules have a tendency to interact with a fresh surface of anhydrite. The two processes are hindered because of the adsorbed layer. When the thickness of the adsorbed layer increases beyond a certain limit, cracks are formed. However, this is a very slow process; however, in the ball mill, the crack formation in the adsorbed layer is accelerated considerably. Water molecules enter through the cracks and come in contact with a fresh surface of anhydrite. When there are sufficient numbers of Ca^{2+} and SO_4^{2-} ions and water molecules at the surface, nuclei of gypsum are formed. A small amount of gypsum is already present in the anhydrite but, because it is an aged one, may not act as an effective nucleus. If the radius of the nucleus is higher than the critical size, crystallization of gypsum starts and will occur at a faster rate. Once a large amount of gypsum is formed, the remaining anhydrite, if any, is covered with that, and further hydration becomes very difficult. But in the ball mill, the possibility of completion of the hydration is much more than in the paste. The overall mechanism is shown in Fig. 9.

From the above discussions it is clear that there is a time lag between the adsorption and the formation of gypsum crystals. As a result, the time for maximum surface area does not coincide with the maximum rate of gypsum formation.

In the presence of activators, the solution compositions are changed, and activators may also retard the evaporation of water due to reduction in vapour pressure, and, therefore, gauge water is available for a longer period to facilitate the hydration for a prolonged time. As a result, the process of adsorption, breaking of adsorbed layer, nucleation and crystal growth are changed. This simply causes change in the time for the appearance of maximum surface area and maximum rate of gypsum formation in the hydrating anhydrite.

4. Conclusions

From the results, following conclusions can be drawn:

1. During the hydration of natural anhydrite in a ball mill, the time for the rate of formation of the maximum

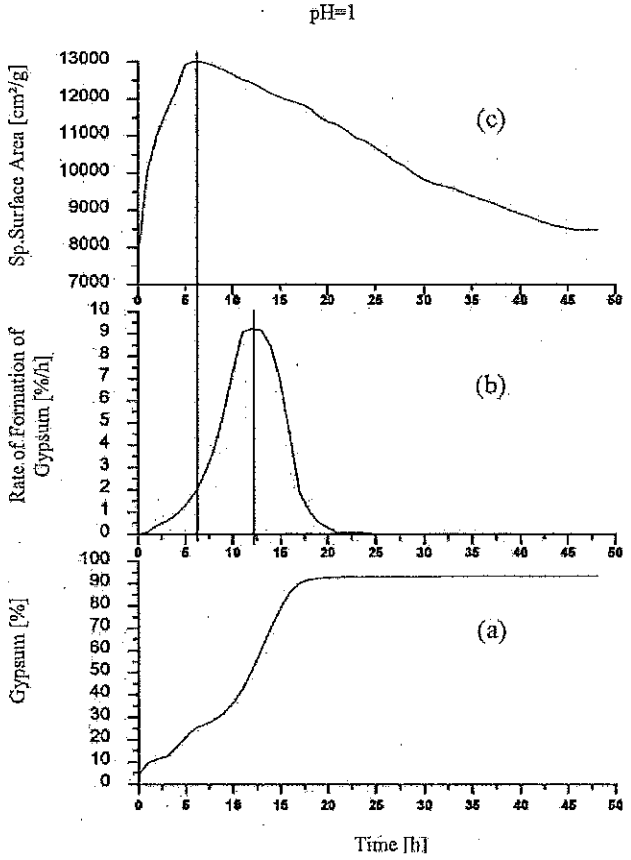

Fig. 5. Variation of (a) percent gypsum formed, (b) rate of formation of gypsum and (c) specific surface area with time in the hydrating anhydrite, in presence of H_2SO_4 (pH 1).

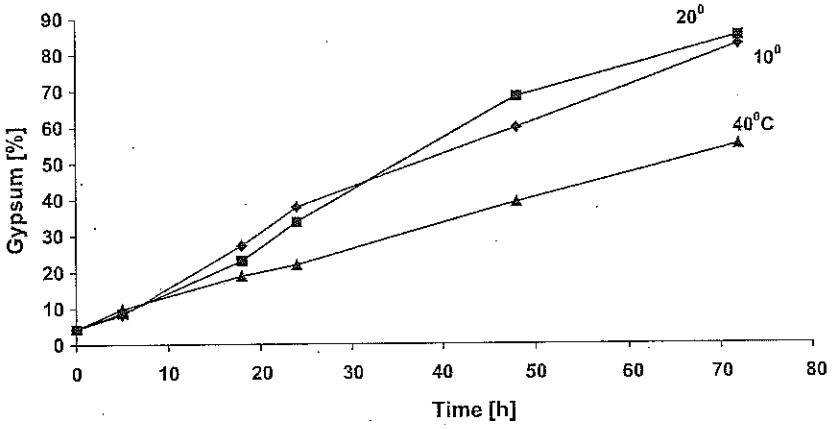

Fig. 6. Variation of amount of gypsum in the hydrating anhydrite, with time, at different temperatures.

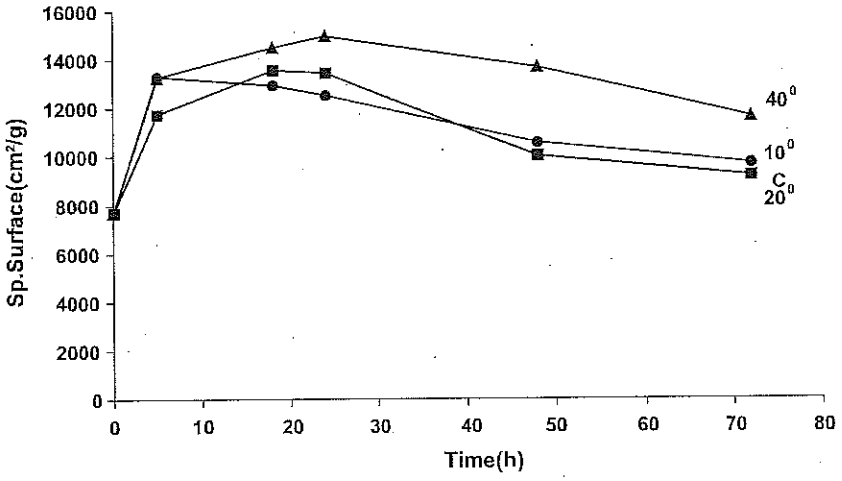

Fig. 7. Variation of specific surface area in the hydrating anhydrite, with time, at different temperatures.

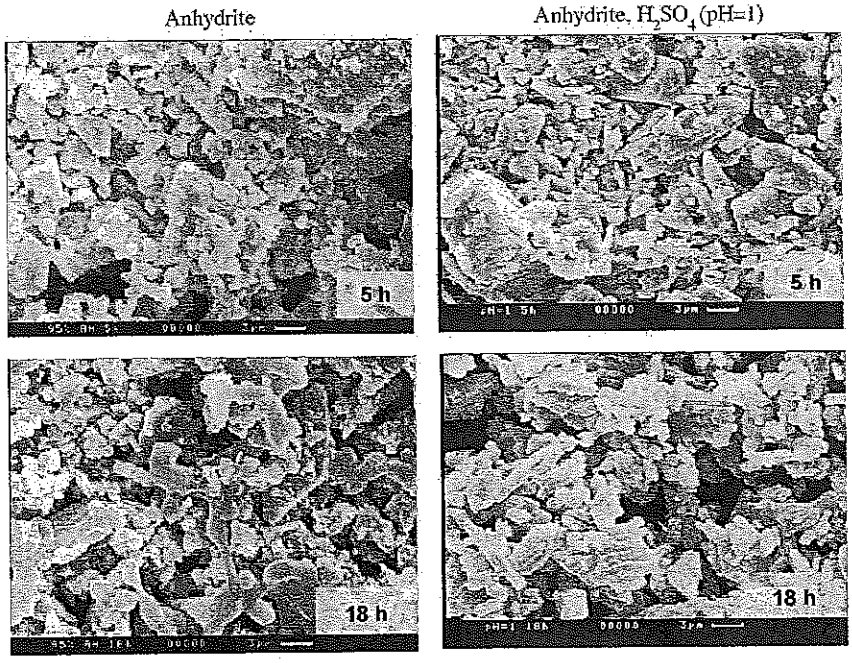

Fig. 8. SEM pictures of anhydrite hydrated for 5 and 18 h in the absence and presence of H_2SO_4 (pH 1).

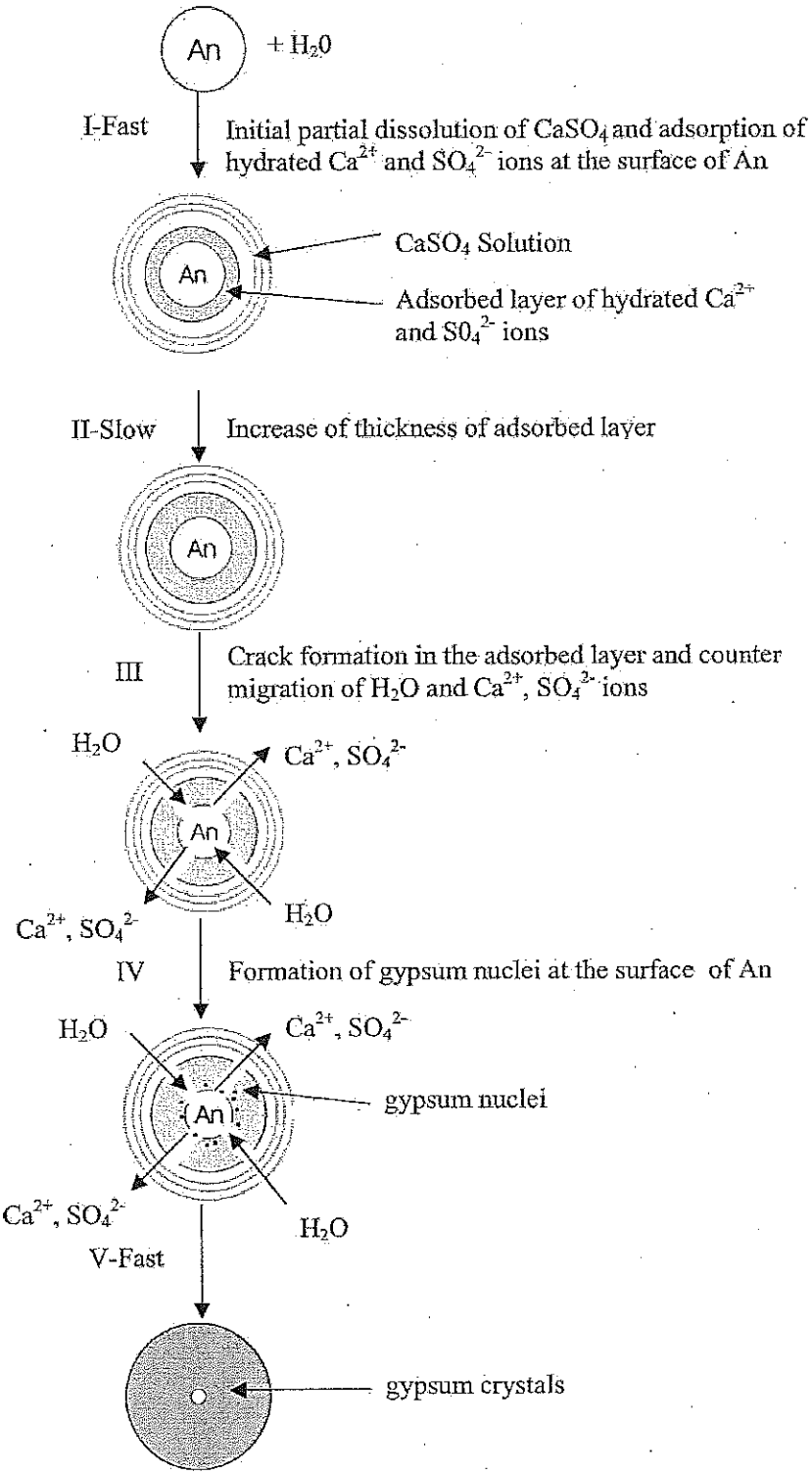

Fig. 9. Mechanism of hydration of anhydrite (An).

amount of gypsum (longer time) does not coincide with the time for the development of maximum specific surface area (shorter time). There is a time lag between the adsorption of ions on the surface of anhydrite increasing the specific surface area and the formation of gypsum.

2. At 40 °C, the amount of gypsum formed was always lower as compared with that formed at 10 and 20 °C, whereas the variation of specific surface area followed the reverse sequence. This simply indicates that the lower the amount of gypsum, the higher the surface area.

3. Activators simply lower the time for the appearance of maximum specific surface area and the rate of formation of maximum gypsum.
4. SEM pictures showed that very little morphological changes occur during the hydration of anhydrite.
5. A plausible mechanism of hydration has been proposed.

Acknowledgements

The authors are thankful to German Gypsum Industry for providing the anhydrite and their interest in the present investigation. Prof. N. B. Singh, Department of Chemistry, DDU Gorakhpur University, Gorakhpur, India, is thankful to Alexander von Humboldt Foundation for providing a fellowship under the follow-up programme.

References

[1] R.J. Hand, Calcium sulphate hydrates: a review, Br. Ceram. Trans. 96 (3) (1996) 116–120.
[2] F. Follner, A. Wolter, A. Preusser, S. Indris, C. Silber, H. Follner, The setting behaviour of α- and β-$CaSO_4.0.5H_2O$ as a function of crystal structure and morphology, Cryst. Res. Technol. 37 (10) (2002) 1075–1087.
[3] M. Murat, A. El Hajjouji, C. Comel, Investigation on some factors affecting the reactivity of synthetic orthorhombic anhydrite with water: I—Role of foreign cations in solution, Cem. Concr. Res. 17 (4) (1987) 633–639.
[4] J. Ottemann, Beziehungen zwischen Hydratation und Festigkeit. Mitteilungen aus den Laboratorien des Geologischen Dienstes Berlin, Neue Folge 2 (1951).
[5] W. Riedel, R. Bimberg, Ch. Göhring, Einfluß von Anregern auf den Eigenschaften eines synthetischen Anhydritbinders aus Fluoranhydrite, Baustoffind 2 (1989) 62–65.
[6] A. El Hajjouji, M. Murat, Strength development and hydrate formation rate. Investigation of anhydrite binders, Cem. Concr. Res. 17 (5) (1987) 814–820.
[7] D. Israel, Investigations into the relationship between the degree of hydration, flexural tensile strength and microstructure of setting anhydrite, Zement-Kalk-Gips 49 (4) (1996) 228–234.
[8] N.B. Singh, Effect of activator K_2SO_4 on the hydration of anhydrite of gypsum ($CaSO_4$.II) J. Amer. Ceram. Soc. (communicated 2003).
[9] Chemische Analyse von Gypsen und gipshaltigen Stoffen, Richtlinie des Deutschen Gipsvereins e.V., Ergänzung zur DIN 1168 Blatt 1 und 2.
[10] Th. Sievert, Rehydratation von Anhydrit, Diplomarbeit, Technical University Clausthal, 2000.